CONSTANT HEAD TEST ANALYSIS IN PARTIALLY PENETRATING WELLS

by

Cem Akgüner

B.S. in C.E., İstanbul Technical University, 1992

Submitted to the Institute for Graduate Studies in Science and Engineering in partial fulfillment of the requirements for the degree of

Master of Science

in

Civil Engineering

Boğaziçi University

1995

ACKNOWLEDGMENTS

There were a lot of people that contributed and got involved throughout the study. I am deeply grateful to all of them. First of all I want to thank God gave me health, strength and reasoning. My thesis supervisor Dr. Erol Güler encouraged, supported and guided me at all stages of this dissertation. I have gained a lot from his experience and knowledge. Dr. Cem B. Avcı was also of valuable help. He was always interested in my work and introduced and linked me to this subject and area of interest. The mathematical model he derived, along with Burak Kılanç, was used for analysis. He also took part in the Examining Committee. Dr. Orhan Yenigün also was a member of the Commitee and made valuable suggestions.

My family was always there when I needed them. They supported me in whatever I did. They made me what I am. My father, Dr. Tayfun Akgüner opened all the locked doors and lightened my path. My mother, Mary Akgüner and my sister, Perim Akgüner Ilgaz were on my side and they gave me encouragement.

Erkan Çetinkaya, Mehmet Tuna, Hasan Demir and Mehmet Özkerem at the Şeker Fabrikaları A.Ş. (EMAF) helped produce the testing tank. I don't know what I would have done without their assistance and suggestions. Şükrü Şıpka of TRT Ankara Television put his great enthusiasm into the project.

Dr. Kutay Özaydın, always interested and guiding, read a draft copy of my dissertation and made suggestions gratefully evaluated. M. Şükrü Özçoban had answers for every question and gave valuable assistance in the design, construction and utilization of the testing device. He was my right hand. Mehmet M. Berilgen was always there to help and listen to my complaints. He was my left hand. Dr. Mustafa Yıldırım gave me support in my work and made wonderful suggestions.

Burak Kılanç created a computer program to compare the mathematical model and the test results. I am thankful to him. Ahmet Ilgaz took the pictures. Havvanur Kılıç, Semra Yavuz, Ayşe Koçak, İrfan Çoşkun, Zafer Kütüğ, Ahmet Şahin, Erhan Erol, Turan Andiç, Şemsettin Tonkuş, construction materials technician Halil took piezometer readings and helped testing. Erhan Erol also conducted laboratory tests. I truly appreciate all of their effort. The staff of the Boğaziçi University Library assisted enthusiastically with finding related materials.

Dr. Ali Pusane provided constant good humored nudging.

The staff at The Film and Printing Center of Istanbul University gave freely of their time and typing skills in preparing the manuscript. Among these were Tabib Derinbay, Fatma Özbir, Berrin Şarakman, İkbal Karadoğan, Tülay Saka, Tuğrul Erçetin, Necdet Kızılca.

I want to dedicate this thesis to my family and all who care for me and what I do. Bless you all.

CONSTANT HEAD TEST IN PARTIALLY PENETRATING WELLS

ABSTRACT

Field tests provide reliable results to determine permeability. A testing device is built to model the in-situ conditions in the laboratory. The device had a circular plan of 1 · 1 square meter and a height of 1.2 meter. Constant head pumping-in tests were conducted in a model well that was centered in the tank. The pore-water pressures were measured by 12 piezometers that had various locations in the tank. The data obtained were compared with a mathematical model derived by Avcı and Kılanç (1994). The mathematical model considered wells partially penetrating anisotropic, homogeneous and finite-depth confined or unconfined aquifers. The test results and their comparison with the mathematical model were given in graphs. Comments and proposals for further study were given. It was seen that the mathematical model provided a good match with test results for points at a certain distance.

KISMİ DELEN KUYULARDA SABİT SEVİYELİ DENEY ANALİZİ

ÖZET

Permeabiliteyi belirlemek için arazi deneyleri güvenilir sonuçlar vermektedir. Arazi koşullarını laboratuarda modellemek için bir deney aleti yapılmıştır. Alet dairesel 1· 1 metrekare kesitli ve 1.2 metre yüksekliğindedir. Tankın ortasında bulunan bir model kuyuda sabit seviyeli su basma deneyleri yürütülmüştür. Boşluk suyu basınçları tankın içinde çeşitli yerlerdeki 12 piezometre ile ölçülmüştür. Elde edilen veriler Avcı ve Kılanç (1994) tarafından çıkarılmış matematik modelle karşılaştırılmıştır. Matematik model anizotropik, homojen ve sonlu derinlikteki basınçlı ya da serbest akiferleri kısmi delen kuyuları gözönüne almaktadır. Deney sonuçları ve matematik model kıyaslamaları grafikler halinde verilmiştir. Yorumlar ve daha ileri çalışmalar için öneriler sunulmuştur. Sonuç olarak matematik modelin belirli mesafedeki noktalarda deney sonuçlarıyla iyi bir uyum sağladığı görülmüştür.

TABLE OF CONTENTS

	Page
TITLE PAGE	i
PAGE OF APPROVAL	ii
ACKNOWLEDGEMENTS	iii
ABSTRACT	iv
ÖZET	v
LIST OF FIGURES	viii
LIST OF TABLES	x
LIST OF SYMBOLS	xii
1. INTRODUCTION	1
2. PERMEABILITY TESTING METHODS	2
2. I. EMPIRICAL RELATIONSHIPS	4
2. I. A. HAZEN FORMULA	4
2. I. B. KOZENY - CARMAN RELATION	4
2. I. C. SAMARASINGHE, HUANG AND DRNEVICH EQUATION	5
2. I. D. AMER AND AWAD RELATION	5
2. I. E. SHAHABI, DAS AND TARQUIN FORMULA	5
2. I. F. MESRI AND OLSON EQUATION	6
2. II. LABORATORY METHODS	7
2. II. A. CONSTANT HEAD PERMEABILITY TEST	8
2. II. B. FALLING (VARIABLE) HEAD PERMEABILITY TEST	9
2. II. C. DOUBLE - RING PERMEAMETER	10
2. II. D. PERMEABILITY IN AN OEDOMETER CELL	11
2. II. E. HORIZONTAL CAPILLARY TEST	12
2. II. F. TRIAXIAL PERMEABILITY	13
2. II. F. I. CONSTANT HEAD TRIAXIAL TEST	13
2. II. F. II. FALLING HEAD TEST USING ONE BACK PRESSURE SYSTEM	14
2. II. F. III. FALLING HEAD TEST USING TWO BURETTES	14
2. III. IN- SITU PERMEABILITY DETERMINATION	18
2. III. A. METHODS DEPENDING ON PUMPING OR VARYING HYDRAULIC HEAD IN HOLES	20

Page

2. III. A. I. PUMPED WELLS WITH OBSERVATION WELLS 20
2. III. A. II. BOREHOLE METHODS 25
2. III. A. III. POROUS PROBES 28
2. III. A. IV. INFILTROMETERS 30
2. III. A. V. LYSIMETERS 34
2. III. A. VI. PERMEABILITY DETERMINATION USING SHAPE FACTORS 37

2. III. B. METHODS DEPENDING ON THE SEEPAGE VELOCITIES 47
2.III.B.I. USE OF AN ELECTROLYTE AND GALVANOMETERS 47
2.III.B.II. USE OF RADIOACTIVATED CHARGES AND GEIGER COUNTERS 20
2.III.B.III. USING DYES 48

3. THEORETICAL SOLUTION 50

3.I. INTRODUCTION 50
3.II. GOVERNING EQUATIONS 50
3. III. SOLUTION PROCEDURES 53

4. TESTING DEVICE AND METHODOLOGY 59

4.I. TEST SET-UP 59
4.II. THE MATERIAL 66
4.III. THE METHODOLOGY 66

5. RESULTS AND EVALUATION 70

6. CONCLUSIONS 91

APPENDIX A 93

APPENDIX B 103

APPENDIX C 116

REFERENCES 127

REFERENCES NOT CITED 133

LIST OF FIGURES

		Page
Figure 2.1.	Permeability, drainage, soil type and methods to determine the coefficient of permeability	3
Figure 2.2.	Permeability of kaolinite to various fluids	7
Figure 2.3.	Schematical constant head laboratory testing device	8
Figure 2.4.	Falling head laboratory permeability device	9
Figure 2.5.	Schematic of a double-ring infiltrometer	10
Figüre 2.6.	Details of the modified base plate to the double-ring permeameter	10
Figure 2.7.	Schematic of an oedometer or consolidation test apparatus	11
Figure 2.8.	Horizontal capillary permeability test	12
Figure 2.9.	Plot of x^2 against time t in horizontal capillary permeability test	13
Figure 2.10.	Arrangement for triaxial constant head permeability test	14
Figure 2.11.	Test set-up for triaxial falling head permeability test	15
Figure 2.12.	Triaxial falling head permeability test with two burettes	15
Figure 2.13.	Pumping test in wells-gravity well	20
Figure 2.14.	Pumping well test-confined aquifer case	20
Figure 2.15.	The range of validity of Dupuit assumption	22
Figure 2.16.	Correction factor C_x variation with r/R	23
Figure 2.17.	View of oa partially penetrating well	24
Figure 2.18.	Open-end tests for permeability determination	25
Figure 2.19.	C aganist H/r	27
Figure 2.20.	The packer test for soil permeability	28
Figure 2.21.	Hydraulic conductivity from porous probe test	29
Figure 2.22.	Open, single-ring infiltrometer	31
Figure 2.23.	Open, double-ring infiltrometer	31
Figure 2.24.	Sealed, single-ring infiltrometer	32

LIST OF SYMBOLS

A	:	area of cross-section
a	:	cross-section of the standpipe, the distance of the top of the screen from the confining lower boundary
α	:	the sorptive number
α^*	:	soil suction parameter
α_v	:	a parameter
A', B'	:	constants
b	:	the distance of the bottom of the screen from the confining lower boundary
C	:	constants for formulas of different researchers
C_s	:	shape factor coefficient
C_u	:	uniformity coefficient, a dimensionless factor
c_v	:	the consolidation coefficient
C_x	:	correction factor
D	:	depth of penetration, aquifer thickness
d_1, d_2	:	particle sizes
D_{10}	:	the effective particle size
Δh	:	head difference
ΔH	:	displacement
e	:	void ratio
f	:	angularity factor
F	:	shape factor
γ_w	:	unit weight of water
$h(r,z,t)$	:	hydraulic head distribution
h_1	:	initial water head, water level in the observation well
h_2	:	water head at the end, level in the observation well

Q	:	volume of collected water, amount of flow
$Q(t)$	:	inflow rate
R	:	radius of influence, casing radius
r	:	casing radius
r_1, r_2	:	horizontal distance of the observation wells
r_s	:	screen radius
r_w	:	well radius
ρ	:	density, radial distance
S	:	specific surface
s	:	build-up or drawdown, distance of the well from the impermeable layer
S'	:	shape factor coefficient
S_c	:	specific storage coefficient
S_d	:	skin factor
S_y	:	specific yield
t	:	time interval, duration of test
T	:	turtuosity of the flow path
v_s	:	seepage velocity
Ψ_f	:	depth of the wetting front
ψ_f	:	wetting front suction head

1. INTRODUCTION

Permeability of a soil is the ability of that soil to be penetrated or permeated by a flowing substance, such as gas or water. Generally the permeability of soils to different permeans is called hydraulic conductivity. These two terms are used synonymously. Permeability is one of the most important concepts both in geotechnical and in rapidly growing geoenvironmental engineering. It governs such major matters as the ground- water regime in stratified deposits, the flow of water through or around engineered structures like dams or wells, the consolidation settlement of fine grained soils under applied loads and the diffusion of leachate through sanitary landfills and liners.

Due to this importance and to the infinite variety of soils, there has been a lot of research conducted and insight gained from numerous testing and analysis methods. The utilization of the correct analytical tool is crucial because wrong figures may lead to errors that have serious economic consequences and cause irreparable damage.

Testing and analysis methods should take into consideration the field situation that is to be confronted. This can be best achieved by using in-situ tests of the actual permeability according to the desired precision. A literature survey on laboratory and field permeability tests and on accompanying analysis methods was conducted. A comparison of their relative advantages and disadvantages was made. Special emphasis was given to in-situ tests and especially to shape factors since these are the most common and easily interpreted methods for precise permeability determination.

The scope of this study was to present an improved analysis method under conditions like those most frequently seen in the field that would allow practitioners to better measure permeability and evaluate their testing data with a design that is economical as well as safe. Also it was aimed that permeability could be calculated even if the steady-state conditions were not reached. Permeability calculation from the transient-state field data will save a considerable time and will provide economy, especially for low permeability soils that necessitate a long time until the steady-state conditions are satisfied.

The main purpose was to test mathematical calculations formulated by Avcı and Kılanç (1994) of a flow towards a well using assumptions more closely simulating field conditions. A laboratory testing device was constructed to obtain an environment that could be continuously monitored and recorded. The testing program included measurements taken directly from the constructed device as well as from standard laboratory testing.

2. PERMEABILITY TESTING METHODS

Determination of permeability means measuring the mean discharge velocity of flow of water (or other permeans) in a soil under the action of a unit hydraulic gradient; the calculation of the coefficient of permeability is, therefore, expressed in the same units as velocity (length per unit time).

Permeability values ranged widely from $1 \cdot 10^{-10}$ to one hundred cm/s as shown in **Figure 2.1.**

Permeability has an important significance for engineering evaluation, treatment and assessment of soils; this requires that the measurement of permeability be done as precisely as possible. For this purpose, several testing methods have been developed and conducted in the laboratory as well as in the field. Several empirical relationships have also been developed from direct observation and experience. Testing methods model and measure the ability of water to diffuse through the voids in a soil under pressure. These methods can be divided into three main groups:

I) Empirical relationships
II) Laboratory methods
III) Field methods (in-situ tests)

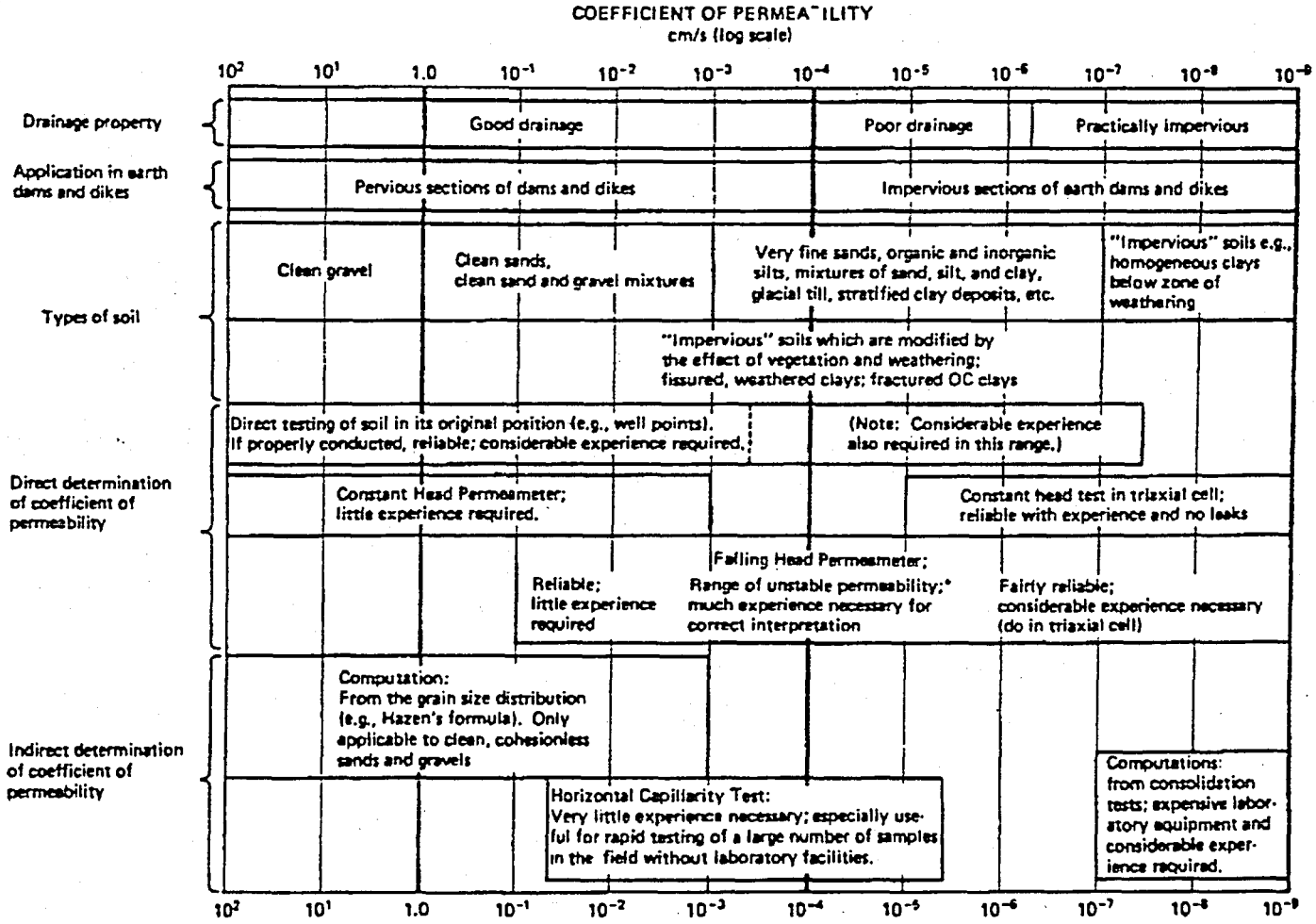

Figure 2. 1 : Permeability, drainage, soil type and methods to determine the coefficient of permeability (Casagrande quoted by Holtz and Kovacs, 1981)

2. I. EMPIRICAL RELATIONSHIPS

Many empirical relations have been developed for the estimation of permeability. Many of these methods depend on the grain size distribution. The particle size and particle shape can be determined by using different sizes of sieves. The empirical formulas also utilize the void ratio in different relations.

2. I. A : Hazen Formula (1911)

$$k = C \cdot (D_{10})^2 \qquad (2.1)$$

where k : the coefficient of permeability in cm/s

D_{10} : the effective particle size, 0.1 mm < D_{10} < 3 mm

C : a constant varying from 0.4 to 1.2. Studies also state that C depends on the uniformity coefficient C_u (Beyer quoted by Hausmann, 1990).

The general formula is valid for clean sands (with less than 5 per cent passing the No. 200 sieve) and for $k \geq 10^{-3}$ cm/s.

Table 2. 1 : C_u - C Variation (Beyer quoted by Hausmann, 1990)

$C_u = D_{60} / D_{10}$	1 - 1.9	2 - 2.9	3 - 4.9	5 - 9.9	10 - 19.9	> 20
C	1.1	1	0.9	0.8	0.7	0.6

2. I. B : Kozeny - Carman Relation (1956)

$$k = \frac{2}{f \cdot S^2} \cdot \left[\frac{e^3}{1+e} \right] = \frac{1}{K_0 \cdot T^2 \cdot S_0^2} \cdot \frac{\rho}{\mu} \cdot \frac{n^3}{(1-n)^2} \qquad (2.2)$$

in which f : angularity factor - 1.1 for rounded grains
- 1.4 for angular grains

S : specific surface (mm^2 / mm^3) of the soil grains; for spherical particles uniformly graded between d_1 (mm) and d_2 (mm) the specific surface is:

$$S = \frac{6}{\sqrt{d_1 \cdot d_2}} \qquad (2.3)$$

K_0 : pore shape factor

T : tortuosity of the flow path

ρ : density of the permeating fluid

μ : viscosity of the permeating fluid

e : void ratio of the soil mass

n : soil porosity.

Taylor (1948) showed that this equation is valid only for sands.

2. I. C : Samarasinghe, Huang and Drnevich Equation (1982)

$$k = C \cdot \frac{e^n}{1+e} \qquad (2.4)$$

where C : a constant depending on the soil characteristics

n : a constant typically of order 4 - 5.

e : void ratio.

C and n are determined experimentally.The formula is valid for normally consolidated clays.

2. I. D : Amer and Awad Relation (1974)

$$k = C \cdot D_{10}^{2.32} \cdot C_u^{0.6} \cdot \frac{e^3}{1+e} \qquad (2.5)$$

here C : a constant

D_{10} : the particle diameter where 10 per cent is finer by weight, effective particle size

C_u : the coefficient of uniformity

e : void ratio.

The relationship is given for sands.

2. I. E : Shahabi, Das and Tarquin Formula (1984)

$$k = 1.2 \cdot C^{0.735} \cdot D_{10}^{0.89} \cdot \frac{e^3}{1+e} \qquad (2.6)$$

where C : a constant

D_{10} : the effective particle size

e : void ratio.

The formula is valid for medium to fine sands.

2. I. F : Mesri and Olson Equation (1971)

$$\log k = A' \log e - B' \qquad (2.7)$$

which A', B' : constants

e : void ratio.

The equation is proposed for clays.

A study comparing the equations presented in 2.I.B, 2.I.C and 2.I.F (Tavenas et. al. 1983) states that any of these equations may be valid for certain clays or certain ranges of void ratio variations, but not for all clays. They also conclude that the in-situ permeability of intact soft clays at their in-situ void ratio is a function not only of void ratio and grain size but also of the plasticity and the fabric of the clay.

2. II. LABORATORY METHODS

Laboratory methods are widely conducted to estimate the coefficient of permeability. The laboratory provides an environment that can be fully controlled, monitored and recorded. On the other hand, there are many problems associated with obtaining field representative samples. This is due to the fact that the field is stratified and differs in characteristics for every layer. The samples that are taken from the field - no matter how much care is given- will be disturbed to some degree. However, for many projects laboratory tests give valuable data on the behavior of the particular site.

The permean being used should be one that will be encountered in the field because the type of permean will affect the coefficient of permeability. For example, the clays for liners should be tested with fluid wastes or gas tank liners should be tested with gasoline; a particular soil may be very impervious to water but can be very pervious to leachate. Results of kaolinite tests with different permeans are given in **Figure 2. 2.** Here the kaolinite was molded in the fluid which was used as the permeant. The variation is quite large reaching to many hundred per cent in absolute permeability K expressed in cm^2.

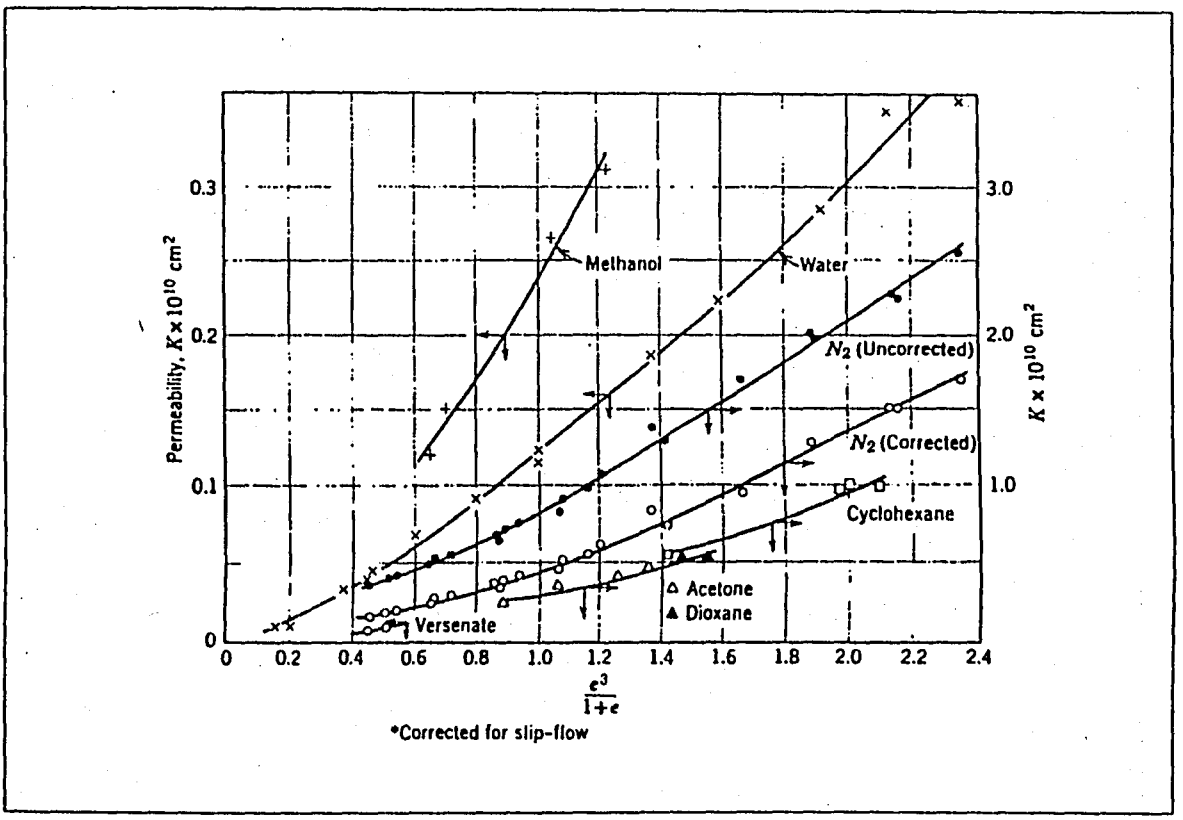

Figure 2. 2 : Permeability of kaolinite to various fluids (Michaels and Lin quoted by Lambe and Whitman, 1979)

2. II. A : Constant Head Permeability Test

This method is mainly used for coarse grained soils. The water head that is applied to the specimen during the test is kept constant. The amount of water that passes through the soil at a certain time difference is collected in a graduated cylinder. A schematical constant head device is given in **Figure 2. 3.** The permeability coefficient is calculated using the formula depending on Darcy's Law ($v = k \cdot i$; where v is the velocity and i is the hydraulic gradient applied):

$$k = \frac{Q \cdot L}{\Delta h \cdot A \cdot \Delta t} \qquad (2.8)$$

here
- Q : volume of water collected
- A : area of cross-section of the soil specimen
- L : length of the specimen
- Δh : the constant water head difference applied to the specimen
- t : duration of collection of water.

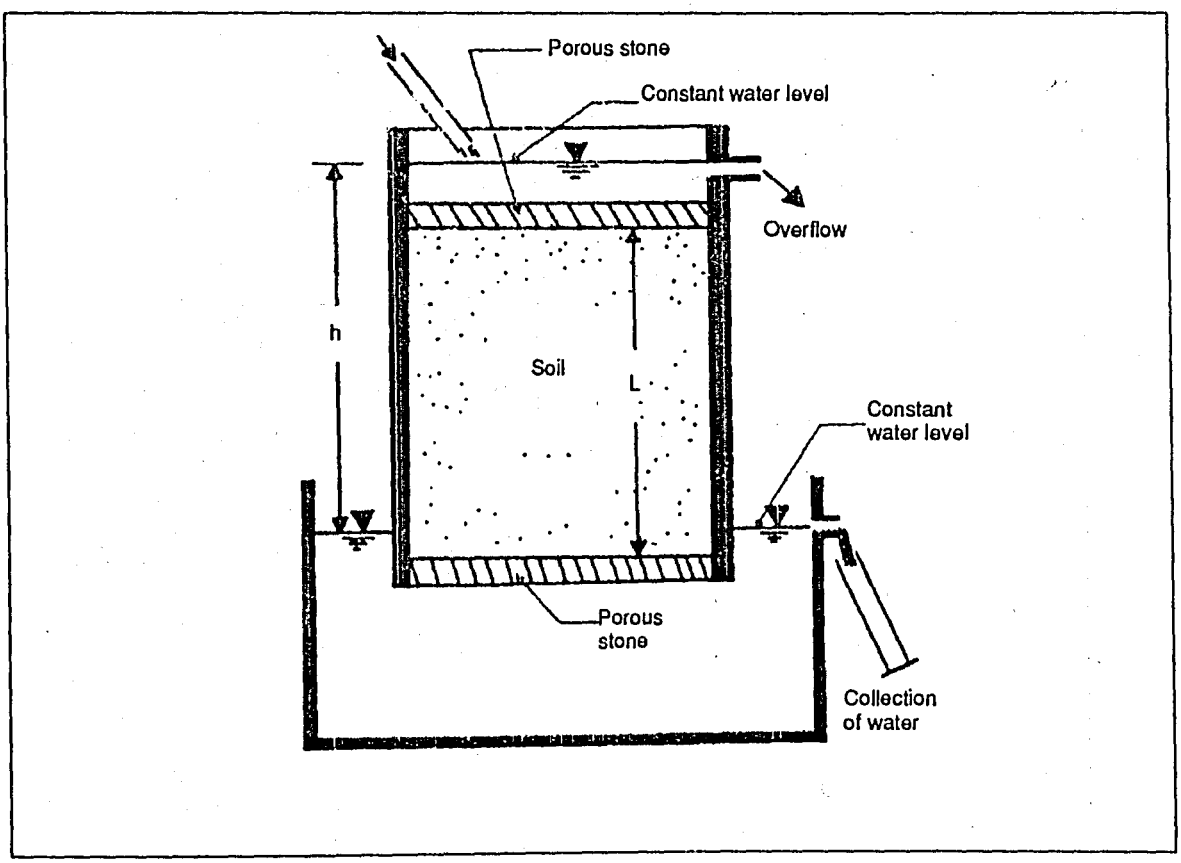

Figure 2. 3 : Schematical constant head laboratory permeability testing device.

2. II. B : Falling (Variable) Head Permeability Test

A falling head set-up is shown in **Figure 2. 4.** This test is conducted primarily for saturated fine grained soils. The water head on the test specimen varies (decreases) with time. The change in water heads is recorded and the permeability is obtained using the principle of the conservation of masses:

$$k = \frac{L \cdot a}{(t_2 - t_1) \cdot A} \cdot \ln\left(\frac{h_1}{h_2}\right) \qquad (2.9)$$

where
- L : length of the test specimen
- a : cross-sectional area of the standpipe
- A : cross-sectional area of the soil specimen
- t : duration of the test
- h_1 : water head applied in the beginning of the test
- h_2 : water head applied at the end of the test.

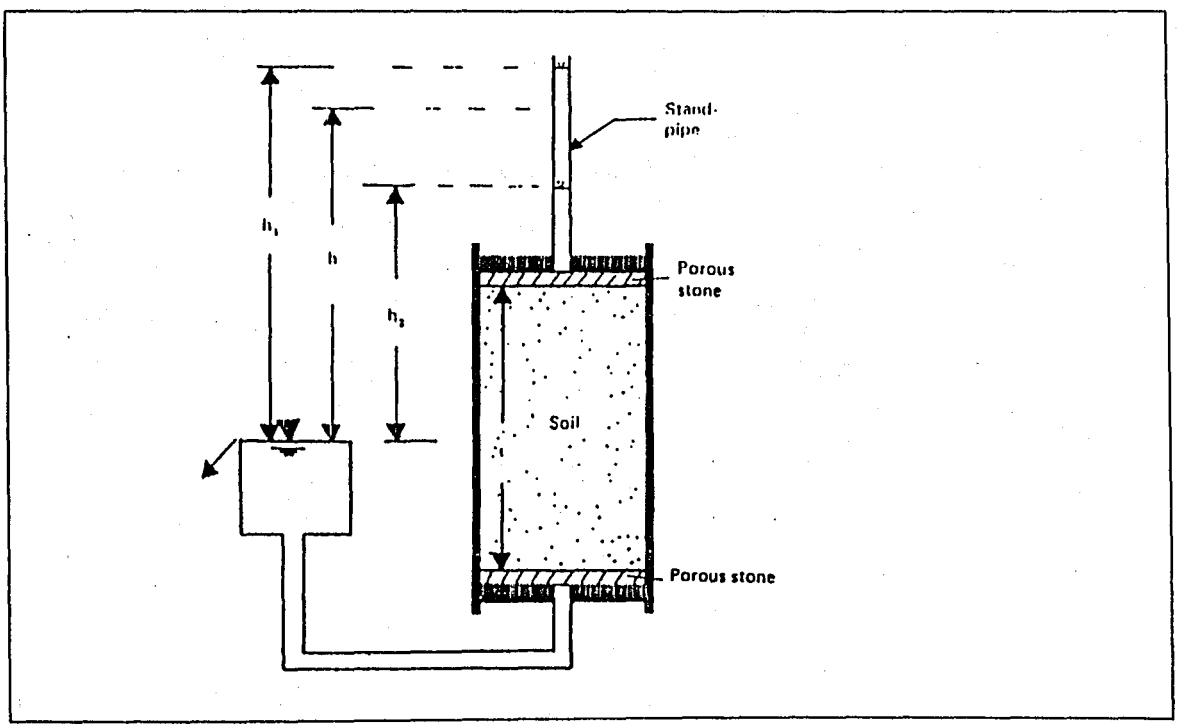

Figure 2. 4: Falling head laboratory permeability test

2. II.C : Double - Ring Permeameter (Anderson et al, 1985)

This type of permeameter is similar to a fixed-wall permeameter, except for the specially modified base plate that separates flow near the permeameter sidewalls from flow through the central portion of the soil core. Details of this permeameter are shown in **Figures 2. 5 and 2. 6.** The calculations are the same as 2. II. A or 2. II. B depending on the type of test conducted.

Double-ring permeameters appear to have the potential to overcome the problems of sidewall flow and confining pressure.

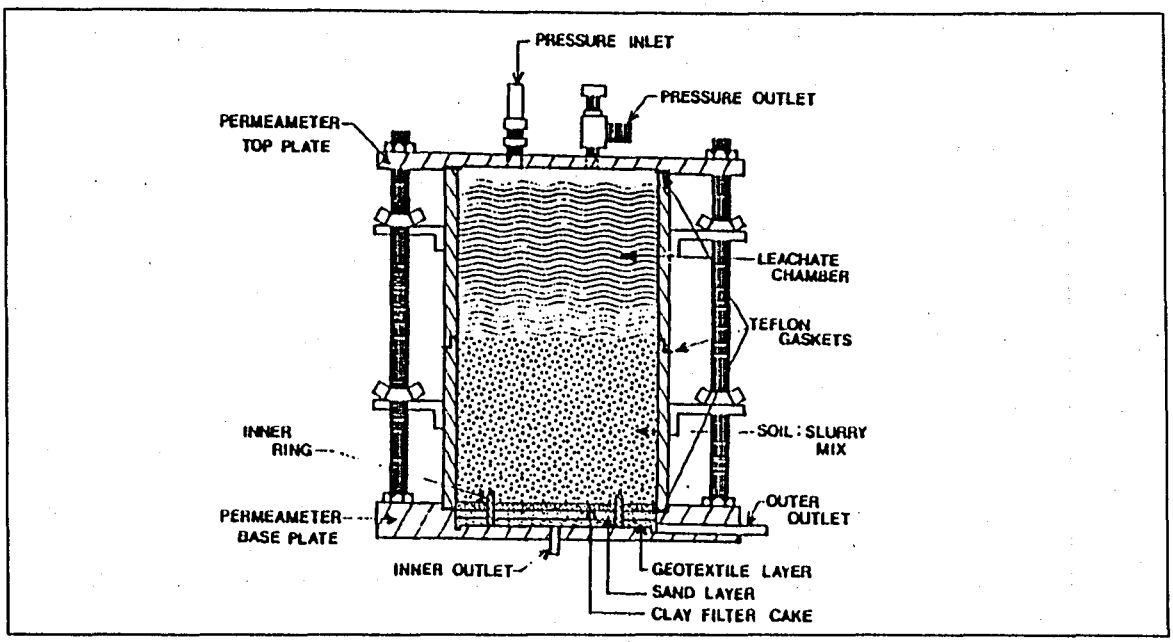

Figure 2. 5: Schematic of a double-ring permeameter (Anderson, et al., 1985)

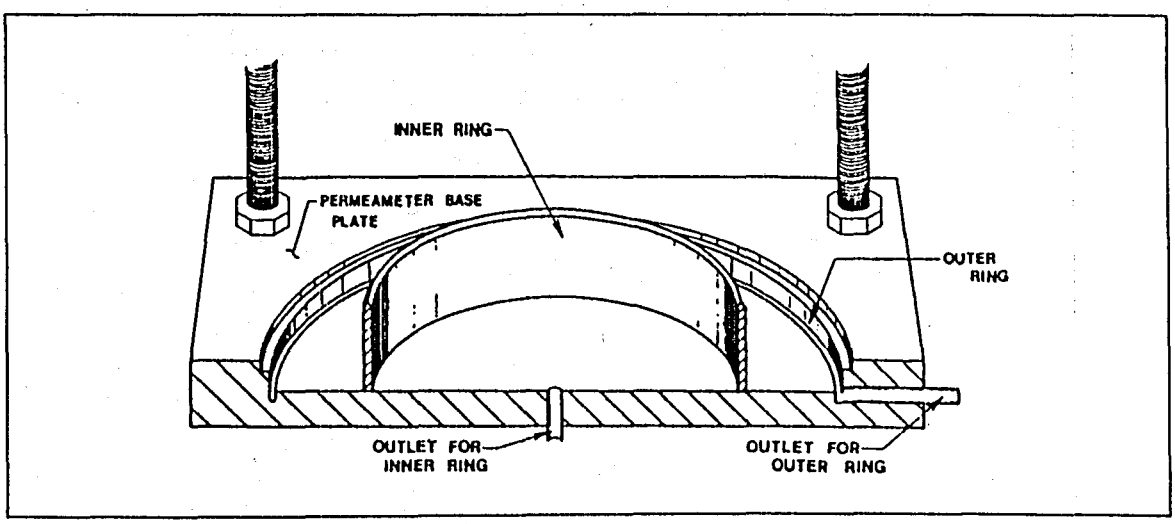

Figure 2. 6: Details of the modified base plate to the double-ring permeameter (Anderson, et al., 1985)

2. II.D : Permeability in an Oedometer Cell

The coefficient of consolidation (c_v) and the coefficient of volume compressibility (m_v) can be obtained from the displacement - logarithm of time (ΔH - log t) curves of Casagrande or from the displacement - square root of time (ΔH - $t^{1/2}$) curves of Taylor or from the computational method of Sivaram and Swamee (1977). The schematical testing oedometer device is shown in **Figure 2.7.**

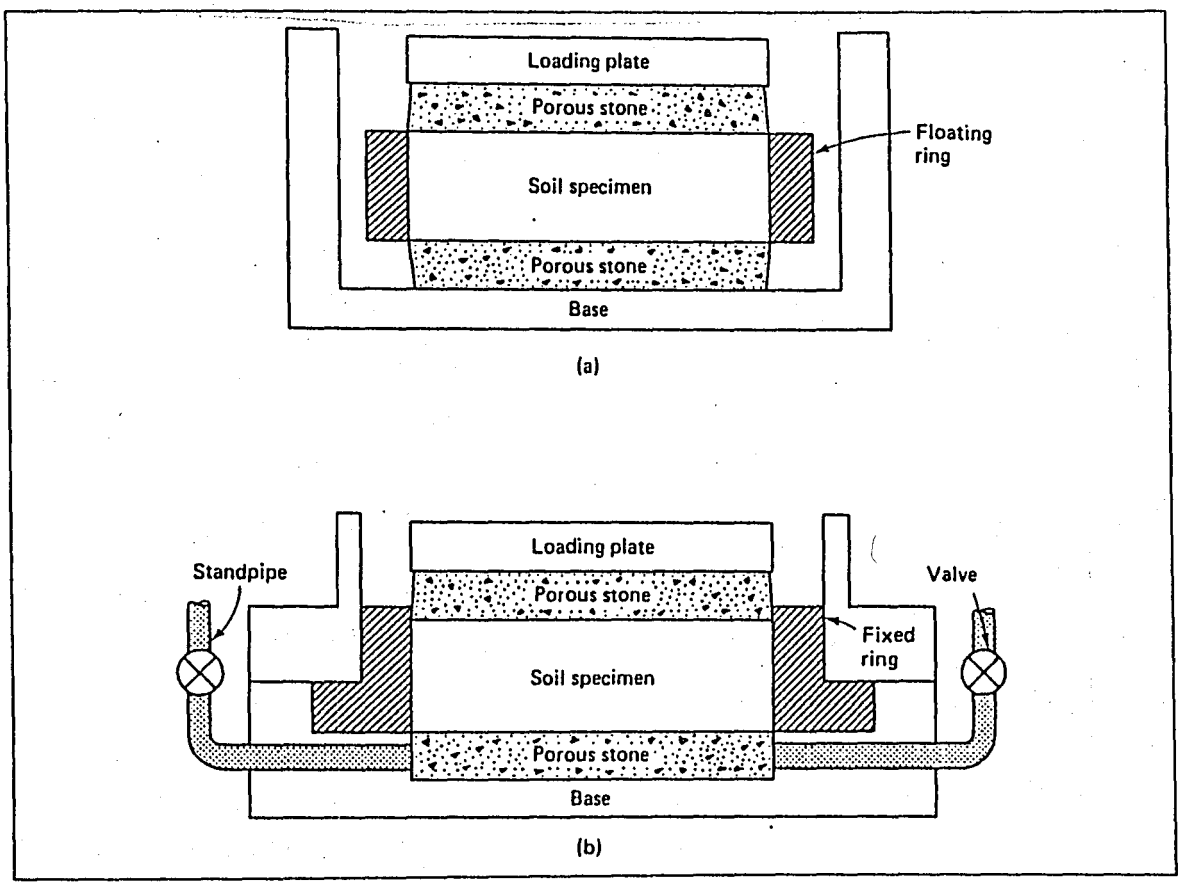

Figure 2. 7: Schematic of an oedometer or consolidation test apparatus: (a) floating-ring oedometer; (b) fixed-ring oedometer

The permeability is then given as:

$$k = c_v \cdot m_v \cdot \gamma_w \qquad (2.10)$$

Here γ_w is the unit weight of water.

It should be noted that the permeability obtained directly from the compression data is not very precise because there are several factors in addition to permeability that enter into the rate of consolidation - permeability relationship.

2. II. E : Horizontal Capillary Test

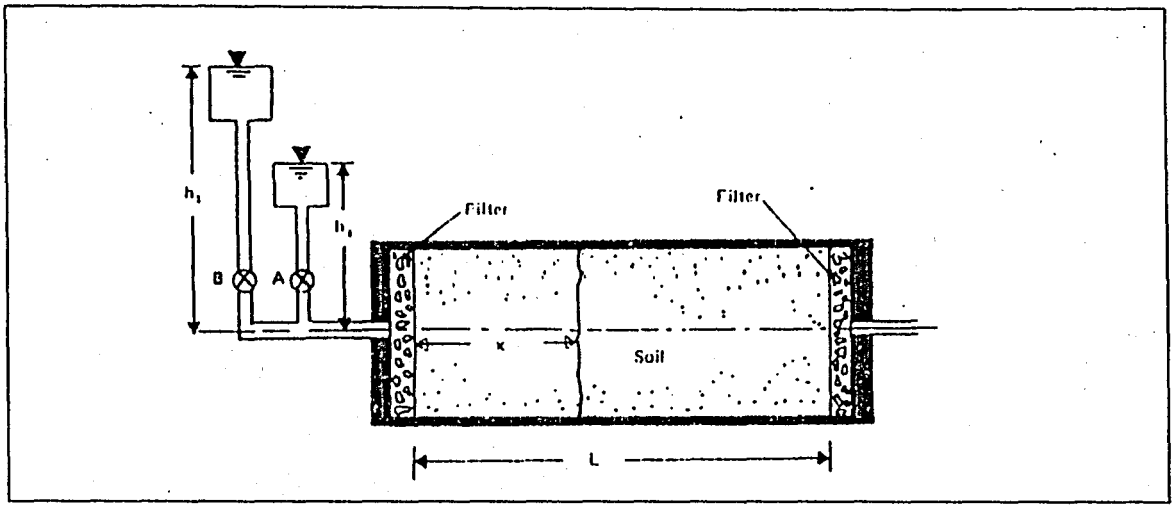

Figure 2. 8 : Horizontal capillary permeability test

The test setup is shown in **Figure 2. 8.** The soil is initially dry inside the horizontal tube. Water penetrates slowly when valves A and B are opened in a sequential order. From the square of the distance of the penetrated water (x^2) to time a graph similar to **Figure 2. 9** is derived. The slopes m_1 and m_2 are then calculated as follows:

$$m_1 = \frac{2k}{n \cdot S_r}(h_1 + h_c) \qquad (2.11)$$

$$m_2 = \frac{2k}{n \cdot S_r}(h_2 + h_c) \qquad (2.12)$$

where n : porosity

S_r : degree of saturation

h_1,h_2 :constant water levels

m_1,m_2: slopes of curves obtained from the readings plotted x^2 against time

h_c : water head in the soil.

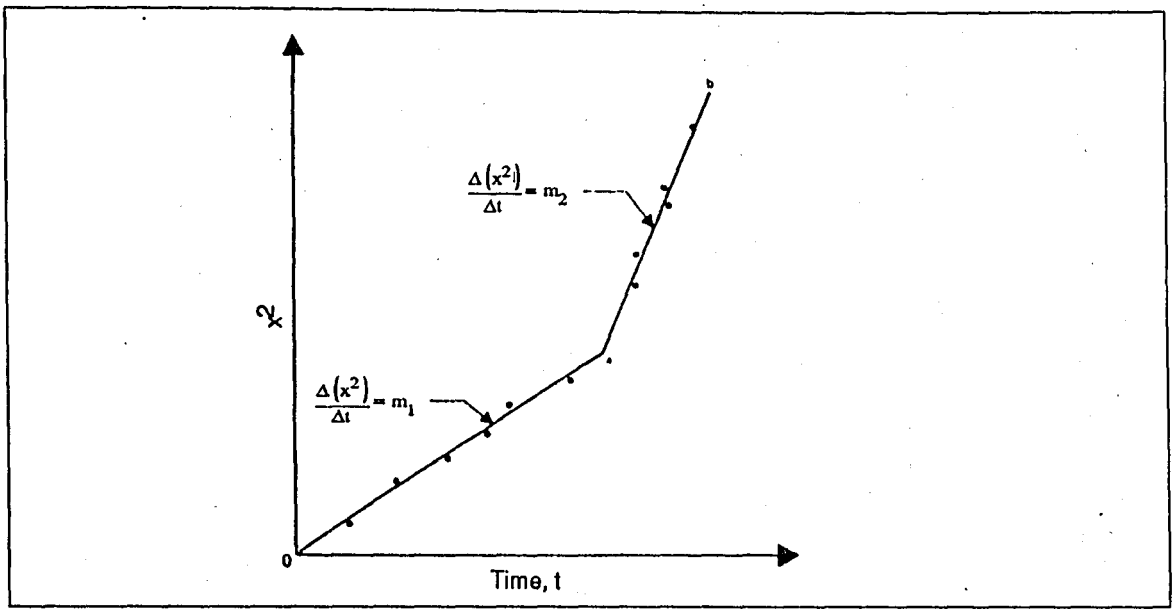

Figure 2. 9 : Plot of x^2 against time t in horizontal capillary permeability test

The permeability coefficient k and the water head h_c can be solved from these two slopes.

2. II. F : Triaxial Permeability

The triaxial cell is a preferable method over other permeameters for soils that have very low permeabilities. The specimen can be saturated and applied stresses and water pressures can be closely controlled. There are three types of triaxial permeability tests conducted on the triaxial cell.

2. II. F. I : Constant Head Triaxial Test. The pressure applied to the specimen is constant over the duration of the test. There are two back pressure systems utilized during the test. The back pressure is used to saturate the tested specimens and to apply the constant pressure as shown in **Figure 2. 10.** The permeability coefficient can be calculated as:

$$k = \frac{Q \cdot L \cdot \gamma_w}{(p_1 - p_2) \cdot A \cdot t} \qquad (2.13)$$

in which p_1, p_2 : the back pressures applied to the specimen at inlet and outlet, respectively.

A : area of the cross-section of the soil specimen

L : length of the testing specimen

Q : the amount of flow

γ_w : the unit weight of water

t : time.

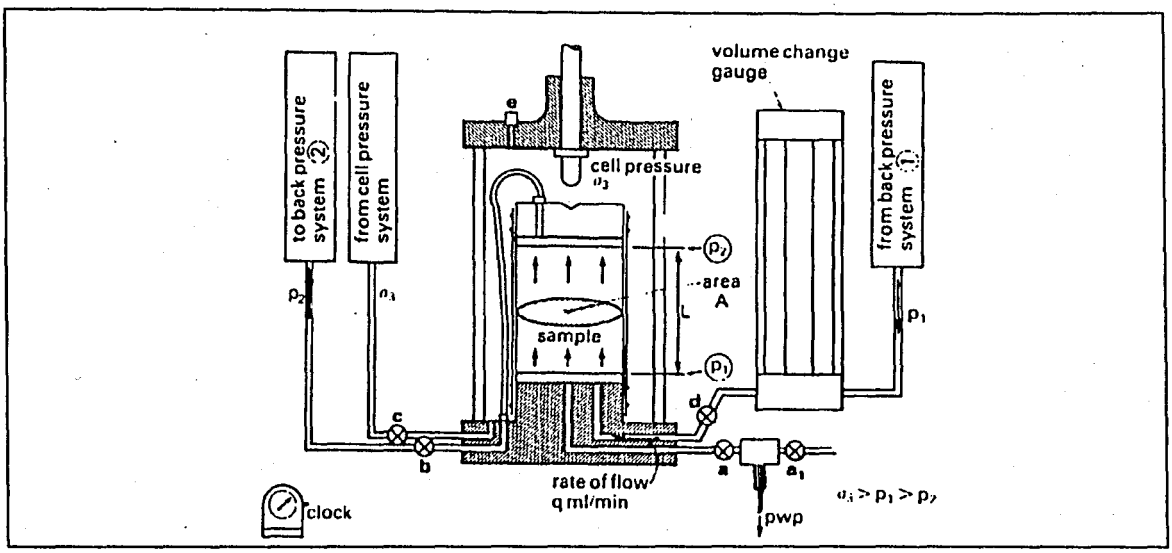

Figure 2. 10 : Arrangement for triaxial constant head permeability test (from Head, 1989)

2. II. F. II : Falling Head Test Using One Back Pressure System. The system is shown in **Figure 2. 11.** The principle is the same as the falling head permeameter. The coefficient of permeability is:

$$k = \frac{a \cdot L}{A \cdot t} \cdot \ln\left(\frac{\frac{p_1}{\gamma_w} - h_0}{\frac{p_2}{\gamma_w} - h_f}\right) \qquad (2.14)$$

here a : the cross-section area of the burette.

L : length of the testing specimen

A : cross-sectional area of the soil specimen

h_0 : height of water level in burette above outlet end of sample initially

h_f: corresponding height after t time

γ_w: unit weight of water

t: time interval.

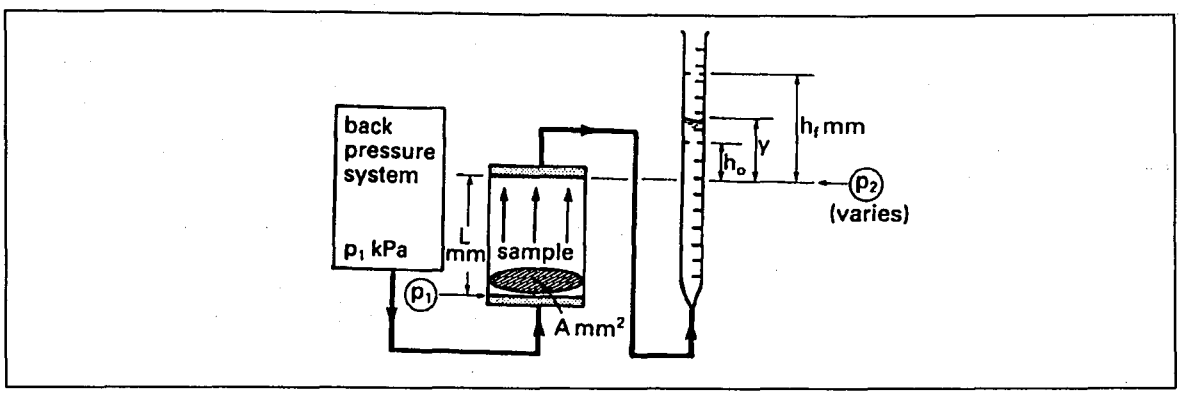

Figure 2. 11 : Test set-up for triaxial falling head permeability test (from Head, 1989)

2. II. F. III : Falling Head Test Using Two Burettes. The schematical testing device is given in **Figure 2. 12.** From known values:

$$k = \frac{Q \cdot L}{(h_0 - h_f) \cdot A \cdot t} \cdot \ln\left(\frac{h_0}{h_f}\right) \qquad (2.15)$$

where Q: volume of water flowing through the sample, measured in either burette, over time t minutes

L: length of the testing specinen

A: area of the cross-section of the soil specimen

h_0: the difference between water levels in the two burettes initially

h_f: the corresponding difference after t time

t: time interval.

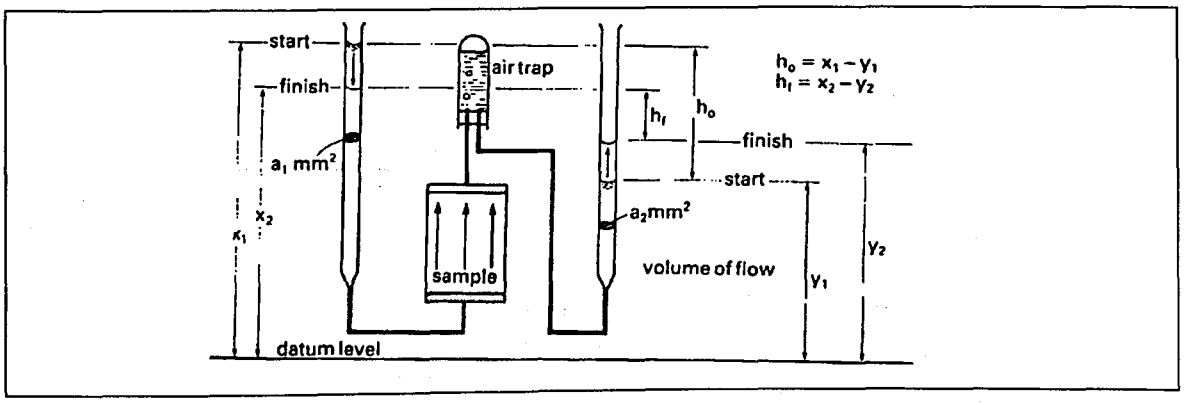

Figure 2. 12 : Triaxial falling head permeability test with two burettes (from Head, 1989)

A study comparing the variable head tests conducted in laboratory compaction mould falling head device, consolidation cell and triaxial cell (Boynton and Daniel, 1984, Daniel et.al., 1985) showed that the effects of different permeameters are not very significant for tests performed on clay specimens permeated with water. The permeability value increases for compaction-mold permeameter when the permean is organic fluids. The differences of various test parameters depending on the type of permeameter are given in **Table 2.2.**

Table 2.2. Differences in various test parameters depending on type of permeameter. (Boynton and Daniel, 1985)

	Type of Permeameter		
Test Parameter	**Compaction Mold**	**Consolidation Cell**	**Flexible Wall**
Side-wall leakage	Leakage is possible.	Applied vertical stress makes leakage unlikely.	Leakage is unlikely.
Void ratio, *e*	Relatively high e because applied vertical stress is zero.	Relatively low *e* because a vertical stress is applied.	Relatively low *e* because an all-round confining pressure is applied.
Degree of saturation	Specimen may be unsaturated.	Specimen may be unsaturated.	Application of backpressure is likely to cause essentially full saturation.
Voids formed during trimming	Impossible; soil is tested in the compaction mold and is not trimmed.	Voids may have formed, but application of a vertical stress should help in closing any voids.	Voids are not relevant; the flexible membrane tracks the irregular surface of the soil specimen.
Portion of sample tested	All of the compacted specimen is tested, including the relatively dense lower portion and the relatively loose upper portion; the dense lower portion may lead to measurement of relatively low *k*.	Only the central portion of the specimen is tested; the upper and lower third of the specimen are trimmed away.	1 cm of soil is trimmed off both ends of the compacted sample.

The relative advantages and disadvantages of various types of permeameters in general can be stated as (Daniel et al., 1985):

- with rigid-wall permeameters, the major advantages are low cost, simplicity, applicability to testing compacted soils, compatibility with a wide range of permeant liquids and lack of a need to apply high confining pressure. The major disadvantages are incomplete control over stresses, inability to measure deformations in most fixed-wall cells, difficulty in trimming soil samples into the containing ring and potential for sidewall leakage.

- flexible-wall permeameters have the advantages of minimizing sidewall leakage, permitting control over vertical and horizontal stresses, enabling one to measure vertical and volumetric deformations, permitting convenient back pressuring of the soil, enabling one to verify saturation and providing the possibility of testing specimens with a range of diameters in the same cell. The disadvantages are higher cost, compatibility problems between the flexible membrane and some permeant liquids.

2. III. IN-SITU PERMEABILITY DETERMINATION

The testing of the coefficient of permeability is easy to conduct and to interpret using laboratory methods. However, these tests often lack the ability to represent the in-situ behavior of soils. This is because it is very difficult to obtain undisturbed samples from the field. Also the samples taken (by either digging or boreholes) are a small portion of the total area that is being investigated. Daniel (1984) gave data from four applied projects of leachete liners. The permeabilities obtained from the actual back-calculated field values exceeded laboratory testing values from 10 to over 100 times. Daniel and Day (1985) and Fernuik and Haug (1990) also conducted tests on prototype liners and compared the data with the laboratory results. Daniel and Day (1985) calculated similar ratios to Daniel (1984).

In-situ permeability tests will provide permeability values that are more representative of actual field conditions. A comparison of field and laboratory test permeabilities is given in **Table 2.3.**

The in-situ permeability tests can be divided into two main sections:

A. Methods Depending on Pumping or Varying Hydraulic Head in Holes
   I. Pumped Wells With Observation Holes
   II. Borehole Methods
   III. Porous Probes
   IV. Infiltrometers
   V. Lysimeters
   VI. Permeability Determination Using Shape Factors

B. Methods Depending on Seepage Velocities
   I. Use of an Electrolyte and Galvanometers
   II. Use of Radioactivated Charges and Geiger Counters
   III. Using Dyes

Table 2. 3: Comparison of laboratory and field hydraulic conductivities (from Olson and Daniel, 1981)

Reference	Site	Soil	Laboratory Test*	Field Test*	k cm/s		Feld k
					Laboratory	Field	Laboratory k
Skempton and Henkel	Bradwell	clay	M	piezometer	4.5×10^{-9}	3.7×10^{-9}	0.8
			KT	rising head	1.2×10^{-9}	3.7×10^{-9}	3.1
Golder and Gass	Netherlands	sandy clay		suction bellows	3.2×10^{-7}	1.2×10^{-7}	0.4
Weber	Pismo	silty clay	KT	P	6.9×10^{-9}	3.4×10^{-5}	4900
		silty clay			2.0×10^{-8}	2.7×10^{-7}	14
		silty clay			1.1×10^{-8}	7.7×10^{-9}	0.7
	Lafayette	silty clay			5.5×10^{-8}	2.5×10^{-7}	4.6
					4.0×10^{-7}	1.7×10^{-5}	43
	Atascadero	sandy silty clay			3.9×10^{-8}	1.8×10^{-3}	46000
		sandy silty clay			8.5×10^{-5}	8.5×10^{-5}	1
	La Trianon	silty clay			2.8×10^{-7}	4.2×10^{-6}	15
		silty clay			1.6×10^{-7}	2.0×10^{-4}	1200
		silty clay			1.2×10^{-7}	6.1×10^{-6}	51
	Napa River	bay mud			3.3×10^{-7}	7.1×10^{-7}	2.2
					2.9×10^{-7}	9.6×10^{-7}	3.3
					2.1×10^{-7}	9.1×10^{-7}	4.3
					3.4×10^{-7}	4.2×10^{-7}	1.2
					1.4×10^{-7}	4.1×10^{-7}	2.9
					1.9×10^{-7}	6.2×10^{-7}	3.3
					1.9×10^{-7}	4.3×10^{-7}	2.3
					4.2×10^{-7}	3.9×10^{-7}	0.9
Wilkinson	Frodsham	organic silty clay			1.2×10^{-7}	3.3×10^{-7}	2.8
					1.8×10^{-7}	5.0×10^{-7}	2.8
					8.0×10^{-7}	5.0×10^{-7}	6.2
					2.7×10^{-8}	5.0×10^{-7}	19
Al-Dhahir Kennard and Morgenstern	Fiddler's Ferry	silty clay	KT	P.C	1.1×10^{-8}	1.2×10^{-7}	11
Raymond and Azzouz	Lyndhurst	peat	M	constant head.	5.0×10^{-5}	3.0×10^{-4}	6.0
		marl		flow into cell	3.3×10^{-6}	2.1×10^{-4}	64
		algae			5.0×10^{-7}	1.9×10^{-4}	38
		AEC (?)			5.7×10^{-7}	1.4×10^{-6}	2.5
		clay			4.2×10^{-7}	5.2×10^{-6}	1.2
					3.7×10^{-7}	1.7×10^{-7}	0.5
					3.0×10^{-7}	8.7×10^{-8}	0.3
					1.0×10^{-7}	1.1×10^{-7}	1.1
Bishop and Al-Dhahir	Balderhead	clay fill	M		1.0×10^{-8}	1.0×10^{-8}	1.0
	M6	clay fill	M		3.4×10^{-8}	5.0×10^{-8}	1.5
	Fiddler's Ferry	alluvium	KT		1.0×10^{-8}	8.0×10^{-8}	8.0
	Selset	cure clay	M	P.C.I	7.7×10^{-8}	7.9×10^{-8}	1.0
	Selset	foundation clay	KT		3.8×10^{-9}	8.4×10^{-9}	2.3
	Diddington	core	KT		1.2×10^{-8}	3.3×10^{-9}	2.8
		foundation clay	KT		4.0×10^{-9}	1.8×10^{-9}	0.4
Casagrande and Poulos	New Jersey Turnpike	varved clay	M.H		2×10^{-6}		
			M.V		2×10^{-7}		
				P. jetted		2×10^{-6}	1.0
				P. driven		2×10^{-7}	0.1
				WP. jetted		6×10^{-6}	3.0
				WP. driven		2×10^{-6}	1.0
				SD. jetted		4×10^{-5}	20
				SD. driven		4×10^{-6}	2
James	Malaya	silty clay	KT	P.V	1.0×10^{-7}	1.0×10^{-5}	100
Murray	Avonmouth	brown clay	KT	P	3.0×10^{-7}	2.0×10^{-6}	6.1
		blue clay	KT	P	1.7×10^{-6}	1.5×10^{-5}	8.6
		peat	KT	P	2.0×10^{-7}	2.0×10^{-6}	10
		silty clay	KT	P	3.4×10^{-7}	1.6×10^{-5}	47
Ritchie, Kissel and Burnett	Houston	clay	M	10 x 10 m	5.7×10^{-6}	3.1×10^{-5}	5.4
					3.5×10^{-6}	3.1×10^{-5}	8.9
					8.1×10^{-7}	3.1×10^{-5}	38
					4.0×10^{-6}	3.1×10^{-5}	7.8
Jezquel and Mieussens	Bordeaux	clay	KT	constant head	3.0×10^{-7}	2.6×10^{-7}	0.9
				flow into soil	8.0×10^{-8}	2.6×10^{-7}	3.2
					5.0×10^{-8}	2.5×10^{-7}	5.0
					8.0×10^{-8}	4.0×10^{-7}	5.0
					1.7×10^{-8}	2.0×10^{-7}	11.8
					5.0×10^{-8}	2.0×10^{-7}	4.0
Goodall and Quigley	Samia, Ontario	silty clay	KT	P.V	1.5×10^{-8}	1.2×10^{-8}	0.8
			M. KT	P.V	1.6×10^{-8}	1.2×10^{-8}	0.8
			M	P.V	2.1×10^{-8}	1.6×10^{-8}	0.7
				P.V	2.6×10^{-8}	4.6×10^{-8}	1.8
Mieussens and Ducasse	France	clay	KT	P	3.0×10^{-7}	2.6×10^{-7}	0.9
					8.0×10^{-8}	2.6×10^{-7}	3.3
					5.0×10^{-8}	2.5×10^{-7}	5.0
					8.0×10^{-8}	4.0×10^{-7}	5.0
					1.7×10^{-8}	2.0×10^{-7}	12.0
					5.0×10^{-8}	2.0×10^{-7}	4.0

(*) Key to symbols used: KT–back-calculate k using Terzaghi's theory; M–measure k directly; H–horizontal; V–vertical; P – piezometer method; A–auger method; I–inflow (water into soil); O–outflow (water out of soil); C–constant head; V–variable head; WP–well points; SD–sand drains.

2. III. A. Methods Depending on Pumping or Varying Hydraulic Head in Holes

2. III. A. I. Pumped Wells with Observation Wells. Water is either extracted from the well or injected into it from a certain distance; observation wells (minimum 2) are located as in **Figures 2. 13** and **2. 14**. The pumping can be continued until the steady state is reached or the test can be performed at a non-steady state. The analysis of the resulst for each of these two methods is different. The duration of pumping for the steady state can be very long depending on the permeability of the soil. Solutions for the non-steady state obtained from differential equations can be used.

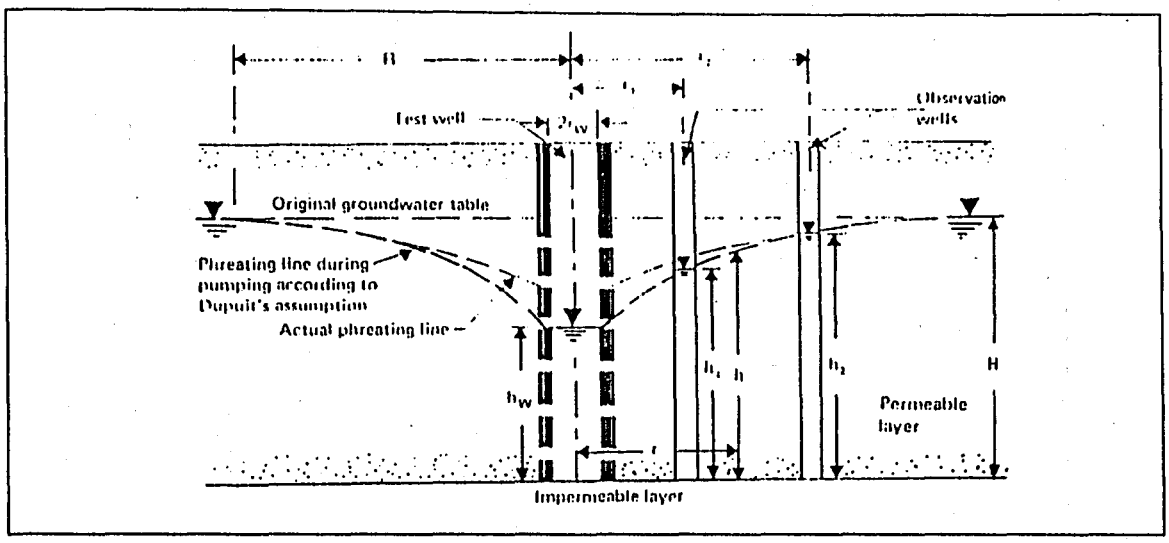

Figure 2. 13 : Pumping test in wells - gravity well

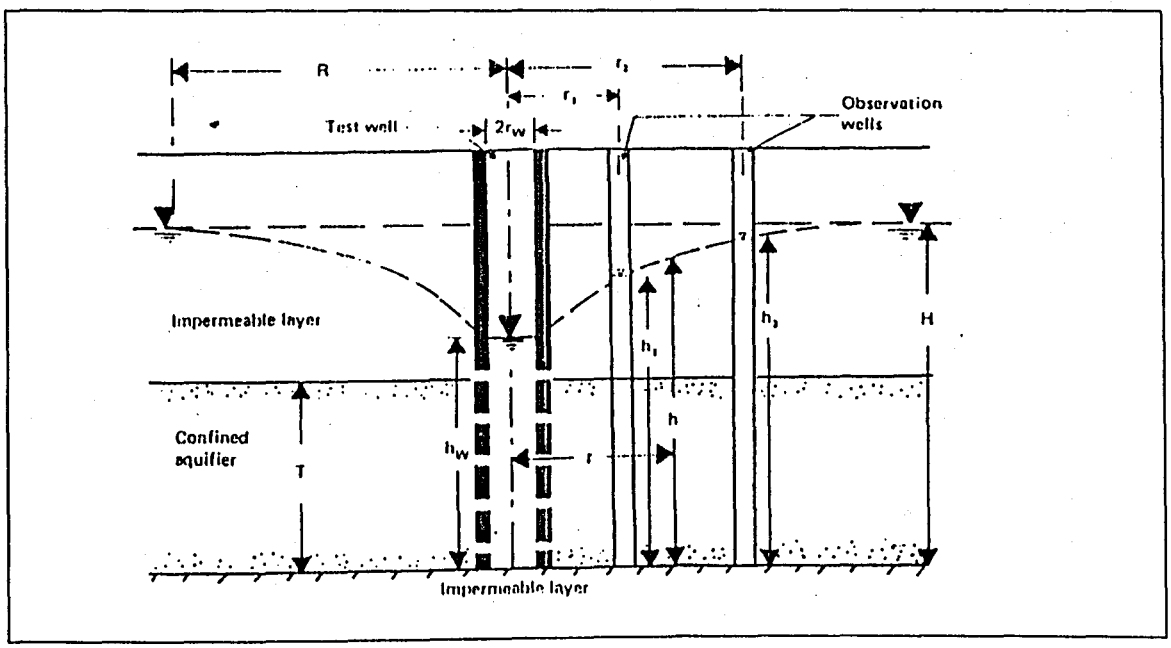

Figure 2. 14 : Pumping well test - confined aquifer case

There are four assumptions underlying the formulas used for analysis in both of the cases:

- the pumping well penetrates the full thickness of the water-bearing formation
- a steady-state flow condition exists
- the water-bearing formation is homogenous, isotropic and extends an infinite distance in all directions
- the Dupuit assumption is valid.

For steady case, the analytical formula for confined aquifers is given by Thiem in 1906 as:

$$k = \frac{q}{\pi\left(h_2^{\,2} - h_1^{\,2}\right)} \ln\left(\frac{r_2}{r_1}\right) = \frac{q}{\pi\left(H^2 - h_w^{\,2}\right)} \ln\left(\frac{R}{r_w}\right) \qquad (2.16)$$

where
- q : the quantity of water flowing toward or from a well in a unit time interval
- H : height of the water bearing strata (pervious formation)
- h_w : water height in the well
- R : radius of influence, the effect of pumping ceases at this distance
- r_w : radius of the well
- r_1, r_2 : horizontal distance of the observation wells from the test well
- h_1, h_2 : water levels in the observation wells.

According to Kozeny (1933), the maximum radius of influence R is:

$$R = \sqrt{\frac{12\,t}{n}\sqrt{\frac{q \cdot k}{\pi}}} \qquad (2.17)$$

here
- n : porosity
- R : radius of influence
- t : time during which discharge or recharge of water from well has been established.

The Dupuit assumption in the general vicinity of the well is not satisfactory. This is due to neglect of the seepage surface (**Figure 2.15**). Babbitt and Caldwell (1948, quoted by Harr) state that the shape of the free surface closely approximates the Dupuit curve at

distances greater than h_2 from the well. If an observation well is located at a radial distance ρ, where $\rho > h_2$, the height of the free surface above the impervious boundary h at any $r > h_2$ can be determined from:

$$h^2 = \frac{h_2^2 - h_1^2}{\ln(R/r_w)} \cdot \ln\frac{r}{\rho} + h_w^2 \qquad (2.18)$$

where h_w is the elevation of the free surface at the observation well (above the impervious boundary). For $r < h_2$, Babbitt and Caldwell recommend that the height h be obtained from the empirical relationship:

$$h = h_2 - \frac{C_x}{h_2} \cdot \frac{h_2^2 - h_1^2}{\ln(R/r_w)} \cdot \ln\frac{R}{0.1h_2} \qquad (2.19)$$

where C_x is a correction factor that is dependent on the ratio of r / R (**Figure 2.16**).

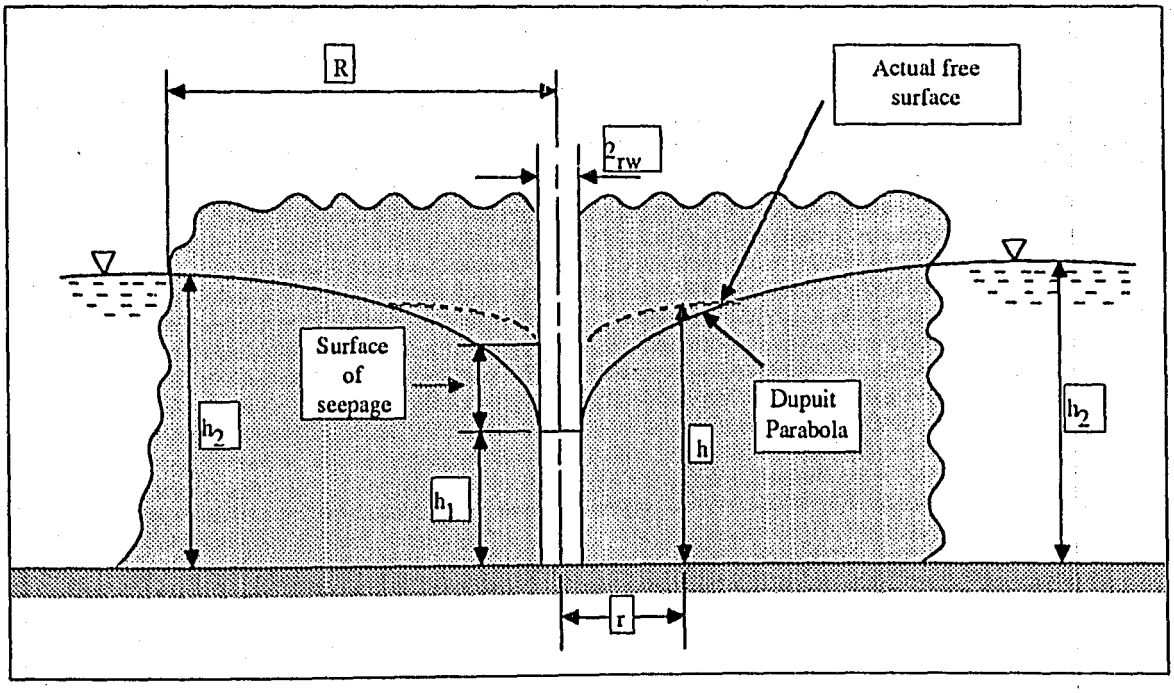

Figure 2. 15 : The range of validity of Dupuit assumption

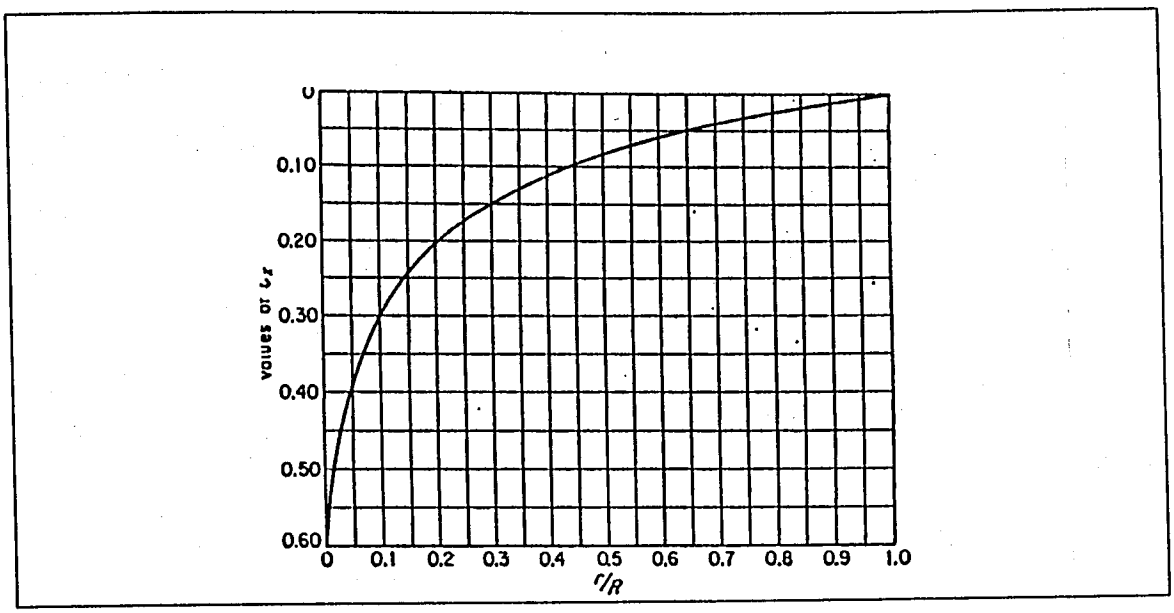

Figure 2. 16 : Correction factor C_x variation with r/R (Babbitt, and Caldwell, 1948)

For the non-steady state from the analytical formula using drawdown or build-up observed in the monitoring well is given by Theis (1935):

$$k = \frac{q}{2\pi \cdot s \cdot H} \int_{\frac{r}{\sqrt{4\alpha \cdot t}}}^{\infty} \frac{e^{-u^2}}{u} du \qquad (2.20)$$

where
- s : build-up or drawdown measured in a piezometer at a known distance from the pumped well
- q : steady rate of discharge or recharge maintained by the pump
- H : aquifer thickness and

$$\int_{\frac{r}{\sqrt{4\alpha \cdot t}}}^{\infty} \frac{e^{-u^2}}{u} du = -\frac{1}{2} E \cdot i\left(-\frac{r^2}{4\alpha \cdot t}\right) \qquad (2.21)$$

$$\alpha = \frac{k \cdot H}{n} \qquad (2.22)$$

where n is the porosity.

Some aquifers are too large to install a fully penetrating well. Partially penetrating wells are then preferable. For partially penetrating wells (**Figure 2. 17**) the following formula can be used:

$$k = \frac{2.303 \cdot q}{\pi \left[(H - s)^2 - t^2 \right]} \log\left(\frac{R}{r_w}\right) \cdot \left[1 + \left(0.30 + \frac{10\, r_w}{H}\right) \sin\frac{1.8\, s}{H} \right]^{-1} \qquad (2.23)$$

here
- R : radius of influence
- r_w : radius of the well
- H : aquifer thickness
- s : the distance of the well from the impermeable layer
- L : the screen length.

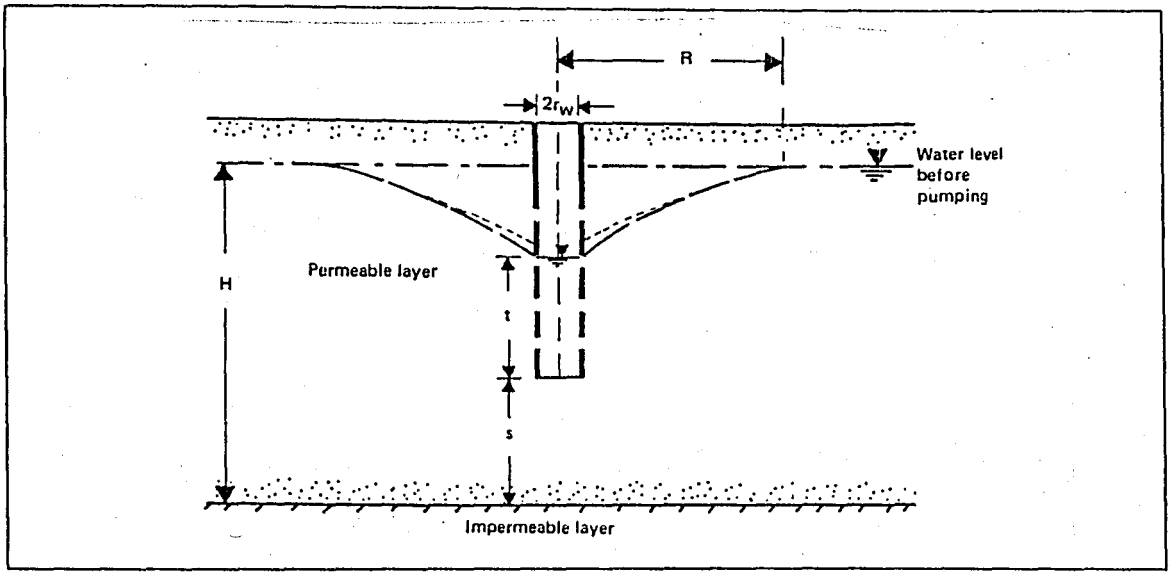

Figure 2. 17 : View of a partially penetrating well

Hantush (1961 a,b) developed equations for the unsteady drawdown around a well partially screened and steadily discharged and applied them to field data. These equations were a modification of the Theis method. Hantush also proposed another modification to Jacob's solution. Boonstra (1990) studied these two methods and compared them to field data. He then concluded that the first modification could lead to a serious overestimation of the tested aquifer thickness and thus recommended the second method. Kono and Nishigaki (1979) also derived a graphical approximation method for unsteady groundwater flow toward a partially penetrating well in an anisotropic confined aquifer. Tavenas et al. (1990) used a finite element analysis to extrapolate transient state observations to steady state conditions.

2. III. A. II. Borehole Methods. The in-situ permeability determination by boreholes without use of observation wells may be preferred due to the cost of the well pumping tests. The pumping can be into or out of the borehole.

2. III. A. II. a) Open End Tests. Casings are inserted in the boreholes extending to the soil layers whose permeability needs to be determined. The test can be conducted either with gravity flow or under pressurized conditions. Pressurized injection may be neccessary when low permeability soils are being tested. The amount of hydraulic head (h) maintained during a constant rate of flow (q) into or out of the hole, the inside diameter casing (r) and the elevations of the top and bottom of the casing are measured **(Figure 2. 18).** The permeability can be calculated from these variables as:

$$k = \frac{q}{5.5\, r \cdot h} \qquad (2.24)$$

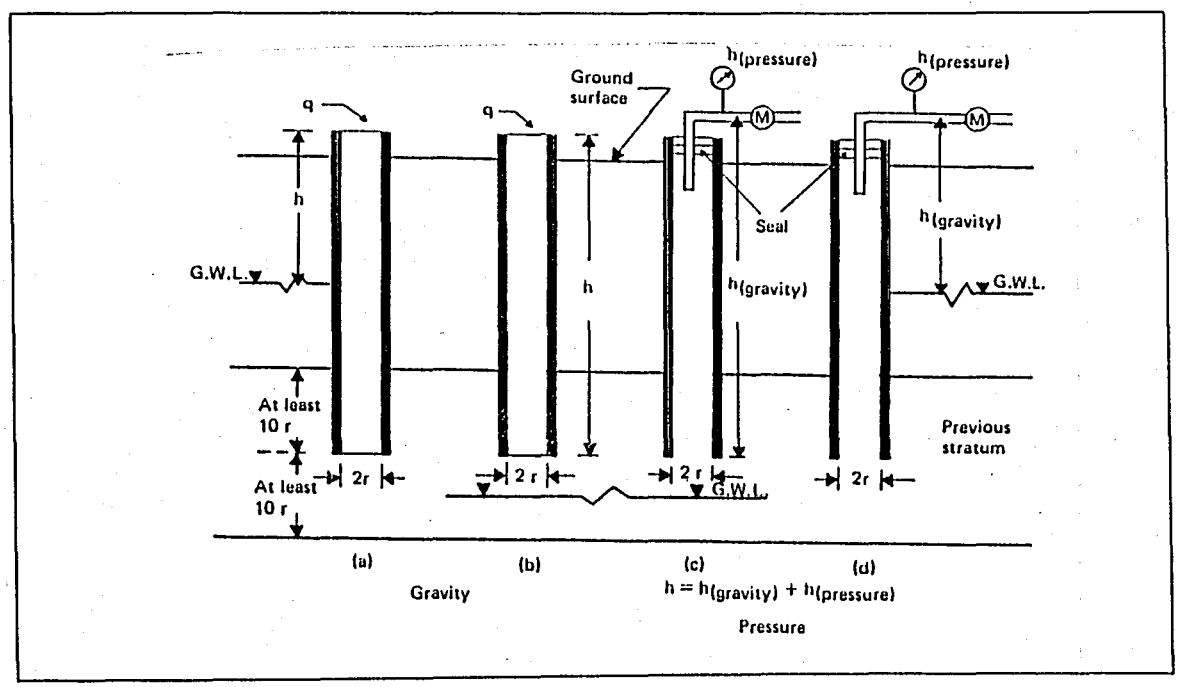

Figure 2. 18 : Open - end tests for permeability determination

The above equation was determined using electric analogue tests. The applied hydraulic head will change depending on whether the test is conducted above or below the ground water level. The formulation was developed assuming that the effects of soil suction were negligible. Improved solutions that account for soil suction have been developed (Stephens and Neuman, 1982 a, b, c; Philip, 1985; Reynolds, et al. 1985). Stephens et al. (1987) performed statistical analyses on numerical models to develop a method for computing hydraulic conductivity k that accounts for soil suction.

The solution of Philip (1985) computes hydraulic conductivity as follows:

$$k = \frac{q}{r^2 \sqrt{R^2 - 1}\left[F_1 + \left(\frac{F_2}{A} \right) \right]} \qquad (2.25)$$

where q : the rate of flow ; $R = H / r$ and

$$F_1 = \frac{4.117\,(1 - R^{-2})}{\ln\left[R + \sqrt{R^2 - 1} \right] - \left[\sqrt{1 - \left(\frac{1}{R^2} \right)} \right]} \qquad (2.26)$$

$$F_2 = \frac{4.280}{\ln\left[R + \sqrt{R^2 - 1} \right]} \qquad (2.27)$$

$$A = \frac{1}{2} \alpha \cdot r \qquad (2.28)$$

α : a parameter (units of L^{-1}) called the "sorptive number" that is a measure of the capillary (suction) properties of the soil and has a typical value of 0.002 cm^{-1}-(Philip, 1985)-0.01 cm^{-1} for fine-grained soil.

The hydraulic conductivity k calculated from Equation 2.5 should be compared with the value of k computed from Stephens et al.'s (1987) regression analysis obtained from numerical simulations:

$$k = \frac{q}{r \cdot H \cdot C_u} \qquad (2.29)$$

where the dimensionless factor C_u is determined as follows from α_v (units of cm^{-1}) and H and r (units of meters):

$$\log (C_u) = [0.653 \log (R)] - [0.257 \log (\alpha_v)] - [0.633 \log (H)] + (0.021 \sqrt{R}) - \left(\frac{0.313}{\sqrt{N}} \right) + (1.456r) + 0.453 \qquad (2.30)$$

and where N and α_v are parameters that have values of about 1.8 and 0.002 cm^{-1}, respectively, for fine-grained soils.

Another procedure that takes soil suction into account for calculating permeability is given by Elrick et al. (quoted by Daniel, 1989)

$$k = \frac{C \cdot q}{2\pi \cdot H^2 + \pi \cdot r^2 \cdot C + \frac{2\pi \cdot H}{\alpha^*}} \qquad (2.31)$$

where C is determined from **Figure 2. 19.** For practical purposes, α^* is equal to α.

The important assumptions are that the soil is homogeneous, isotropic, and uniformly saturated and infinite in extent. Soil is not smeared across the surface of the borehole and it does not swell when wetted.

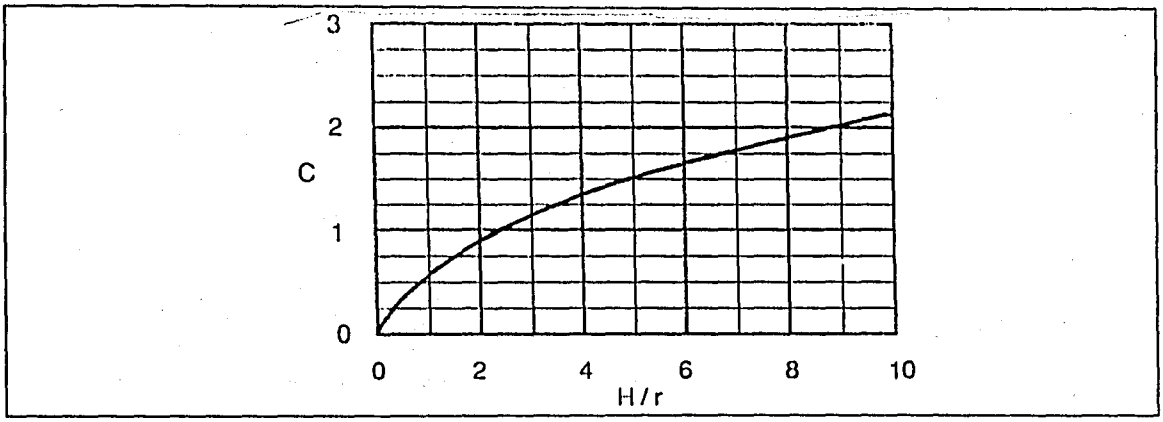

Figure 2. 19 : C against H/r (Reynolds and Elrick, 1987)

Reynolds and Elrick (1985) compared the permeability calculations obtained from Laplace and Richards analyses of Guelph permeameter data to tests on undisturbed samples in the laboratory. They considered a heterogeneous, anisotropic and structured loam soil. They expressed that the permeability would be overestimated neglecting the capillarity.

<u>2. III. A. II. b) Packer Tests.</u> Packer tests are conducted on soils that can remain open without the use of casing. The test can be performed either above or below the water table. These tests are found to provide more accurate results in testing below the groundwater level than above (**Figure 2. 20**). The permeability is :

$$k = \frac{q}{2\pi \cdot L \cdot h} \ln \frac{L}{r} \qquad \text{for } L \geq 10r \qquad (2.32)$$

$$k = \frac{q}{2\pi \cdot L \cdot h} \sinh^{-1} \frac{L}{2r} \qquad \text{for } 10r > L \geq r \qquad (2.33)$$

in which q : contant rate of flow into the borehole
a : constant rate of flow into borehole
L : length of test hole
r : radius of borehole
h : differential head of water.

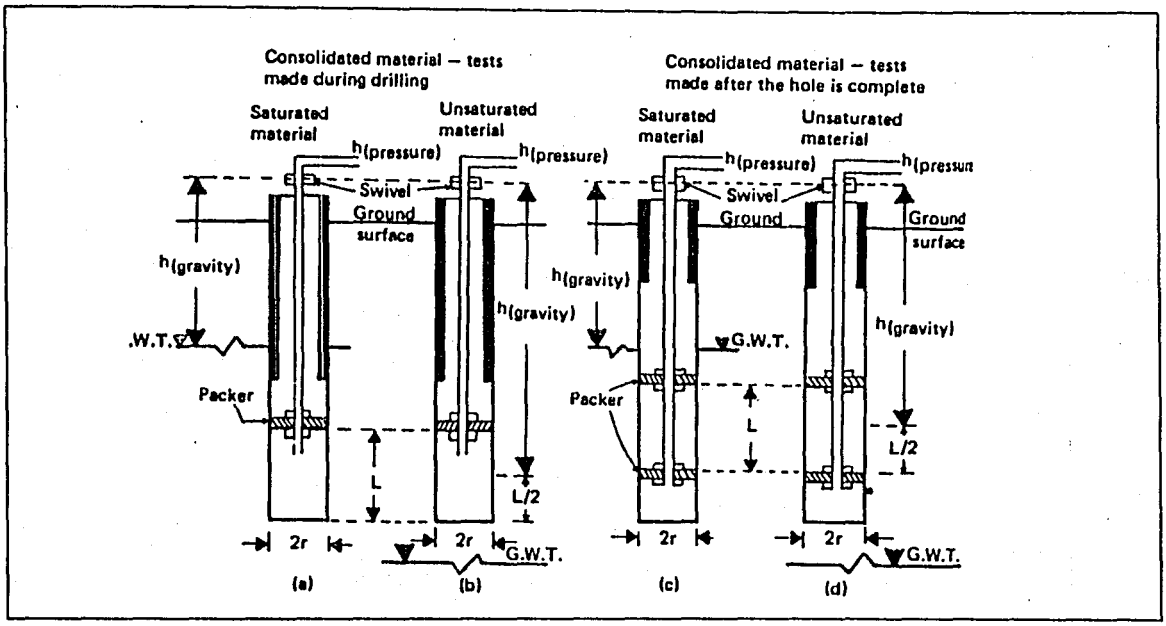

Figure 2. 20 : The packer test for soil permeability

Kabala (1993) introduced a new borehole test which is called the dipole-flow test using three packers. He also derived a mathematical model for the evaluation of this type of test data.

2. III. A. III. Porous Probes. Porous probes are pushed and driven into the soil and subsequently constant or falling head tests are performed. The probes are usually used for measuring permeability of saturated clays. The usual configurations and equations recommended for calculation of permeability coefficient are given in **Figure 2. 21.** The BAT permeameter was developed for more accurate measurement (Torstensson, 1984). This device can be used on unsaturated compacted clays. The assumptions are:

- soil is homogeneous, isotropic uniformly soaked and incompressible
- infinite boundaries
- soil is not smeared across the surface of the porous element
- no soil suction
- conditions are isothermal
- there is no effect from dissolutioned gas in the pressure chamber.

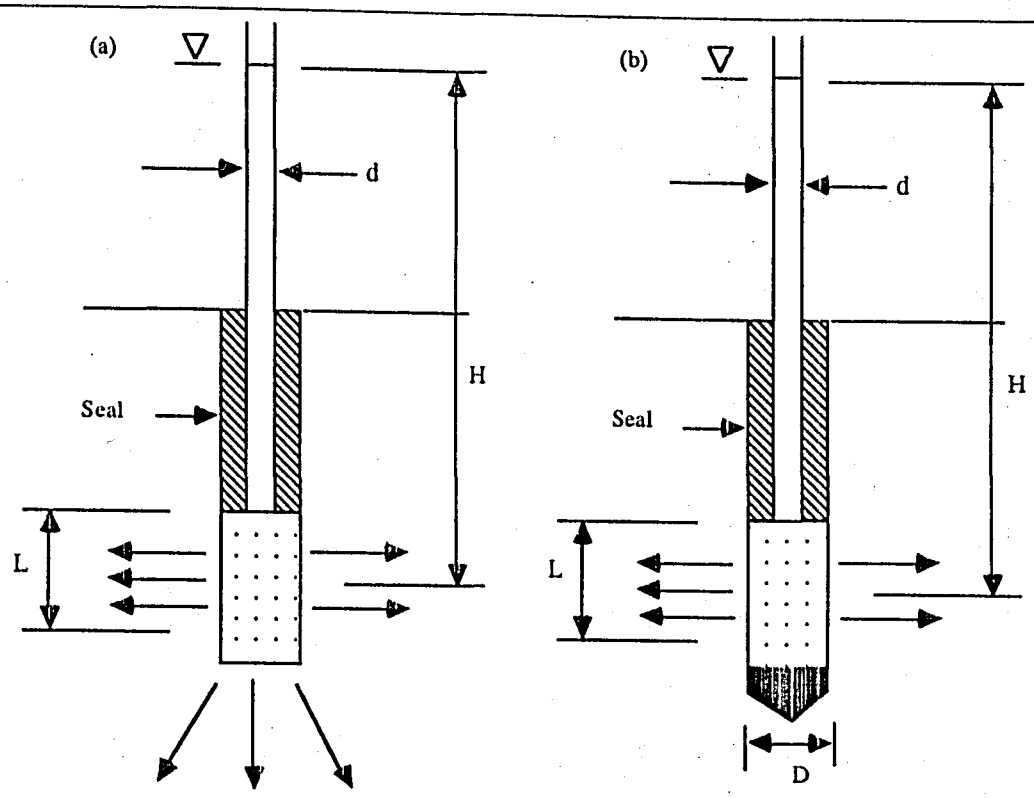

Constant Head: $$k = \frac{q}{F \cdot H}$$

Falling Head: $$k = \frac{\pi \cdot d^2 / 4}{F\,(t_2 - t_1)} \ln\left(\frac{H_1}{H_2}\right)$$

Case A: $$F = \frac{2\pi \cdot L}{\ln\left(\frac{L}{D} + \sqrt{1 + (L/D)^2}\right)}$$

Case B: $$F = \frac{2\pi \cdot L}{\ln\left(\frac{L}{D} + \sqrt{1 + (L/D)^2}\right)} - 2.8D$$

Figure 2. 21 : Hydraulic conductivity from porous probe test:
a)Case A -Probe with permeable base
b) Case B-Probe with impermeable base

Detailed analysis techniques and examples depending on various boundaries, state of flow, rate of discharge, aquifer types and penetration for **2. III. A. I, 2. III. A. II and 2. III. A.III** can be found in Kruseman and de Ridder (1983). Methods of conducting these are quite well standardized and can be found in any groundwater manual.

2. III. A. IV. Infiltrometers. Infiltrometers are divided to five subgroups:

2. III. A. IV. a) Open Single-Ring Infiltrometers. Open single-ring infiltrometers are the simplest infiltrometer (**Figure 2.22**). The ring is placed in a trench that is sealed with a bentonitic grout. The water is introduced into the ring and the infiltration rate(I) is monitored and recorded. The key assumptions are the following:

- the soil is homogeneous and uniformly soaked behind a wetting front
- the rate of infiltration is sufficiently large that it can be measured accurately
- there is no leakage through the seal between the infiltrometer and soil
- evaporative losses can be taken into account
- either the wetting front does not pass below the bottom of the ring or lateral spreading below the ring is properly considered
- the wetting-front suction head can be determined or taken as zero without introducing excessive error
- any swelling of the soil is complete by the time that the final hydraulic conductivity k is determined
- the effect of boundary conditions beneath the ring are negligible.

The permeability formulation is given by:

$$k = \frac{I}{i} = \frac{q}{A \cdot i} = \frac{I \cdot L_f}{(H + L_f + \psi_f)} \qquad (2.34)$$

where
- q : the rate of flow
- A : the area of the ring
- t : the elapsed time
- i : the hydraulic gradient
- H : the depth of ponded water
- L_f : the depth of the wetting front
- ψ_f : the wetting-front suction head.

ψ_f is often taken as zero, which leads to higher permeabilities and thus to a higher safety factor. The wetting front is measured by probes in the ground or by water content calculation at the end of the test. The evaporation must be taken into account for correct interpretation.

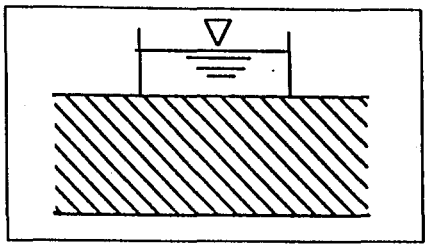

Figure 2. 22 : Open, single ring infiltrometer

2. III. A. IV. b) Open Double-Ring Infiltrometers. Double ring infiltrometer tests are performed with two rings or boxes that are sealed in the soil, filled with water and covered to minimize evaporation (**Figure 2. 23**). The purpose of the outer ring is to limit lateral spreading of water originating from the inner ring. The analysis is performed with the following assumptions:

- the soil is homogeneous and uniformly wetted
- the rate of infiltration is large enough to be measured accurately
- evaporative losses are properly taken into account
- seepage beneath the inner ring is one-dimensional
- the wetting front suction can be determined or taken as zero without introducing excessive error
- any swelling of the soil is either complete or can be taken into account
- the effect of boundaries beneath the ring either are negligible or can be taken into account.

The calculation of permeability is equal to the previous single-ring case.

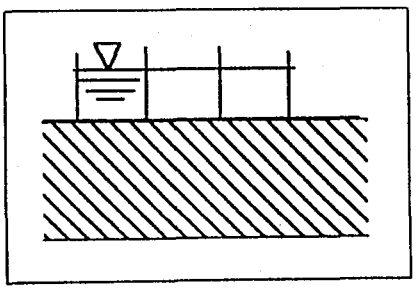

Figure 2. 23 : Open, double-ring infiltrometer

2. III. A. IV. c) Sealed, Single-Ring Infiltrometers. The seal of this type of infiltrometer ensures that there is very little evaporation and minimal temperature changes for long periods of time (**Figure 2.24**). Assumptions and calculation of permeability are the same as for open-single ring infiltrometers.

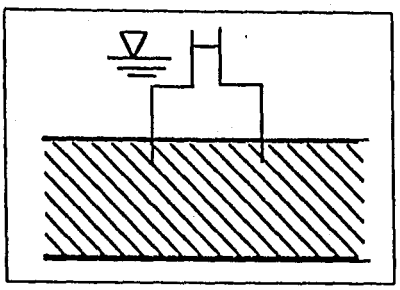

Figure 2. 24 : Sealed, single ring infiltrometer

2. III. A. IV. d) Sealed, Double-Ring Infiltrometers. The sealed double ring infiltrometer consists of a sealed inner ring and an open outer ring that are embedded into trenches and sealed with bentonitic grout. The rings are filled with water and a small, flexible bag is attached to the inner ring. The entire infiltrometer is covered so that there is no evaporation loss. The inside bag is periodically removed, weighed to determine the quantity of flow and, when necessary, refilled (**Figure 2. 25**). The important assumptions in the analysis are:

- the soil is homogeneous and uniformly soaked behind a wetting front
- the wetting-front suction head can be determined or taken as zero without introducing excessive error
- temperature fluctuations in the inner ring are minimal
- seepage beneath the inner rings is one dimensional
- any swelling of the soil is either cmoplete when the final k is determined or can somehow be taken into account
- the effects of boundaries beneath the rings are negligible.

The permeability is calculated in a similar manner to the other infiltrometers.

2. III. A. IV. e) Air-Entry Permeameters. The air-entry permeameter device was developed by Bouwer (1978) (**Figure 2.26**). It consists of a sealed ring (approximately 60 cm in diameter) embedded about 10 cm into the soil. There are two stages during the test. It is assumed:

- the soil is homogeneous and uniformly soaked behind a sharp wetting front
- the gauge reading is directly related to the air-entry value of a soaked zone of soil
- the water-entry value is one-half the air-entry value computed from the gauge reading
- the soil does not swell when wetted.

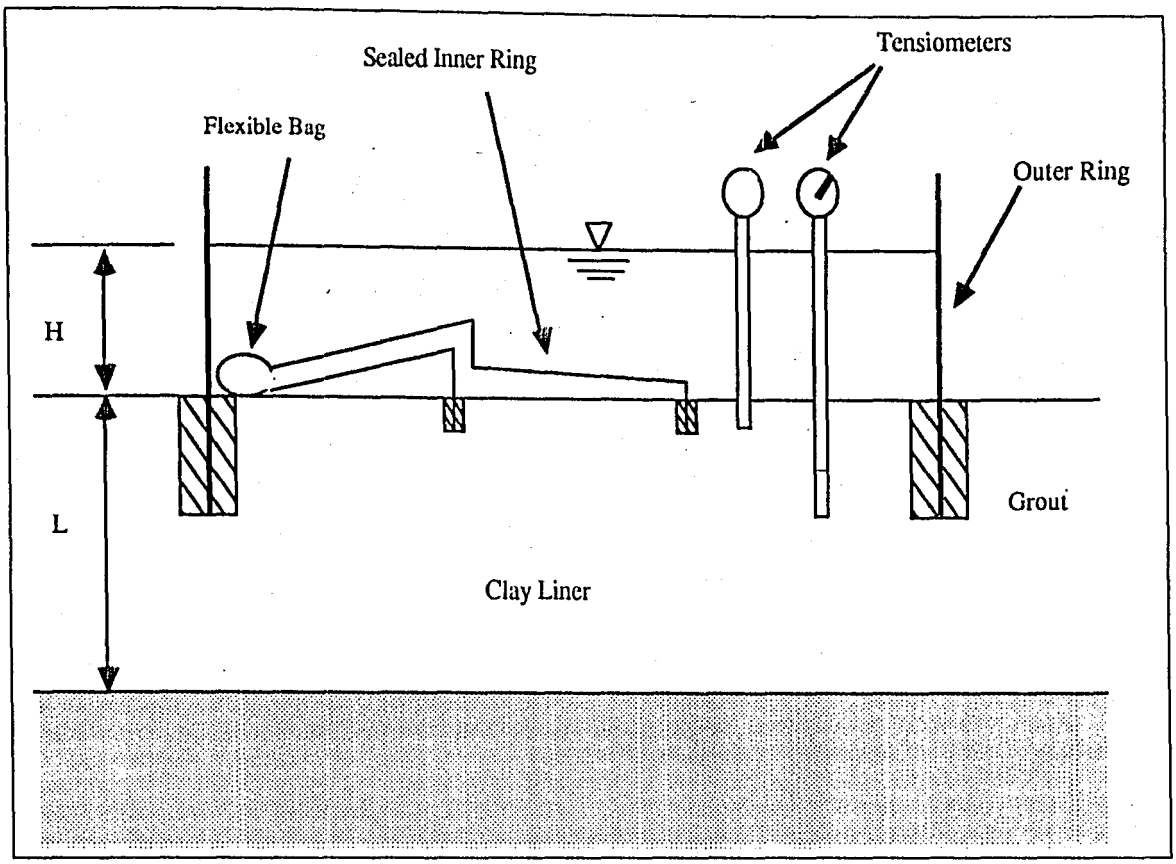

Figure 2. 25 : Sealed, double ring infiltrometer

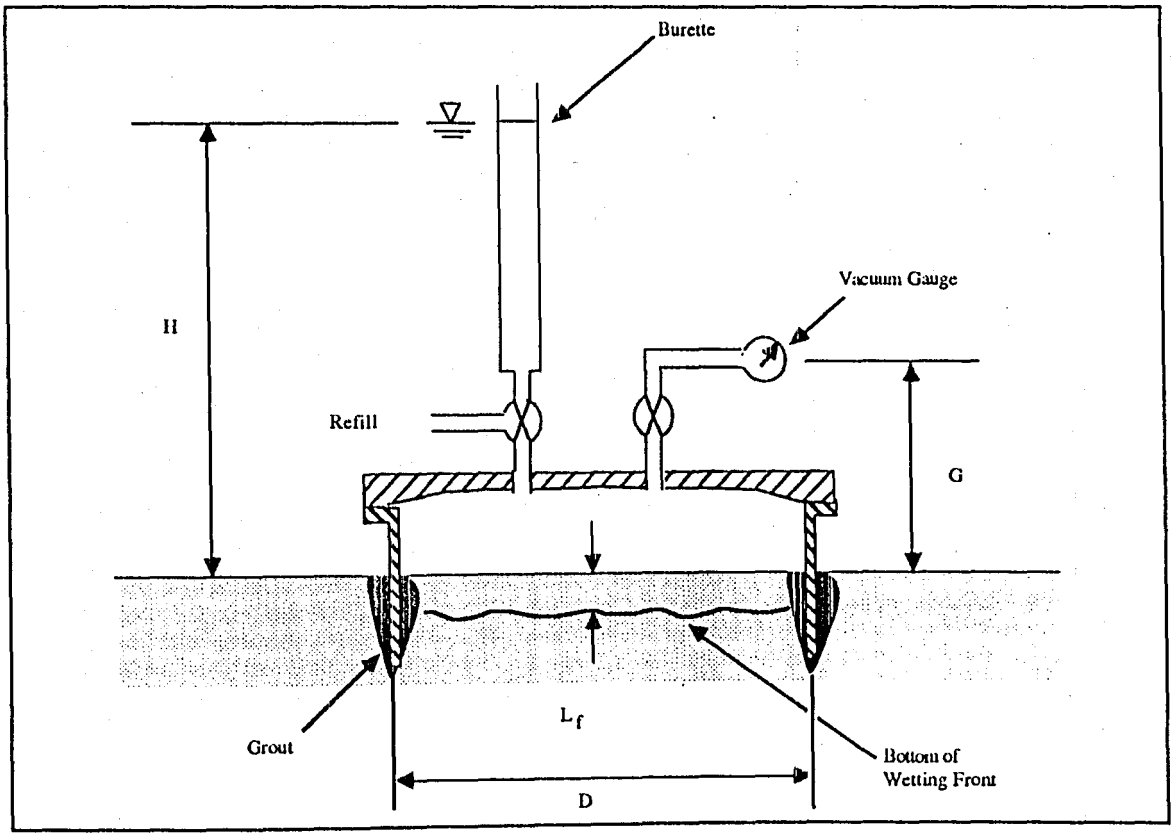

Figure 2. 26 : Air-entry permeameter

2. III. A. V. Lysimeters. A lysimeter pan is an underdrain placed beneath the soil strata that is being tested (**Figure 2.27**). The pan can be constructed from any impervious material. The pan is backfilled with drainage material, soaked and covered with a filter fabric. It is assumed that the flow has reached the steady state and that water flows one-dimensionally into the pan. The permeability calculation is made through Darcy's law and the measured rate of flow into the pan.

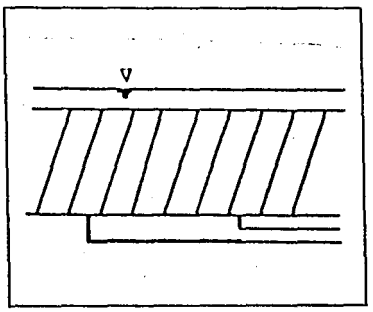

Figure 2. 27 : Lysimeter

The comparison of methods 2.III.A.II, 2.III.A.III, 2.III.A.IV and 2.III.A.V are given in Daniel (1989). The advantages and the disadvantages of each testing method are tabulated in **Table 2.4**.

Table 2. 4 : Advantages and disadvantages of methods of testing (Daniel, 1985)

Type of test	Device	Advantages	Disadvantages
Borehole	Boutwell permeameter	Low equipment cost (< $ 200 per unit). Easy to install. Hydraulic conductivity is measured in vertical and horizontal direction. Can measure low hydraulic conductivity (down to about 10^{-9} cm/s). Can be used at great depths and on slopes.	Volume of soil tested is small. Unsatured nature of soil not properly taken into account. Testing times are somewhat long (typically several days to several weeks for hydraulic conductivities < 10^{-7} cm/s).
	Constant head permeameter	Low eqipment cost (< $ 1.000 per unit). Easy to install. Unsaturated nature of soil taken info account relatively rigorously. Relatively short testing times (a few hours to several days). The hydraulic conductivity that is measured is primarily the horizontal value. (which is an advantage if this is the desired value). Can be used at great depths.	Volume of soil tested is small. The hydraulic conductivity that is measured is primarily the horizontal value (in some applications, the value in the vertical direction is desired). The device is not well suited to measuring very low hydraulic conductivies (less than 10^{-7} cm/s).
Porous probe	BAT permeameter	Easy to install. Short testing times (usually a few minutes to a few hours). Probe can also be used to measure pore-water pressures. Can measure low hydraulic conductivity (down to about 10^{-10} cm/s). The hydraulic conductivity that is measured is primarily the horizontal value (which is an advantage if this is the desired value). Can be used at great depths.	High equipment cost (> $ 6.000). Volume of soil tested is very small. Soil smeared across probe during installation may lead to underestimation of hydraulic conductivity. The hydraulic conductivity that is measured is primarily the horizontal value (in some applications the value in the vertical direction is desired). The unsaturated nature of the soil is not properly taken into account.
Infiltrometer	Open. single ring infiltrometer	Low cost (< $ 1,000). Easy to install. Very large infiltrometer can be used to test a large volume of soil. Hydraulic conductivity in the vertical direction is determined.	Low hydraulic conductivity (< 10^{-7} cm/s) is difficult to measure accurately. Must eliminate, or make a correction for evaporation. May need to correct for lateral spreading of water beneath infiltrometer. Testing times are relatively long (usually several weeks to several months for hydraulic conductivities < 10^{-7} cm/s). Must estimate wetting front suction head.

Table 2. 4 : Advantages and disadvantages of methods of testing (Daniel, 1985) (continued)

Type of test	Device	Advantages	Disadvantages
	Open double ring infiltrometer	Low equipment cost (< $ 1,000). Hydraulic conductivity in the vertical direction is determined. Minimal lateral spreading of water that infiltrates from inner ring.	Cannot be used on steep slopes unless a flat bench is cut. Low hydraulic conductivity (10^{-7} cm/s) is difficult to measure accurately. Must eliminate or make a correction for evaporation. Testing times are somewhat long (usually several days to several months for hydraulic conductivites < 10^{-7} cm/s). Must estimate wetting front suction head. Cannot be used on steep slopes unless a flat bench is cut.
	Closed, single-ring infiltrometer	Low equipment cost ($ 1,000). Hydraulic conductivity in the vertical direction is measured. Can measure low hydraulic conductivity (down to 10^{-8} - 10^{-9} cm/s).	Volume of soil tested is somewhat small because diameter of ring is < 1 m. Need to correct for lateral spreading of water if wetting front penetrates below the base of the ring. Testing times are long (usually several weeks to several months). Must estimate wetting front suction head. Very difficult to use on steeply sloping ground.
	Sealed double-ring infiltrometer	Moderate equipment cost (< $ 2,500). Hydraulic conductivity in the vertical direction is determined. Can measure low hydraulic conductivity (down to about 10^{-8} cm/s). Minimal lateral spreading of water that infiltrates from inner ring. Relatively large volume of soil is permeated.	Testing times are relatively long (usually several weeks to several months). Must estimate wetting front suction head. Cannot be used on slopes unless a flat bench is cut.
	Air entry permeameter	Modest equipment cost (< $ 3,000). Relatively short testing times (a few hours to a few days). Hydraulic conductivity in the vertical direction is measured. Can measure low hydraulic conductivity (down to 10^{-8} - 10^{-9} cm/s). Wetting front suction head is estimated in second stage of test.	A relatively small volume of soil is permeated because the wetting front usually does not penetrate more than a few centimeters into compacted clay. Cannot be used on slopes unless a flat bench is cut. Several important assumptions are required.
Underdrain	Lysimeter pan	Low cost. Hydraulic conductivity in the vertical direction is measured. Large volumes of soil can be tested. Few experimental ambiguities. No disturbance of soil.	Must install underdrain before the liner is constructed. Relatively long testing times (usually several weeks to several months for hydraulic conductivities less than 10^{-7} cm/s). Must collect and measure seepage from underdrain, which usually necessitates a sump and a pump.

2. III. A. VI. Permeability Determination Using Shape Factors. The permeability can be calculated by measuring the rate of flow of uncased auger and boreholes and by using the appropriate shape factors. These are obtained by either electrical analogies or mathematical approximations. During the constant head permeability tests in clay or other low-permeability soil the steady-state conditions can take a long time and they are often not realized. Therefore, the observations made in short-duration tests should be extrapolated to the steady-state flow.

The Laplace equation, which is the governing equation for steady-state flow problems, is encountered in many engineering applications and physics. Among these are the problems of the steady flow of electricity and heat and various aspects of elastic theory, such as the plane theory of torsion annd bending. The reason for this correspondence becomes evident when one considers the nature of the governing laws in these various disciplines; that is, the counterparts of Darcy's law are Fourier's law for heat conduction, Maxwell's law for electrostatics, Ohm's law for current cunduction and Hooke's law and the nature of Airy stress components in plane elastic theory. The most productive model analogy is the one of the electrohydrodynamic type. The correspondence between the steady-state flow of water through a porous medium and the steady flow of electric current in a conductor is presented in **Table 2.5.**

Table 2. 5: Correspondence between seepage and flow of electric current

Steady-state seepage	Electric current
Total head h	Voltage V
Coefficient of permeability k	Conductivity σ
Discharge velocity v	Current I
Darcy's law : $v = -k \cdot i$	Ohm's law : $I = -\sigma \cdot V$
$\Delta^2 h = 0$	$\Delta^2 V = 0$
Equipotential lines : h = constant	Equipotential lines : V = constant
Impervious boundary : $\partial h / \partial n = 0$	Impervious boundary : $\partial V / \partial n = 0$

From Table 2. 4 it is evident that the formal analogy between confined seepage flow and current flow is perfect. Thus, to obtain the pattern of equipotential lines for a seepage problem, the flow domain can be transferred into an electrical conductor of similar geometrical form (**Figure 2.28**). This was first developed by Pavlovsky in 1918. This analogy provides the equipotential lines with the following limitations: the electrical potential is unaffected by gravity; hence the investigated system should be confined; the finite dimensions of the conducting material severely limit this method for large spatial problems.

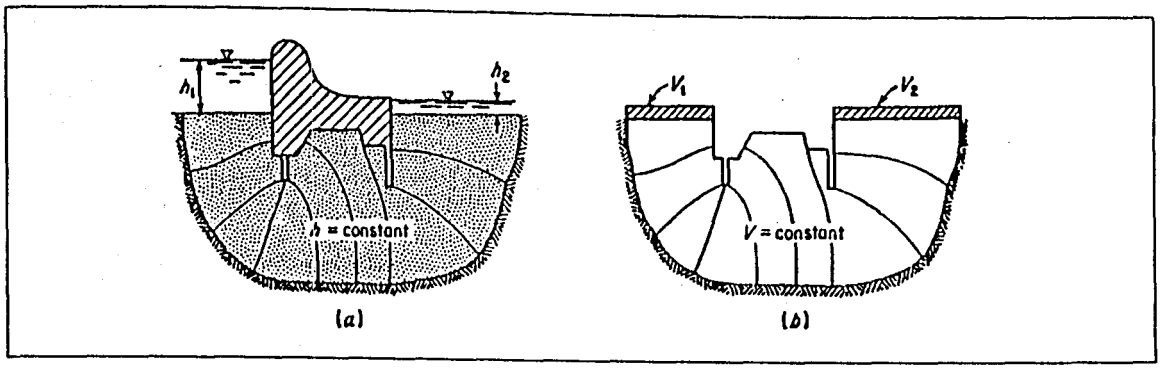

Figure 2. 28 : The equipotential lines simulated by the electrical conductor

Mathematical approximations include finite differences method, finite element analysis and boundary element method. There are also simplified equations of exact solutions. Kruseman and de Ridder (1983) provide details of these simplified relations.

The U.S. Department of the Navy has adopted some standard variable head tests for determining the permeability by means of piezometer observation wells (**Table 2.6**). The calculation methods are explained in **Figures 2.29, 2.30 and 2.31.**

Hvorslev also developed shape factors for the U. S. Corps of Engineers (1951). He applied Dachler's solution for the flow from a line source for which the equipotential surface was a hemispheroid to cylindrical piezometer by representing the cylinder by its inscribed prolate spheroid. This equation was only approximate. A time lag concept was introduced for the time difference of reacting the measuring device and the true porewater pressure. The magnitude of the time lag was determined to be inversely proportional to the permeability of the soil and varied with the size and type of pressure measuring device.

Lambe and Whitman (1979) summarized the formulas for various piezometer geometries and penetration conditions proposed by Hvorslev as shown in **Table 2.7.**

Table 2. 6: Computation of permeabiltiy from variable head tests (for observation well of constant cross section)

Condition	Diagram	Shape factor F	Permeability k by variable head test	Applicability
Observation well or piezometer in saturated isotropic stratum of infinite depth				
(A) Uncased hole	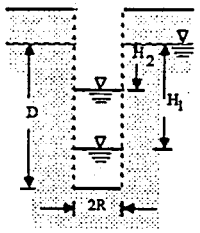	$F = 16\,\pi \cdot D \cdot S' \cdot R$	$k = \frac{R}{16\,D \cdot S'} \cdot \frac{H_2 - H_1}{t_2 - t_1}$ for $\frac{D}{R} < 50$	Simplest methods for permeability determination. Not applicable in stratified soils. For values of S', see Figure 29.
(B) Cased hole, soil flush with bottom	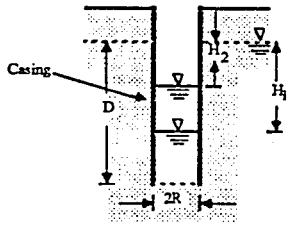	$F = \frac{11\,R}{2}$	$k = \frac{2\,\pi\,R}{11\,(t_2 - t_1)} \ln \frac{H_1}{H_2}$ for 6 in (0.1524 m) ≤ D ≤ 60 in (1.524 m)	Used for permeability determination at shallow depths below the water table. May yield unreliable results in falling-head test with silting of bottom of hole.
(C) Cased hole, uncased or perforated extension of length L	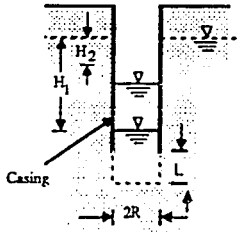	$F = \frac{2\,\pi \cdot L}{\ln (L/R)}$	$k = \frac{R^2}{2\,L\,(t_2 - t_1)} \cdot \ln \frac{L}{R} \ln \frac{H_1}{H_2}$ for $\frac{L}{R} > 8$	Used for permeability determination at greater depths below water table.
(D) Cased hole, column of soil inside casing to height L	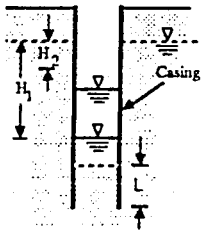	$F = \frac{11\,\pi \cdot R^2}{2\,\pi \cdot R + 11\,L}$	$k = \frac{2\,\pi \cdot R + 11\,L}{11\,(t_2 - t_1)} \cdot \ln \frac{H_1}{H_2}$	Principal use is for permeability in vertical direction in anisotropic soils.

Table 2. 6: Computation of permeabilty from variable head tests (for observation well of constant cross section) (continued)

Condition	Diagram	Shape factor F	Permeability k by variable head test	Applicability
Observation well or piezometer in acquifer with impervious upper layer				
(E) Cased hole, opening flush with upper boundary of aquifer of infinite depth	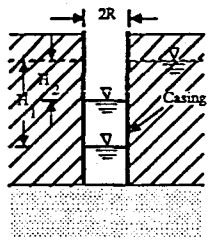	$F = 4\,R$	$k = \frac{\pi \cdot R}{4\,(t_2 - t_1)} \cdot \ln \frac{H_1}{H_2}$	Used for permeability determination when surface impervious layer is relatively thin. May yield unreliable results in falling-head test with silting of bottom of hole.
(F) Cased hole, uncased or perforated extension into aquifer of finite thickness:		(1) $F = C_s \cdot R$	$k = \frac{\pi \cdot R}{C_s (t_2 - t_1)} \cdot \ln \frac{H_1}{H_2}$	Used for permeability determinations at depths greater than about 5 ft (1.524 m). For values of C_s, see Figure 30.
(1) $\frac{L_1}{T} \leq 0.20$ (2) $0.2 < \frac{L_2}{T} < 0.85$ (3) $\frac{L_3}{T} = 1.00$	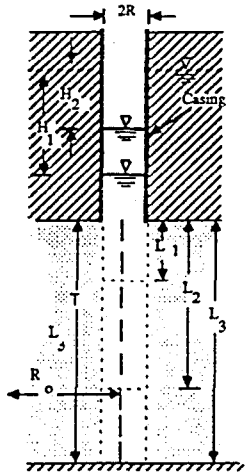	(2) $F = \frac{2\pi \cdot L_2}{\ln (L_2 / R)}$	$k = \frac{R^2 \cdot \ln (L_2/R)}{2\,L_2 (t_2 - t_1)} \cdot \ln \frac{H_1}{H_2}$ for $\frac{L}{R} > 8$	Used for permeability determinations at greater depths and for fine-grained soils using porous intake point of piezometer.
Note: R_0 is the effective radius to source at constant head		(3) $F = \frac{2\pi \cdot L_3}{\ln (R_0 / R)}$	$k = \frac{R^2 \cdot \ln (R_0/R)}{2\,L_3 \cdot (t_2 - t_1)} \cdot \ln \frac{H_1}{H_2}$	Assume value of $R_0 / R = 200$ for estimates unless observation wells are made to determine actual value of R_0.

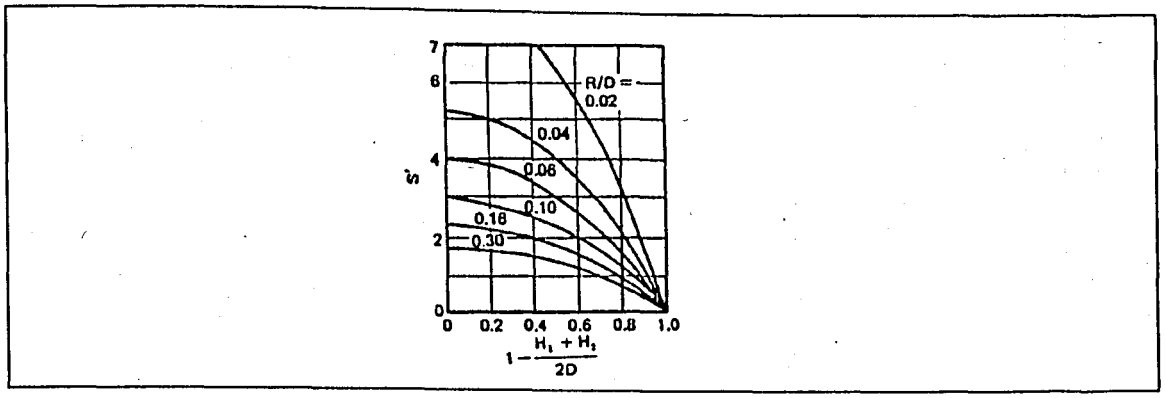

Figure 2. 29 : Shape factor coefficient S' used for condition A of Table 2.6

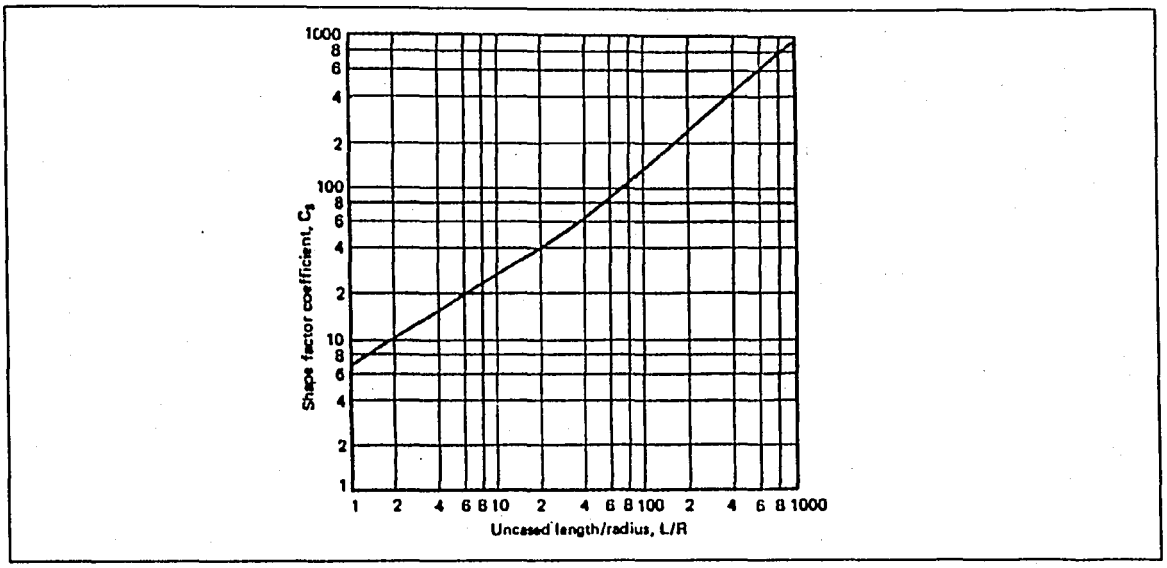

Figure 2. 30 : Shape factor coefficient C_s used for condition (F-1) of Table 2.6

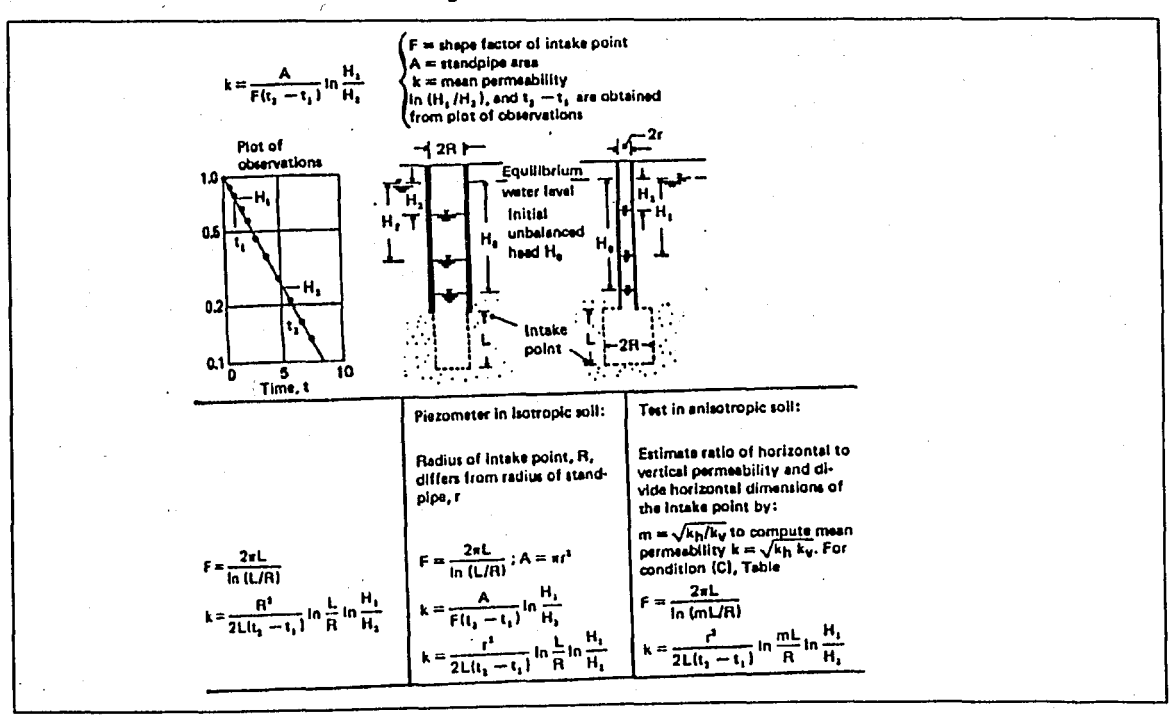

Figure 2. 31 : Analysis of permeability by variable-head tests (U. S. Navy, 1971) (in general)

Table 2. 7: Formulas for determination of permeability (Hvorslev, 1951)

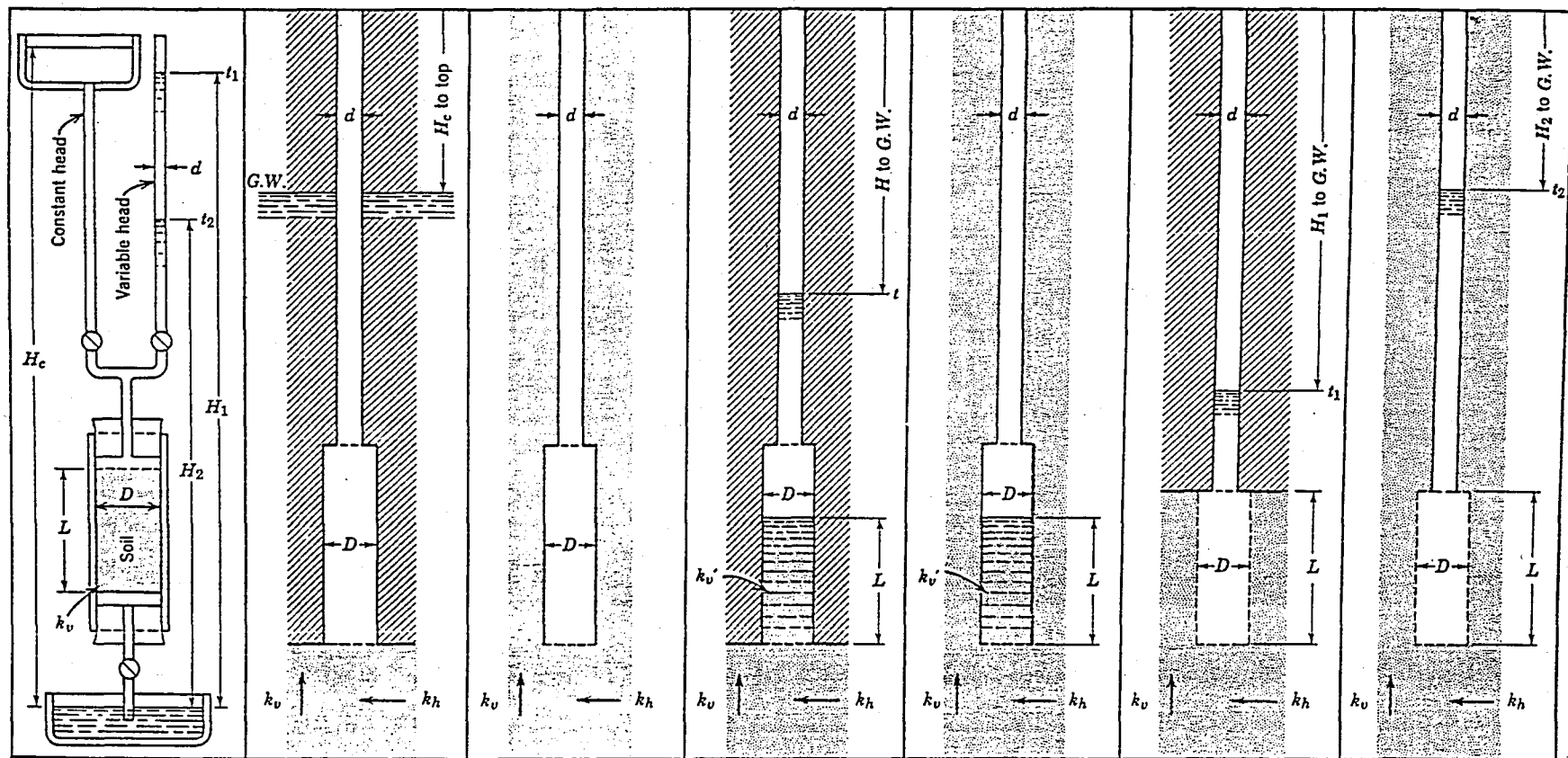

Laboratory permeameter	Flush bottom at impervious boundary	Flush bottom in uniform soil	Soil in casing at impervious boundary	Soil in casing in uniform soil	Well point-filter at impervious boundary	Well point-filter in uniform soil
A	*B*	*C*	*D*	*E*	*F*	*G*

Case	Constant head	Variable Head	Basic Time Lag	Notation
A	$k_v = \frac{4 \cdot q \cdot L}{\pi \cdot D^2 \cdot H_c}$	$k_v = \frac{d^2 \cdot L}{D^2 \cdot (t_2 - t_1)} \cdot \ln \frac{H_1}{H_2}$ $k_v = \frac{L}{t_2 - t_1} \cdot \ln \frac{H_1}{H_2}$ for d=D	$k_v = \frac{d^2 \cdot L}{D^2 \cdot T}$ $k_v = \frac{L}{T}$ for d=D	D = Diameter, intake, sample (cm) d = Diameter, standpipe (cm) L = Length, intake, sample (cm) H_c = Constant piez. head (cm) H_1 = Piez. head for t=t 1 (cm) H_2 = Piez. head for t=t 2 (cm) q = Flow of water (cm^3/sec) t = Time (sec) T = Basic time lag (sec) k_v' = Vert. perm. casing (cm/sec)
B	$k_m = \frac{q}{2 \cdot D \cdot H_c}$	$k_m = \frac{\pi \cdot d^2}{8 \cdot D \cdot (t_2 - t_1)} \cdot \ln \frac{H_1}{H_2}$ $k_m = \frac{\pi \cdot D}{8 \cdot (t_2 - t_1)} \cdot \ln \frac{H_1}{H_2}$ for d=D	$k_m = \frac{\pi d^2}{8 \cdot D \cdot T}$ $k_m = \frac{\pi \cdot D}{8 \cdot T}$ for d=D	
C	$k_m = \frac{q}{2.75 \cdot D \cdot H_c}$	$k_m = \frac{\pi \cdot d^2}{11 \cdot D \cdot (t_2 - t_1)} \cdot \ln \frac{H_1}{H_2}$ $k_m = \frac{\pi \cdot D}{11 \cdot (t_2 - t_1)} \cdot \ln \frac{H_1}{H_2}$ for d=D	$k_m = \frac{\pi \cdot d^2}{11 \cdot D \cdot T}$ $k_m = \frac{\pi \cdot D}{11 \cdot T}$ for d=D	
D	$k_v' = \frac{4 \cdot q \left(\frac{\pi}{8} \cdot \frac{k_v'}{k_v} \cdot \frac{D}{m} + L \right)}{\pi \cdot D^2 \cdot H_c}$	$k_v' = \frac{d^2 \cdot \left(\frac{\pi}{8} \cdot \frac{k_v'}{k_v} \cdot \frac{D}{m} + L \right)}{D^2 \cdot (t_2 - t_1)} \cdot \ln \frac{H_1}{H_2}$ $k_v = \frac{\frac{\pi}{8} \cdot \frac{D}{m} + L}{t_2 - t_1} \cdot \ln \frac{H_1}{H_2}$ for $k_v = k_v'$; d=D	$k_v' = \frac{d^2 \cdot \left(\frac{\pi}{8} \cdot \frac{k_v'}{k_v} \cdot \frac{D}{m} \right) + L}{D^2 \cdot T}$ $k_v = \frac{\frac{\pi}{8} \cdot \frac{D}{m} + L}{T}$ for $k_v' = k_v$; d=D	k_v = Vert. perm. ground (cm/sec) k_h = Horz. perm. ground (cm/sec) k_m = Mean coeff. perm. (cm/sec) m = Transformation ratio $k_m = \sqrt{k_h \cdot k_v}$ $m = \sqrt{k_h / k_v}$ $\ln = \log_e = 2.3 \log_{10}$
E	$k_v' = \frac{4 \cdot q \left(\frac{\pi}{11} \cdot \frac{k_v'}{k_v} \cdot \frac{D}{m} + L \right)}{\pi \cdot D^2 \cdot H_c}$	$k_v' = \frac{d^2 \cdot \left(\frac{\pi}{11} \cdot \frac{k_v'}{k_v} \cdot \frac{D}{m} + L \right)}{D^2 \cdot (t_2 - t_1)} \cdot \ln \frac{H_1}{H_2}$ $k_v = \frac{\frac{\pi}{11} \cdot \frac{D}{m} + L}{t_2 - t_1} \cdot \ln \frac{H_1}{H_2}$ for $k_v = k_v'$; d=D	$k_v' = \frac{d^2 \cdot \left(\frac{\pi}{11} \cdot \frac{k_v'}{k_v} \cdot \frac{D}{m} + L \right)}{D^2 \cdot T}$ $k_v = \frac{\frac{\pi}{11} \cdot \frac{D}{m} + L}{T}$ for $k_v' = k_v$; d=D	
F	$k_h = \frac{q \cdot \ln \left[\frac{2mL}{D} + \sqrt{1 + \left(\frac{2mL}{D} \right)^2} \right]}{2 \cdot \pi \cdot L \cdot H_c}$	$k_h = \frac{d^2 \cdot \ln \left[\frac{2mL}{D} + \sqrt{1 + \left(\frac{2mL}{D} \right)^2} \right]}{8 \cdot L \cdot (t_2 - t_1)} \cdot \ln \frac{H_1}{H_2}$ $k_h = \frac{d^2 \cdot \ln \left(\frac{4mL}{D} \right)}{8 \cdot L \cdot (t_2 - t_1)} \cdot \ln \frac{H_1}{H_2}$ for $\frac{2mL}{D} > 4$	$k_h = \frac{d^2 \cdot \ln \left[\frac{2mL}{D} + \sqrt{1 + \left(\frac{2mL}{D} \right)^2} \right]}{8 \cdot L \cdot T}$ $k_h = \frac{d^2 \cdot \ln \left(\frac{4mL}{D} \right)}{8 \cdot L \cdot T}$ for $\frac{2mL}{D} > 4$	
G	$k_h = \frac{q \cdot \ln \left[\frac{mL}{D} + \sqrt{1 + \left(\frac{mL}{D} \right)^2} \right]}{2 \cdot \pi \cdot L \cdot H_c}$	$k_h = \frac{d^2 \cdot \ln \left[\frac{mL}{D} + \sqrt{1 + \left(\frac{mL}{D} \right)^2} \right]}{8 \cdot L \cdot (t_2 - t_1)} \cdot \ln \frac{H_1}{H_2}$ $k_h = \frac{d^2 \cdot \ln \left(\frac{2mL}{D} \right)}{8 \cdot L \cdot (t_2 - t_1)} \cdot \ln \frac{H_1}{H_2}$ for $\frac{mL}{D} > 4$	$k_h = \frac{d^2 \cdot \ln \left[\frac{mL}{D} + \sqrt{1 + \left(\frac{mL}{D} \right)^2} \right]}{8 \cdot L \cdot T}$ $k_h = \frac{d^2 \cdot \ln \left(\frac{2mL}{D} \right)}{8 \cdot L \cdot T}$ for $\frac{mL}{D} > 4$	

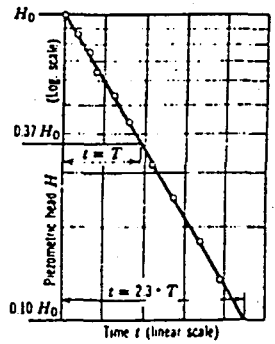

Determination basic time lag T

Table 2.7: Formulas for determination of permeability (Hvorslev, 1951) (continued)

The steady-state flow q -according to Hvorslev, may be expressed by the following simplified expression, when water flows into or out of a casing or other pore pressure sensing device:

$$q = F \cdot k \cdot h = F \cdot k \cdot (z - y) \qquad (2.35)$$

F : shape factor, a constant that depends on the piezometer as well as formation geometry

h : the active head, the water level maintained above or under the initial water level

z : the distance from the reference level to the piezometer level in the transient well (**Figure 2.32**).

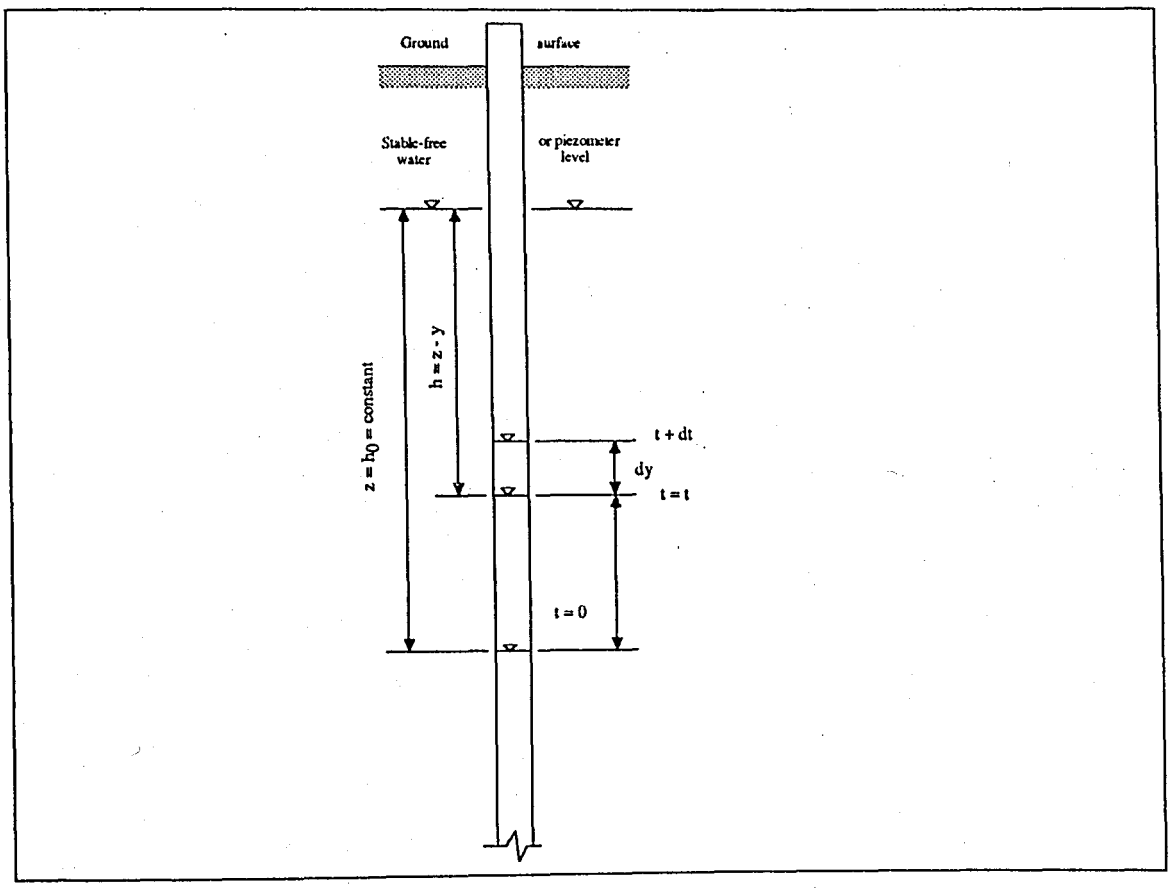

Figure 2. 32 : General conditions for the Hvorslev equation (1951)

Precise values of shape factor are vital to the accurate interpretation of in-situ methods to determine coefficient of permeability, consolidation and earth pressure. Shape factors differ for various piezometers depending on their physical dimensions. They are

independent of the soil permeability. The shape factor is generally a characteristic of an axisymmetrical flow net, since the porous element of a piezometer is nearly always axisymmetrical in shape. Because the flow net is affected by the shape and size of the body of soil in which the piezometer is placed, the value of the shape factor is also affected by the physical dimensions of the flow regime and by the conditions at its boundaries. For a spherical piezometer in a spherical or infinite body of soil, it is possible to integrate directly the governing equation of flow to obtain a closed-form solution for shape factor. This was presented and improved for various effects by Gibson (1963, 1966, 1970) on the basis of Terzaghi's consolidation theory. For piezometers of practical shape however, the partial differential equation which governs the flow cannot usually be solved by analytical means. No closed-form solutions are available for the commonly used cylindrical piezometers.

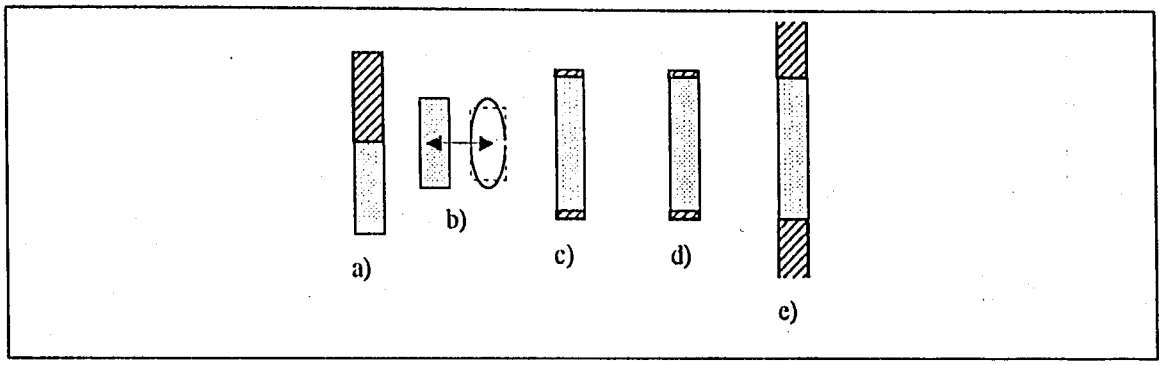

Figure 2. 33: Geometry of porous element and range of aspect ratio l/d analyzed by different authors: a) Hvorslev (1951) and Smiles and Young (1965) b) Wilkinson (1968) c) $1 \leq 4$, AL-Dhahir and Morgenstern (1969) d) $2 \leq l/d$ 15, Brund and Premchitt (1980) e) $0,1 \leq l/d \leq 10$, Randolph and Booker (1982).

Kallstenius and Wallgren (1956) presented an alternative derivation by considering the steady state flow to a spherical piezometer. They suggested that a piezometer of any shape could be represented by an equivalent surfaced spherical piezometer. Smiles and Youngs (1965) used an electric analogue model to measure directly shape factors for cylindrical cavities such as that in **Figure 2.33. a.** They found values 15 per cent higher than those obtained by Hvorslev (1951). Wilkinson (1968) extended Gibson's solution of spherical piezometers to establish the time dependent behavior of the flow rate into the casing in a cylindrical piezometer with pervious bottom. He noted utilizing finite difference method, that Hvorslev's expression slightly underestimated the shape factor and suggested that a more accurate value could be obtained by representing the cylinder as an inscribed prolate spheroid with its major axis adjusted so that its volume was equal to that of the cylinder (**Figure 2.33. b**). Al-Dhahir and Morgenstern (1969) applied a finite difference formulation of Laplace's equation to examine flow to cylindrical probes in an infinite porous medium for the case shown in **Figure 2.33. c.** Raymond and Azzouz (1969)

used a similar technique to obtain shape factors. Mieussens and Ducasse (1977) developed a solution for the case of the cylindrical probe with impervious ends (**Figure 2.33. e**), which is more representative of permeameters used in practice. They solved the governing equations for transient flow with consolidation for driven piezometers or selfboring permeameters and introduced an additional term for end effects but did not take into account the effects of partial penetration in a finite-depth water bearing formation. Dagan (1978) proposed numerical shemes for determining permeability of unconfined formations by recovery, packer and slug tests. He used this sheme to interpret constant head tests at steady-state. The limitation here is that the well screen length or the test section should be about 50 times larger than the well radius. For cases that this sheme is not applicable, Hayashi et al. (1987) proposed another analysis. They obtained the pressure distribution in the formation using Bessel function of the second kind of order n and the inversion theorem for the Laplace transformation and the Fourier cosine transformation. Brand and Premchitt (1980) used both a finite difference solution and an electrical analogy model to determine the shape factors applicable to a cylindrical probe with the geometry shown in **Figure 2.33. d.** They suggested a modification to Hvorslev's solution by using $1.2l$ instead of l. Randolph and Booker (1982) obtained a closed-form solution of Laplace's equation for a cylindrical probe (**Figure 2.33. e**), making an assumption on the flow velocity distribution around the probe. Tavenas et al. (1990) used a finite element method to provide a basis for evaluating the transient state observations in steady-state calculations. Chapuis (1989) proposed a correction for the shape factors considering impervious or recharging boundaries at finite distance as symmetrical planes between either discharging or recharging image piezometers. This technique of images gave a correction factor. Novakowski (1993) solved the governing equations similar to the one being presented. However, the main objective was to obtain the influences of the skin zone and the effects of partial penetration on the transient flow rates in constant head tests performed in confined clay formations. The unconfined case and the steady-state analysis was not given. Lastly, Hyder et al. (1994) used a finite element analysis to obtain a solution for the flow of groundwater to or from a partially penetrating well in an anisotropic medium and used this model to investigate errors in estimating the permeability by accepted practices.

The spatial variation of shape factor computations reflect the complexity of the investigations. The shape factors proposed by different researchers differ up to 100 per cent compared to Hvorslev. This can be better seen in **Figure 2.34.** There are a lot of factors that can affect the test results and analyses require assumptions that are always not possible to satisfy. Shape factors that are applicable to each individual case should be taken into consideration.

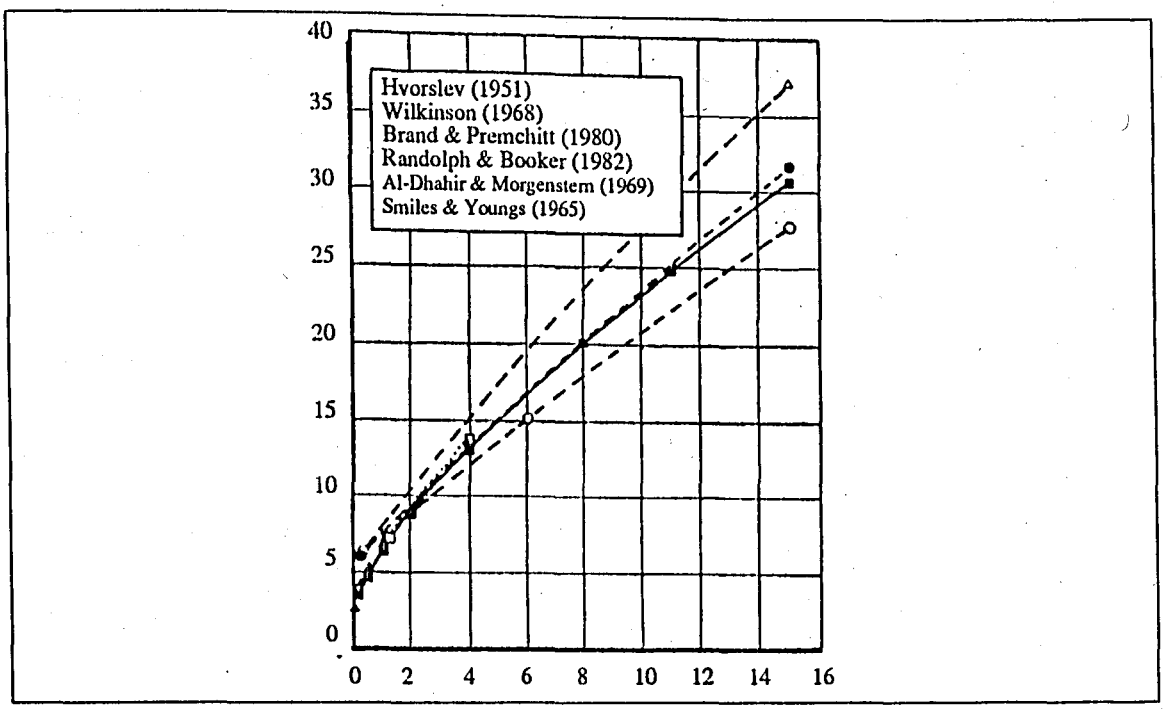

Figure 2. 34 : Comparison of shape factors computed by different authors for cylindrical piezometers

2. III. B. Methods Depending on the Seepage Velocities

Permeability calculations described in this section make use of the principle that permeability is related to the seepage velocity as follows:

$$k = v_s \cdot n_e / i$$

where n_e : the effective porosity

i: the hydraulic gradient

This equation allows the determination of the permeability of soil formations by methods that do not require pumping equipment. When, the velocity of the flowing water and the hydraulic gradient are known at a common point, the permeability can be estimated. Frequently, the hydraulic gradient of an existing water table can be estimated from wells in the area. If not, observation wells must be installed (Cedergren, 1967).

2. III. B. I. Use of an Electrolyte and Galvanometers. An electrolyte is inserted into a test hole and galvanometers are used to detect the time required for the electrolyte to pass a known distance through the soil.

2. III. B. II. Use of Radioactivated Charges and Geiger Counters. Radioactivated charges are used and geiger counters or other measuring instruments are utilized to determine the time required for the charge to travel a known distance through the soil.

2. III. B. III. Using Dyes. A dye such as fluorescein sodium is inserted into a test hole and observations are made to detect the time taken for it to emerge in a nearby test pit or on banks from which seepage is emerging.

The procedure used in these types of tests is illustrated in **Figure 2.35.** An electrolyte or radioactive charge is inserted into the sloping water table in hole A, the time for the charge to reach hole B is measured with suitable instruments and the seepage velocity is determined by dividing distance L by time t. The effective porosity n_e is determined from test data for the in-place soil, or if no tests are available it is estimated.

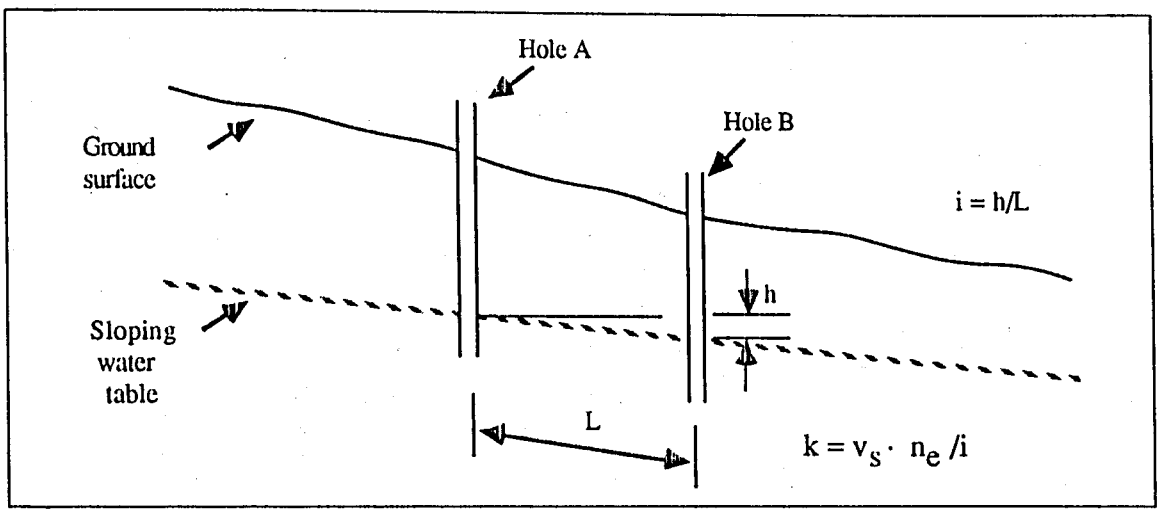

Figure 2. 35 : The typical arrengement for permeability by the seepage velocity method

When dyes or other tracers are used in measuring the velocity of groundwater for permeability determinations or other purposes, the relatively sluggish nature of moving groundwaters should not be overlooked. Unless the formations contain extremely permeable strata, the time required for tracers to move even short distances can be very long **(Table 2.8).**

Table 2. 8 : Relationship between permeability and rate of movement of groundwater ($n_e = 0.25$)

Permeability			**Time to move 30 cm**	
(cm/s)	**i**	**v_s (m/day)**	**Days**	**Hours**
$3{,}5 \cdot 10^{-6}$	0,01	$1{,}2 \cdot 10^{-4}$	2500	
	0,02	$2{,}4 \cdot 10^{-4}$	1250	
	0,05	$6{,}1 \cdot 10^{-4}$	500	
	0,10	$12{,}2 \cdot 10^{-4}$	250	
$3{,}5 \cdot 10^{-5}$	0,01	$1{,}2 \cdot 10^{-3}$	250	
	0,02	$2{,}4 \cdot 10^{-3}$	125	
	0,05	$6{,}1 \cdot 10^{-3}$	50	
	0,10	$12{,}2 \cdot 10^{-3}$	25	
$3{,}5 \cdot 10^{-4}$	0,01	$1{,}2 \cdot 10^{-2}$	25	600
	0,02	$2{,}4 \cdot 10^{-2}$	12,5	300
	0,05	$6{,}1 \cdot 10^{-2}$	5	120
	0,10	$12{,}2 \cdot 10^{-2}$	2,5	60
$3{,}5 \cdot 10^{-3}$	0,01	$1{,}2 \cdot 10^{-1}$	2,5	60
	0,02	$2{,}4 \cdot 10^{-1}$	1,3	30
	0,05	$6{,}1 \cdot 10^{-1}$	0,5	12
	0,10	$12{,}2 \cdot 10^{-1}$	0,25	6
0,035	0,01	1,2	0,25	6
	0,02	2,4	0,13	3
	0,05	6,1	0,05	1,2
	0,10	12,2	0,025	0,6
0,35	0,01	12	0,025	0,6
	0,02	24	0,013	0,3
	0,05	61	0,005	0,12
	0,10	122	0,0025	0,06

3. THEORETICAL SOLUTION

3.I. INTRODUCTION

Constant head field tests are recommended for soils with very low permeability; especially for clays. The methodology of conducting this type of test and analysis are depicted in the previous section.The constant head test model that is used to derive the equations is a cylindrical piezometer with an impervious bottom partially penetrating an anisotropic, finite-depth water bearing formation under confined or unconfined conditions at steady-state. **Figure 3.1 (a,b)** illustrates the piezometer and the hydrogeologic settings.

In the present analysis the equations governing the hydraulic head distribution in the soil are solved for the above conditions. The effects of partial penetration of the piezometer and the hydraulic boundary conditions at the upper and lower boundaries are considered within the analysis.

3. II. GOVERNING EQUATIONS

The thickness of the confined formation or the water column in the unconfined formation is represented by the variable D. The radial and vertical hydraulic conductivities, specific storage coefficient and specific yields are defined as K_r, K_z, S_c and S_y, respectively. The piezometer casing and screen radii are given by r_w and r_s whereas the screen length L is defined by the variables a and b representing the distance from the top and bottom of screen, respectively, to the confining lower boundary. A constant water level change h_o is imposed above the initial water level present in the casing through an inflow rate Q(t). The hydraulic head distribution in the formation is given by h(r, z, t). The cylindrical coordinate system used to define the governing ground water flow equation is shown in **Figure 3.1 (a,b)**.

The following variables are used to nondimensionalize the governing equations:

$$h_d = \frac{h}{h_0},\ h_{wd} = \frac{h_w}{h_0},\ t_d = \frac{t \cdot K_r}{r^2 \cdot S_c},\ r_d = \frac{r}{r_s},\ \gamma = \frac{L}{D} \qquad (3.1)$$

$$z_d = \frac{z}{r_s},\ S_d = \frac{S \cdot K_r}{r_s},\ Q_d = \frac{Q}{2\pi \cdot K_r \cdot L \cdot h_0},\ \zeta = \frac{K_z}{K_r},\ S_{yd} = \frac{S_y}{S_c \cdot r_s \cdot \zeta}$$

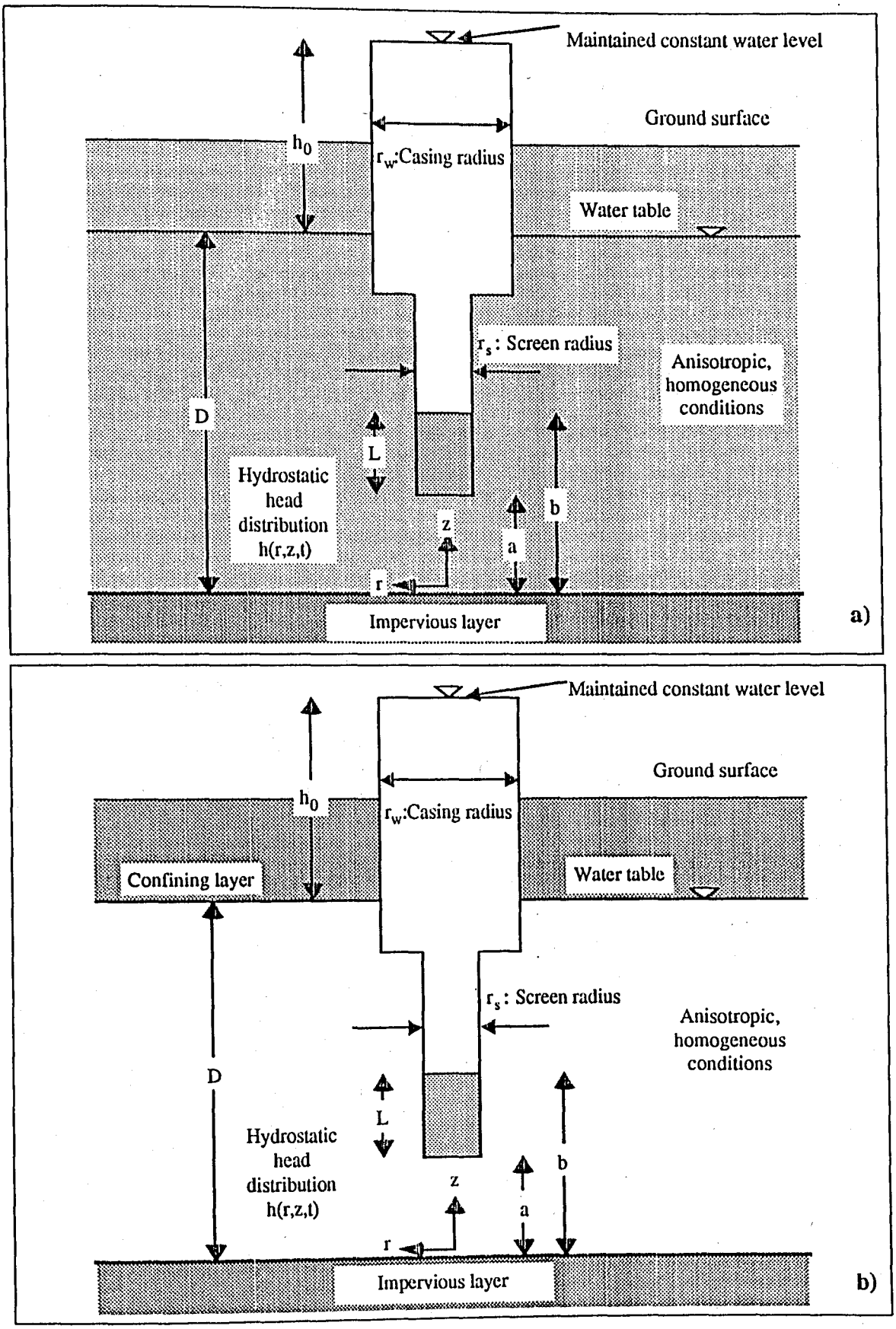

Figure 3. 1 : Schematic of the constant head in-situ test a)unconfined aquifer b) confined aquifer

The dimensionless equation governing the ground water flow during the constant head test is given by:

$$\frac{\partial^2 h_d}{\partial r_d^2} + \frac{1}{r_d}\frac{\partial h_d}{\partial t_d} + \zeta \frac{\partial^2 h_d}{\partial z_d} = \frac{\partial h_d}{\partial t_d} \qquad (3.2)$$

There are accompanying conditions which must be formulated to complete the mathematical statement of the problem. Two options are available for specifiying the conditions existing along the screened zone of the piezometer: either the hydraulic head or the flux across the screen can be assumed to be constant with respect to depth. Constant flux conditions across the screen were selected as boundary conditions for the present investigation based on the successful match between theory and field data obtained in variable head test data analysis by Avcı and Kılanç (1994) using constant flux conditions across the screened zone and formulated as:

$$Q_d = -\frac{\partial h_d}{\partial r_d}\Big|_{r_d = 1} \qquad (3.3)$$

The constant hydraulic head at the casing is equated to the hydraulic head in the water bearing formation at the screened zone by taking into account the losses that occur across the screen as well as any smear zone which might have been created during the installation of the piezometer as follows:

$$1 = h_d^*\Big|_{r_d = 1} - S_d \frac{\partial h_d}{\partial r_d}\Big|_{r_d = 1} \qquad (3.4)$$

where S_d represents the dimensionless skin factor (Sageev, 1986) taking into account the head losses between the screened zone and the undisturbed portion of the water bearing zone. The average head in the screen is given by:

$$h_d^*\Big|_{r_d = 1} = \frac{1}{L_d}\int_{a_d}^{b_d} h_d\Big|_{r_d = 1}\, dz_d \qquad (3.5)$$

The flux conditions along the cylindrical area above and below the screened zone are formulated as:

$$\frac{\partial h_d}{\partial r_d}\Big|_{r_d = 1} = 0 \quad z_d < a_d \text{ and } z_d > b_d \qquad (3.6)$$

Several boundary condition options exist for the upper horizontal extent of the water bearing formation which must be individually examined:

Confined conditions:

$$\frac{\partial h_d}{\partial r_d} = 0 \quad z_d = 0, D_d \tag{3.7}$$

Unconfined conditions:

$$\text{a)} \quad h_d = 0 \quad z_d = D_d \; ; \; \frac{\partial h_d}{\partial z_d} = 0 \quad z_d = 0 \tag{3.8}$$

$$\text{b)} \quad S_{yd} \frac{\partial h_d}{\partial t_d} = - \frac{\partial h_d}{\partial z_d} \quad z_d = D_d \; ; \; \frac{\partial h_d}{\partial z_d} = 0 \quad z_d = 0 \tag{3.9}$$

Type a) unconfined boundary conditions are equivalent to stating that initial water level present in the formation will remain constant throughout the testing period and will not increase from the influx of water; this condition may occur if the permeability of the formation is low or the screened zone is located well below the initial water level elevation. Type b) unconfined boundary conditions, on the other hand, are formulated to take into account possible increases in the water table which may occur from the influx of water into the formation. The rate of increase in the level of the saturation surface is related to the velocity of the water particle at the surface through the specific yield and hydraulic conductivity parameters; this boundary condition formulated by Neuman (1972) was successfully applied in the analysis of well pump test in unconfined aquifers.

The initial conditions are given by:

$$h_d = 0 \; , \; h_{wd} = 1 \; , \; t_d = 0 \tag{3.10}$$

3.III. SOLUTION PROCEDURES

The aim of the analysis is to obtain an expression for inflow rate Q_d (t) in the Laplace for confined and unconfined water bearing formations using the previously derived governing equation and corresponding boundary conditions; these expressions can then be inverted into the real time domain using numerical methods to establish the

behavior of the inflow rate during constant head tests. This is a common method used in the development of analysis procedures for in-situ permeability tests (Moench and Ogata, 1984; Karasaki et al., 1988; Novakowski, 1993 and Avcı 1994). The Laplace expressions for the inflow rate were obtained using the Laplace and Fourier transforms; this solution procedure has previously been used by several investigators including Dougherty and Babu (1984) in the investigation of hydraulic problems in fractured porous reservoirs, Novakowski (1993) in the analysis of transient inflow rates in constant head tests performed in clay formations and Avcı and Kılanç (1994) in the study of variable head tests in partially penetrating wells.

The Laplace transform defined as:

$$\bar{h}_d = \int_0^{\infty} e^{-pt_d} \cdot h_d \, dt_d \qquad (3.11)$$

is applied to the dimensionless equation and boundary conditions to yield:

$$\frac{\partial^2 \bar{h}_d}{\partial r_d^2} + \frac{1}{r_d}\frac{\partial \bar{h}_d}{\partial r_d} + \zeta \frac{\partial^2 \bar{h}_d}{\partial z_d^2} = p \cdot \bar{h}_d \qquad (3.12)$$

$$\bar{Q}_d = -\frac{\partial \bar{h}_d}{\partial r_d}\Big|_{r_d = 1} \qquad (3.13)$$

$$\frac{1}{p} = \bar{h}_d^*\Big|_{r_d = 1} - S_d \frac{\partial \bar{h}_d}{\partial r_d}\Big|_{r_d = 1} \qquad (3.14)$$

$$\frac{\partial \bar{h}_d}{\partial r_d}\Big|_{r_d = 1} = 0 \quad z_d < a_d \text{ and } z_d > b_d \qquad (3.15)$$

The Laplace expressions for the conditions along the upper and lower extent of the water bearing formation become:

Confined conditions:

$$\frac{\partial \bar{h}_d}{\partial r_d} = 0 \quad z_d = 0, D_d \qquad (3.16)$$

Unconfined conditions:

$$a)\ \bar{h}_d = 0 \quad z_d = D_d; \quad \frac{\partial \bar{h}_d}{\partial r_d} = 0 \quad z_d = 0 \tag{3.17}$$

$$b)\ p \cdot S_{yd} \cdot \bar{h}_d = -\frac{\partial \bar{h}_d}{\partial r_d} \quad z_d = D_d; \quad \frac{\partial \bar{h}_d}{\partial r_d} = 0 \quad z_d = 0 \tag{3.18}$$

The derivation of $\bar{Q}_d$ for the constant head test performed under confined conditions is explained in the following sections. The expression for $\bar{h}_d$ is taken to be an infinite series expansion as follows:

$$\bar{h}_d = \sum_{n=0}^{\infty} \alpha_n (r_d, p) \cdot \cos\left(\frac{n \cdot \pi \cdot z_d}{D_d}\right) \tag{3.19}$$

which automatically satisfies the confined aquifer boundary conditions. The following expression is obtained from Equation (3.12):

$$\sum_{n=0}^{\infty} \left[\frac{d^2 \alpha_n}{dr_d^2} + \frac{1}{r_d} \frac{d\alpha_n}{dr_d} - \left(p + \frac{\zeta n^2 \pi^2}{D_d^2} \right) \alpha_n \right] \cos\left(\frac{n \cdot \pi \cdot z_d}{D_d}\right) = 0 \tag{3.20}$$

The following ordinary differential equation is obtained from this expression:

$$\frac{d^2 \alpha_n}{dr_d^2} + \frac{1}{r_d} \frac{d(\alpha_n)}{dr_d} - \left(\rho + \frac{\zeta \cdot n^2 \cdot \pi^2}{D_d^2} \right) \alpha_n = 0 \tag{3.21}$$

The solution to the above ordinary differential equation is given by:

$$\alpha_n = \beta_n(p) \cdot K_0(g_n r_d) \qquad n = 0,1,2,\cdots \tag{3.22}$$

where K_0 is the modified Bessel function of the second kind of order zero and:

$$g_n = \left[p + \frac{\zeta n^2 \cdot \pi^2}{D_d^2} \right]^{1/2} \tag{3.23}$$

The hydraulic head distribution is given by:

$$\bar{h}_d = \sum_{n=0}^{\infty} \beta_n \cdot K_0(g_n r_d) \cdot \left(\frac{n \cdot \pi \cdot z_d}{D_d} \right) \qquad (3.24)$$

The unknown β_n are determined using the flux boundary along the screen and casing conditions as follows:

$$\frac{\partial \bar{h}_d}{\partial r_d}\Big|_{r_d = 1} = \begin{cases} 0 & z_d > b_d \\ -\bar{Q}_d & a_d < z_d < b_d \\ 0 & z_d < a_d \end{cases} \qquad (3.25)$$

The β_n coefficients are obtained using the following expression:

$$-\int_0^{D_d} \frac{\partial \bar{h}_d}{\partial r_d}\Big|_{r_d = 1} \cos\left[\frac{n \cdot \pi \cdot z_d}{D_d} \right] dz_d \quad n = 0,1,2\cdots \qquad (3.26)$$

with Equations (3.25) and the derivative of Equation (3.19) with respect to the radius as follows:

$$\beta_n = \frac{\bar{Q}_d}{-g_o K_1(g_o)} \qquad (3.27)$$

$$\beta_n = \frac{2\bar{Q}_d}{-g_n \cdot K_1(g_n) \cdot n \cdot \pi} \left[\sin\left(\frac{n \cdot \pi \cdot b_d}{D_d} \right) - \sin\left(\frac{n \cdot \pi \cdot a_d}{D_d} \right) \right] \quad n > 0 \qquad (3.28)$$

The expression for $\bar{h}_d$ becomes:

$$\bar{h}_d = \frac{\bar{Q}_d}{-g_0 \cdot K_1(g_0)} \cdot K_1(g_0 r_d) + -\frac{2\bar{Q}_d}{\pi} \sum_{n=1}^{\infty} \frac{K_0(g_n r_d)}{g_n K_1(g_n) n} \left[\sin\left(\frac{n \cdot \pi \cdot b_d}{D_d} \right) - \sin\left(\frac{n \cdot \pi \cdot a_d}{D_d} \right) \right] \cos\left(\frac{n \cdot \pi \cdot z_d}{D_d} \right) \qquad (3.29)$$

The average hydraulic head in the screened zone is given by:

$$\bar{h}_d^*\Big|_{r_d = 1} = \frac{\bar{Q}_d}{g_0 \cdot K_1(g_0)} \cdot K_0(g_0) + -\frac{2\bar{Q}_d}{\gamma \cdot \pi^2} \sum_{n=1}^{\infty} \frac{K_0(g_n)}{g_n \cdot K_1(g_n) \cdot n^2} \left[\sin\left(\frac{n \cdot \pi \cdot b_d}{D_d} \right) - \sin\left(\frac{n \cdot \pi \cdot a_d}{D_d} \right) \right]^2 \qquad (3.30)$$

Equation (3.14) is formulated as follows:

$$\frac{1}{p} = \bar{Q}_d \cdot A + - S_d \cdot \bar{Q}_d \qquad (3.31)$$

where:

$$A = \frac{K_0(g_0)}{g_0 \cdot K_1(g_0)} + \frac{2}{\gamma \cdot \pi^2} \sum_{n=1}^{\infty} \frac{K_0(g_n)}{g_n \cdot K_1(g_n) \cdot n^2} \left[\sin\left(\frac{n \cdot \pi \cdot b_d}{D_d}\right) - \sin\left(\frac{n \cdot \pi \cdot a_d}{D_d}\right) \right]^2 \qquad (3.32)$$

Equations (3.32) yields the following expression for $\bar{Q}_d$

$$\bar{Q}_d = \frac{1}{p\,(A + S_d)} \qquad (3.33)$$

The settings for unconfined water bearing formations can be solved in a similar procedure depicted in the preceding sections. The expressions for $\bar{Q}_d$ remain the same while the variable A are determined to be as follows:

Unconfined a) condition

$$A = \frac{\gamma \cdot K_0(g_0)}{g_0 \cdot K_1(g_0)} + \frac{2}{\gamma \cdot \pi^2} \sum_{n=1}^{\infty} \frac{K_0(g_n)}{n^2 \cdot g_n \cdot K_1(g)} \left[\sin\left(\frac{n \cdot \pi \cdot b_d}{D_d}\right) - \sin\left(\frac{n \cdot \pi \cdot b_d}{D_d}\right) \right]^2 \qquad (3.34)$$

where

$$g_n = \left(p + \frac{\zeta \cdot n^2 \cdot \pi^2}{D_d} \right)^{1/2} \qquad (3.35)$$

Unconfined b) Condition

$$A = \frac{2}{\gamma} \sum_{n=1}^{\infty} \frac{K_0(g_n) \left[\sin\left(\frac{\rho_n \cdot b_d}{D_d}\right) - \sin\left(\frac{\rho_n \cdot a_d}{D_d}\right) \right]^2}{g_n \cdot K_1(g_n) \cdot \rho_n \left[\rho_n + \frac{\sin(2\rho_n)}{2} \right]} \qquad (3.36)$$

where

$$g_n = \left(p + \frac{\zeta \cdot \rho_n^2}{D_d^2} \right)^{1/2} \qquad (3.37)$$

and ρ_n is obtained from the solutions of

$$\tan(\rho) = \frac{\rho \cdot S_{yd} \cdot D_d}{\rho} \qquad (3.38)$$

4. TESTING DEVICE AND METHODOLOGY

4.I. TEST SET - UP

The testing set-up was inspired and improved from the experimental studies of Chapuis et al. (1990), Smiles and Youngs (1965) and Gefell et al. (1994). Chapuis et al. used a circular tank of height 122 centimeters and of diameter of 61 centimeter. They introduced water from a circular model well centered in the tank and obtained shape factors for various conditions. Smiles and Youngs' study which had a square plan and larger dimensions (10 · 10 · 15 cubic meters) compared values obtained from different analysis methods with those from their laboratory tests. Gefell et al. studied the maximum drawdown in a well with data from the oservation wells. These three studies all used sand as the testing material.

A circular tank was built in order to evaluate the pressure distribution in the soil. The tank consisted of an inner diameter of one meter and an outer diameter of 1.02 meter. The height of the tank was 1.2 meters. The test set-up is shown in **Figure 4.1.** The thickness of the pipe was one centimeter. The total weight of the tank was approximately one ton. The tank could move around on the four wheels situated on the bottom. Drainage was provided through the opening at the bottom center.

The tank consisted of three equally sized parts of 40 centimeters for convenience. The parts were connected to each other with a flange that had the same inner diameter as the outer diameter of the steel pipe and an outer diameter of 1230 millimeters; i.e. the flange was 10.5 centimeters wide. The thickness of the flange was three centimeters and it had holes for steel bolts of 33 millimeters. The bolts were 10 centimeters long. Parts were tightened using steel nuts, washers and spring washers.

A clinker of five millimeters thickness was used to ensure that there was no leakage between the parts. Silicon seals were also used to secure water-tightness.

The middle and upper part of the pipe were open on the sides to holes for the piezometers and enable water head readings at various depths and distances of the partially penetrating model well when the constant head that was applied. The water head pressure readings were taken on the six millimeter plastic pipes that were covered with geotextile and connected to each other by a wooden support. There were three holes on the middle

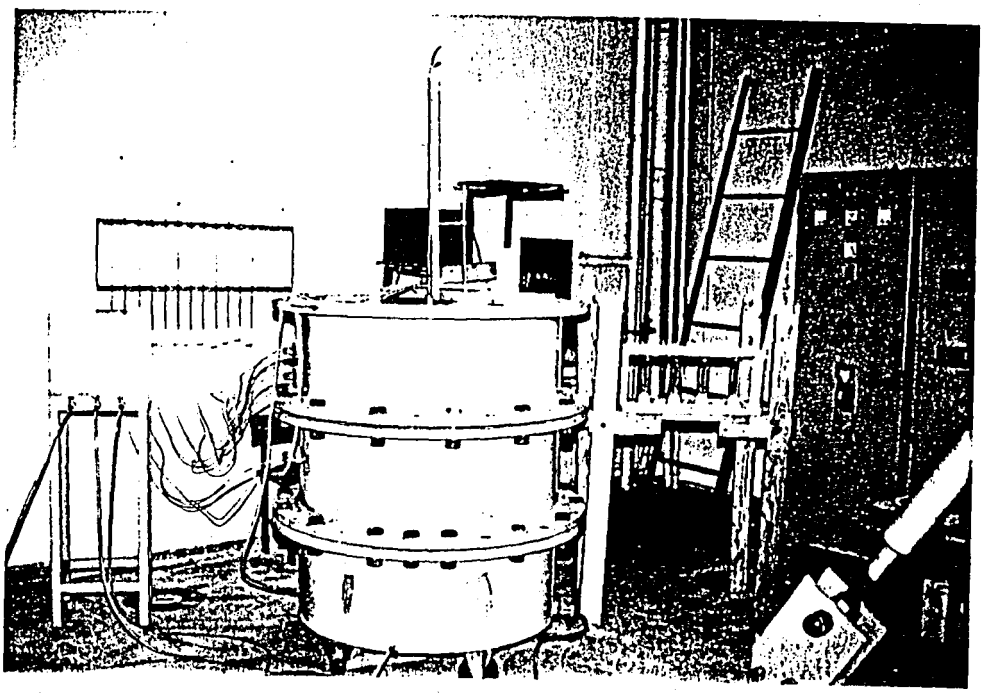

a

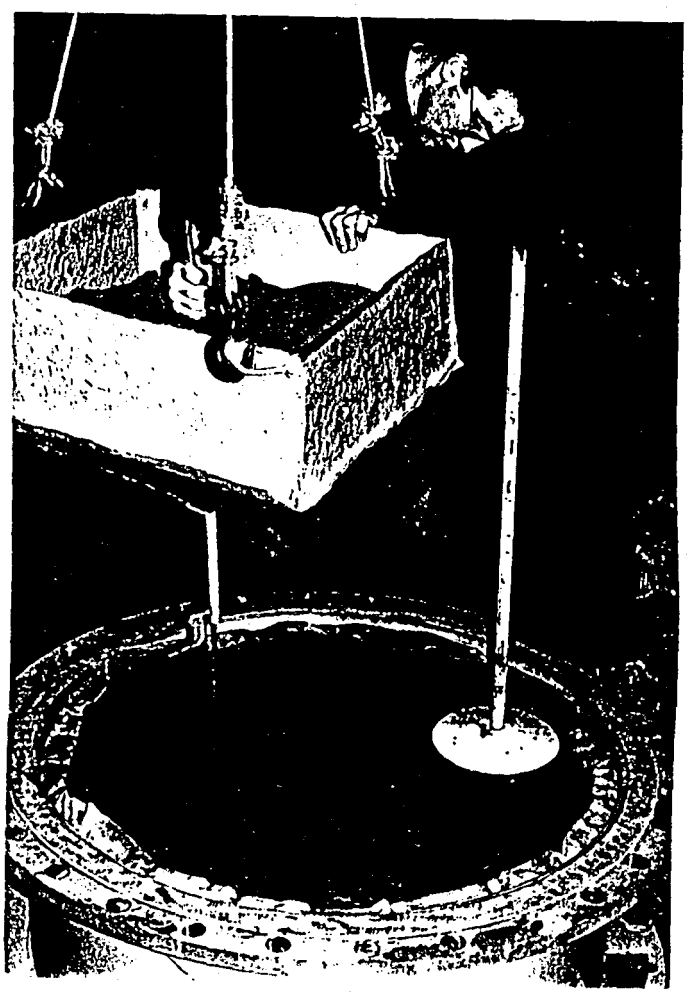

b

Figure 4. 1: Various views of the testing device: a) general view b) sand laying procedure (funnel and compactor)

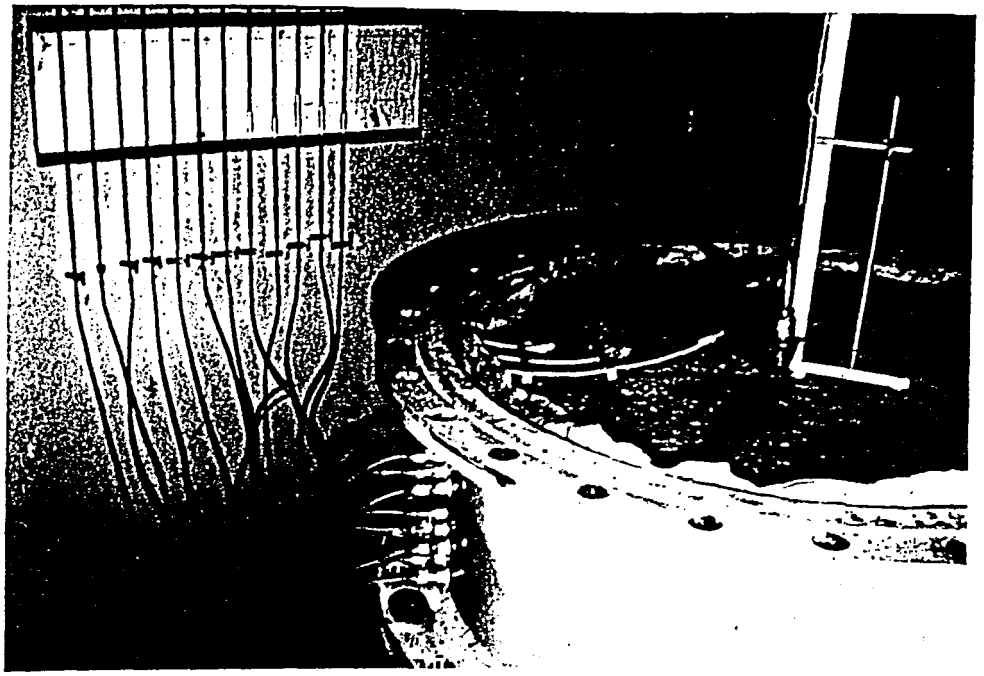

c

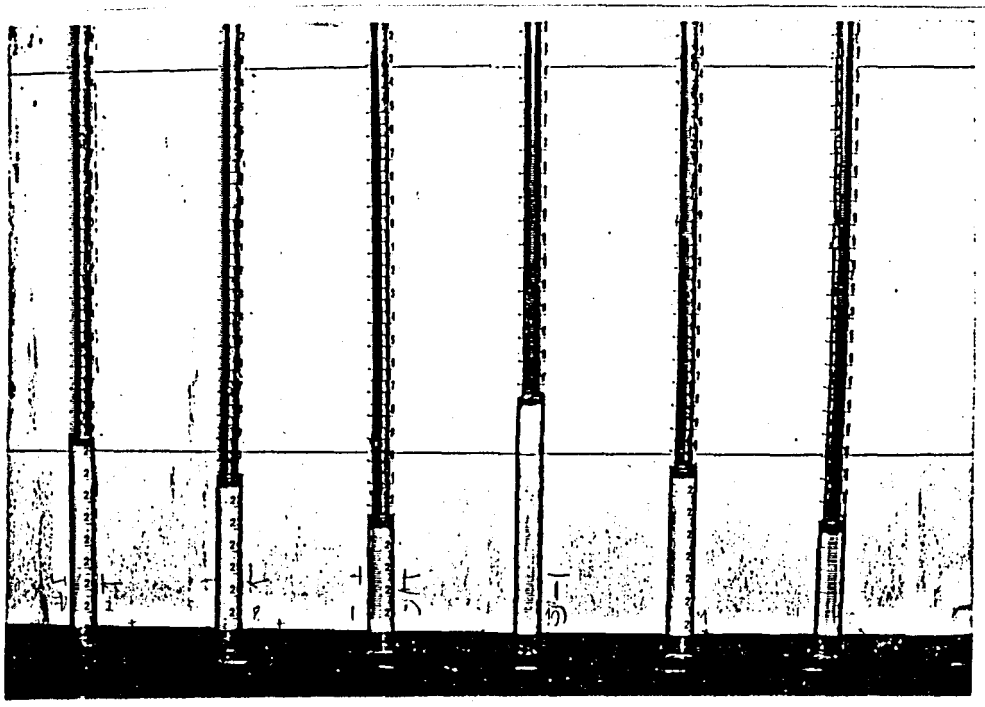

d

Figure 4. 1: Various views of testing device (continued): c) the placement and location of the piezometer d) the pore-water pressures as observed in the piezometer

part and nine on the upper part. Holes were placed three on the same horizontal plane. The vertical distances from the surface of the tank (**Figure 4.2, 4.3**) were 20, 30, 35 and 60 centimeters. On each hole a valve was placed to control the in- and outflow of water. The valves were connected to the piezometers with plastic pipes of six millimeters outer diameter. Piezometers consist of burettes, that is graduated cylinders that were equally divided at every millimeter for 50 milliliters. A correction factor was applied to the levels that were recorded versus time to obtain right values of water head build-ups.

The water was introduced into the pipe and the material placed in the tank through a 2.04 centimeter inner and 2.7 centimeter outer diametered pipe that was 40 centimeters long. The bottom 20 centimeters of the tank were perforated acting as a screen with a closed tip. The screen was covered with geotextile that was used for filter designs.

The constant head that was injected through the model well was applied by the water reservoir. The reservoir had a square cross-section of 36 centimeters and 28 centimeters height. These connections were made with 12 millimeter plastic pipes. The applied water was controlled with a valve that was opened at the beginning of the test. The water level was kept constant at 30 centimeters by a floater. The floater opened the valve to the tap when there was a drop in the water level. The water coming into the constant head tank first flowed through a watermeter. The watermeter could measure flows of one 10000'th of a cubic meter, i.e. its sensivity was 100 milliliters.

The water was initially introduced from the four valves at the bottom of the tank with the help of another reservoir. This was continued until the desired saturated thickness was reached.

The inside of the main circular tank was covered on the sides and on the bottom with very permeable geotextile utilized for drainage purposes.

The sand was laid with a pouring funnel that had a single opening. The funnel had a square top of 58 centimeters and a triangular prism of height 30 centimeters. The opening had a 1.5 centimeter diameter and a 20 centimeters length. The pouring funnel served for one layer of sand in the tank when it was about filled to the top. The average height of the funnel's opening to the bottom of the tank or the last laid layer was 44.5 centimeters.

The sand was compacted to the desired relative density and height with a circular compacting device weighing nine kilograms. The compaction method was to simply drop the weight from 40 centimeters until the desired height was reached. The sand was laid dry.

The excess water that penetrated the aquifer was taken out through the four valves on the bottom of the main tank. The outflow from these were collected separately in graduated cylinders of 250 milliliters capacity. The level of the collection was the same as the water level of the initial saturated thickness of the aquifer.

Tap water was used during the test. This was deemed to be more representative of natural conditions.

The model tank, having a one meter inside diameter and filled with sand, modeled the field conditions. The boundary conditions were:

- the aquifer was unconfined
- the aquifer had a finite radial extent
- the aquifer was homogeneous
- the aquifer had a finite depth
- the well was partially penetrating.

The finite radial extent was obtained by the placement of geotextile on the sides. The water that passed through the formation and reached the geotextile went directly to the bottom outlet that was discharged into the graduated cylinders each of 250 milliliters capacity. The geotextile on the sides and bottom mainly served for drainage purposes. The sides were assumed to have the same water head, i.e. the water head gradually decreased towards the sides.

The tank was divided into three parts just for simplicity: three parts of 40 centimeters are easier to handle than one big tank of 120 centimeters. Another reason was the system flexibility. The height could vary from a minimum of 40 centimeters to any height with additional parts.

The piezometer inlets were covered with geotextile. The geotextile kept the piezometers from getting clogged by particles that could be carried in with the flowing water ("wash-out effect"). Water could only penetrate into the piezometer from the tip of it.

The sand was laid with a pouring funnel for the following reasons:

1) the test could be reproduced for subsequent trials, and

2) the sand could be laid uniformly in the tank so that stratification could be avoided. This was done by the constant rate of intensity of the sand raining procedure.

Sand was placed inside the tank before water was introduced to minimize the grain-size stratification and achieve a relatively homogeneous aquifer medium.

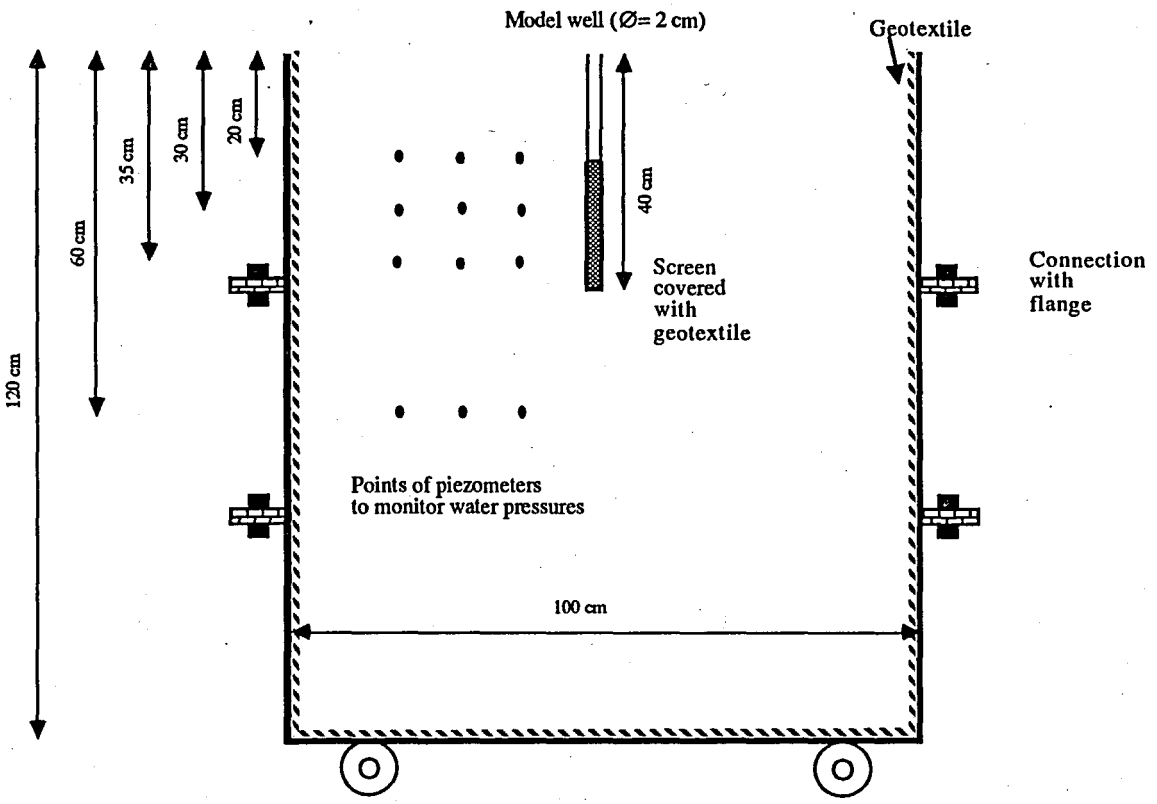

Figure 4. 2: The schematical unconfined aquifer model and the arrengement of the piezometers (the A - A section)

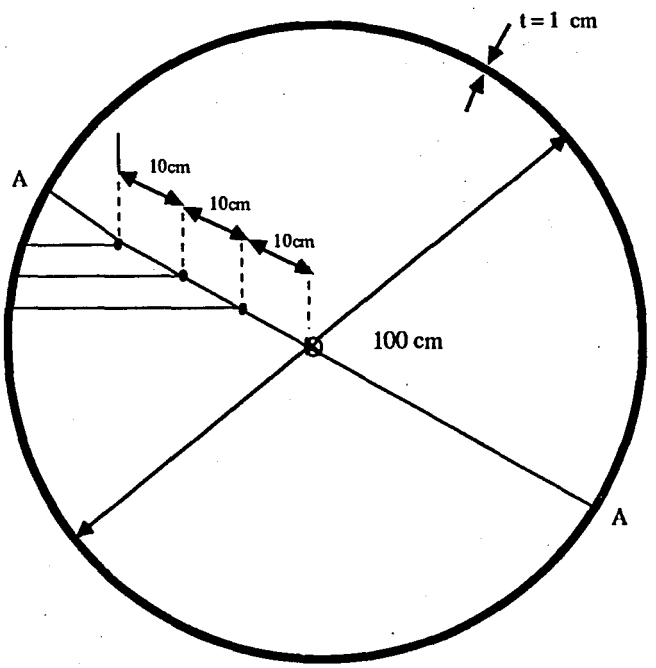

Figure 4. 3: The plan of the aquifer model

4.II. THE MATERIAL

The silty-sand that served as the aquifer medium was brought from Kilyos, İstanbul. The material was taken directly from nature and was dried and sifted through a one millimeter opening sieve. The properties of the tested soil are depicted in **Table 4.1.**

Table 4. 1: The properties of the testing material and the material in the tank

PROPERTIES OF THE TESTING MATERIAL

Sand (%)	85.2
Silt (%)	14.8
D_{60} (mm)	0.19
D_{10} (mm)	0.7
D_{30} (mm)	0.16
C_u	0.27
C_c	0.19
w_L (%)	19
w_P (%)	N.P.
w_{opt} (%)	14
$\gamma_{k_{max}}$ (kN/m^3)	17.51
k (cm/s)	1 ◊ 10^{-2}
USC	SM
AASHTO	A - 2 - 6
e_{max}	1.25
e_{min}	0.59

THE MATERIAL IN THE TANK

Dry	
D_r (%)	70
9 cm layers 107 kg for each layer Compaction 9 kg's from 40 cm	

4.III. THE METHODOLOGY

The test started first with the placement of the very pervious geotextile on the sides and bottom of the bottom 40 centimeters of the circular tank. This was followed by the filling of the pouring funnel specially designed for nine centimeter 107 kilogram lifts. After every lift the sand was compacted to nine centimeter height with a compactor that weighs nine kilograms and that has a circular cross-section diameter of 15 centimeters. The

compaction effort continued until the elevations reach the plane for the piezometers to be placed. These planes are 60 centimeters, 85 centimeters, 90 centimeters and 100 centimeters from the bottom.

The piezometers are plastic pipes open only at the tip allowing the water levels to be measured.

The geotextile on the side was cut into three pieces due to the difficulty of holding it upright and in place. Each part was sewn to the previous one after the completion of the sand laying of the main circular tank. The model well was centered when the level of the sand in the tank reached 80 centimeters. The tank was filled to the top with this model well in place.

The water was introduced from the bottom to prevent air from getting clogged in the voids of the tested material. The rise of the water level was measured with a pipe at the bottom and by the piezometers. The desired level was 100 centimeters from the bottom (Stage I) **(Figure 4. 4).**

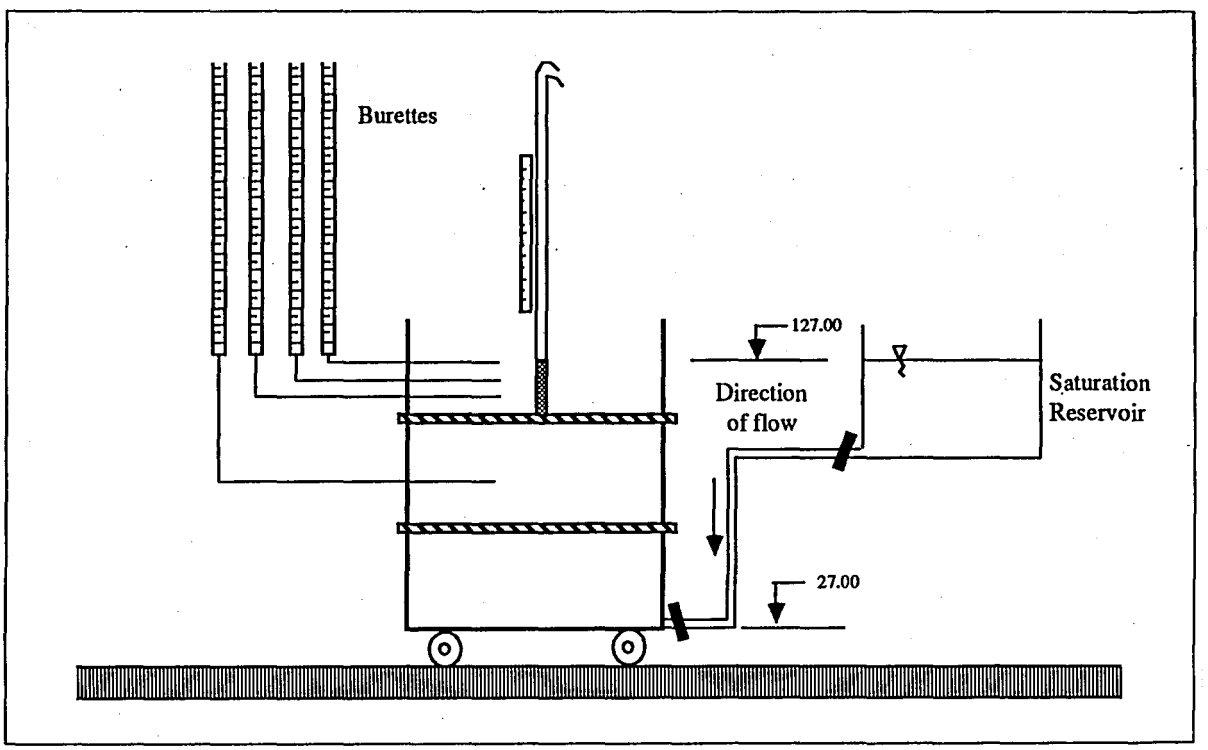

Figure 4. 4: The schematic of the saturation process (Stage I)

The constant head reservoir applied a 50 centimeter head taking the initial water level as the datum. This was kept constant by a floater (Stage II) **(Figure 4.5).**

The rise of the water in the piezometers was recorded. The amount of outflow from the bottom was collected in volumetrically graduated cylinders. The constant water level in the model well was controlled with a meter. The inflow was monitored by the watermeter at the inlet of the reservoir.

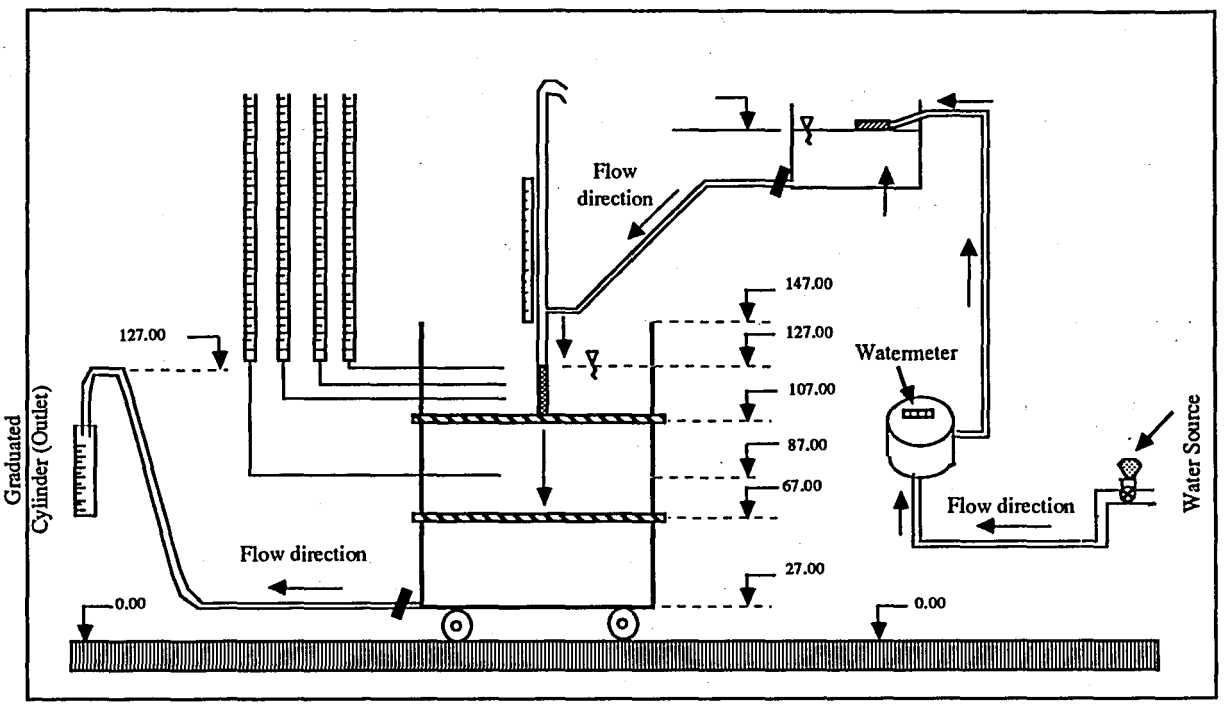

Figure 4. 5: Recharging of the model well and monitoring (Stage II)

The test was run until there was no rise of water in the piezometers or until the hydraulic gradient equalized. Thus, the duration of the test was approximately 25 minutes.

A simple flow chart explaining the general testing procedure is presented in **Figure 4.6.**

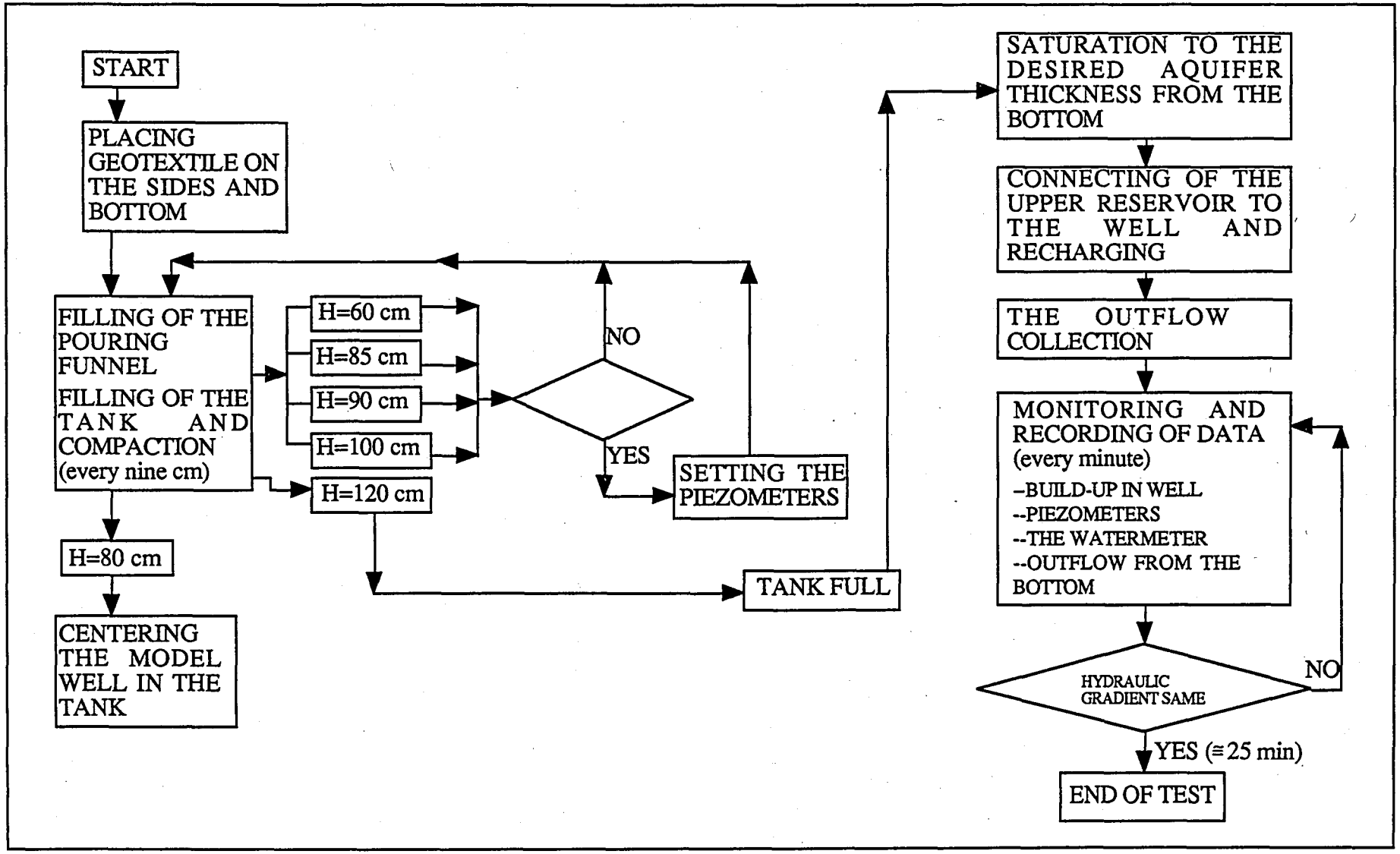

Figure 4. 6 : Flow chart of the test

5. RESULTS AND EVALUATION

The conducted experiments measured the buildup in piezometer that were at 20 centimeter, 30 centimeter, 35 centimeter and 60 centimeter depth from the top of the tank and at 10 centimeter, 20 centimeter and 30 centimeter radius from the model well in the center. The results of the observations are presented in **Figures 5.1** through **5.3** for various radiuses. Here the piezometer at the same vertical plane are plotted. The expression for the legends is the same for all the graphs given as the depth over the radial distance. For example, 60/10 means that the piezometer is located at 60 centimeter depth from the top of the tank and at 10 centimeter radially from the centered model well.

It can be seen from Figure 5.1 that the water head in the piezometer at 60 centimeters depth developed slower than the others. This was due to the closed tip of the model well and due to the distance of the location of the piezometer. The difference decreased when the radius was 20 centimeter (Figure 5.2) and for 30 centimeter (Figure 5.3) it vanished. This trend was measured at every testing. Nevertheless, the progress of each graph is similar to each other. The increase of the water heads is rapid in the beginning, but it steadily decreases with time. The graphs of the some other tests are presented in **Appendix A.**

Figures 5.4 through **5.7** show measurements at the same radial plane plotted at the semi-logarithmic scale. The measurements were the same ones as the Figures 5.1, 5.2 and 5.3. The piezometer readings closest to the model well showed a higher value than the other two that are located further. The graphs are curved in the beginning which follows the same pattern as the rapid increase at the early stages of the test. The graphs become almost linear after a certain time interval and at about the end where a steady-state was barely reached, the graphs form a lateral plot. Further semi-logarithmic plots of different tests are presented in **Appendix B.**

The water levels of each piezometer in time are depicted in **Figures 5.8** through **5.12.** The differences were higher at the first six minutes. Then the differences got smaller as this is visual by the densification of the plots. The water levels at the same radial plane showed a steeper decline from 10 centimeter to 20 centimeter than that from 20 centimeter to 30 centimeter which is similar to the previous graphs. The effect of recharging was not very significant at 60 centimeters depth. The changes and the levels of piezometric heads at

this depth were very close to each other and generally the piezometer at 30 centimeter radius gave higher measurements than those of 20 centimeter.This was not seen at other depths. The further graphs obtained are provided in **Appendix C.**

The match between the proposed mathematical model and the test results are given in **Figures 5.13, 5.14** and **5.15.** The 60 centimeter depth was neglected in light of the insignificant effect of recharging at this depth. The variables used in the mathematical model were the radial hydraulic conductivity of $1 \cdot 10^{-6}$ m/s, the anisotrophy ratio of 1 which states that the vertical and the radial permeabilities are the same, the storage coefficient of 0.01 and the skin friction of zero. The match of the plots of mathematical model to the test results for radiuses 10 centimeter and 20 centimeter gave a weak correlationce. However, 30 centimeter match is quite well, especially at 20 and 30 centimeter depths. It can be seen that the progress of both graphs are of a similar trend. The match of results of some other testings are shown in **Appendix D.**

An attempt was made to obtain the appropriate match between the mathematical model and the measurements taken. **Figure 5.16** shows the match at 20 centimeter depth. The measurements taken at 10 centimeter radius was matched with 21 centimeter, 20 centimeter readings with 25 centimeter and the 30 centimeter with 28 centimeter by using the same variables as in the previous analysis. For 30 centimeter depth (**Figure 5.17**) the matched radiuses were 22 centimeter, 25.5 centimeter and 29 centimeter for 10, 20 and 30 centimeter, respectively. For 35 centimeter these were 23, 26 and 28 centimeter (**Figure 5.18**) for the same variables of the material and the geometry of the testing device and model well.

There was difference observed in the amount of water collected from the bottom in the graduated cylinders and the amount of water charged from the constant head reservoir that is measured with the watermeter. Tests were conducted to obtain the correlation of this phenomenon. Water was taken out of the system until the watermeter starts to measure the flow and then the amounts were compared. **Figure 5.19** shows the measurements taken from the watermeter over the actual amount of flow.

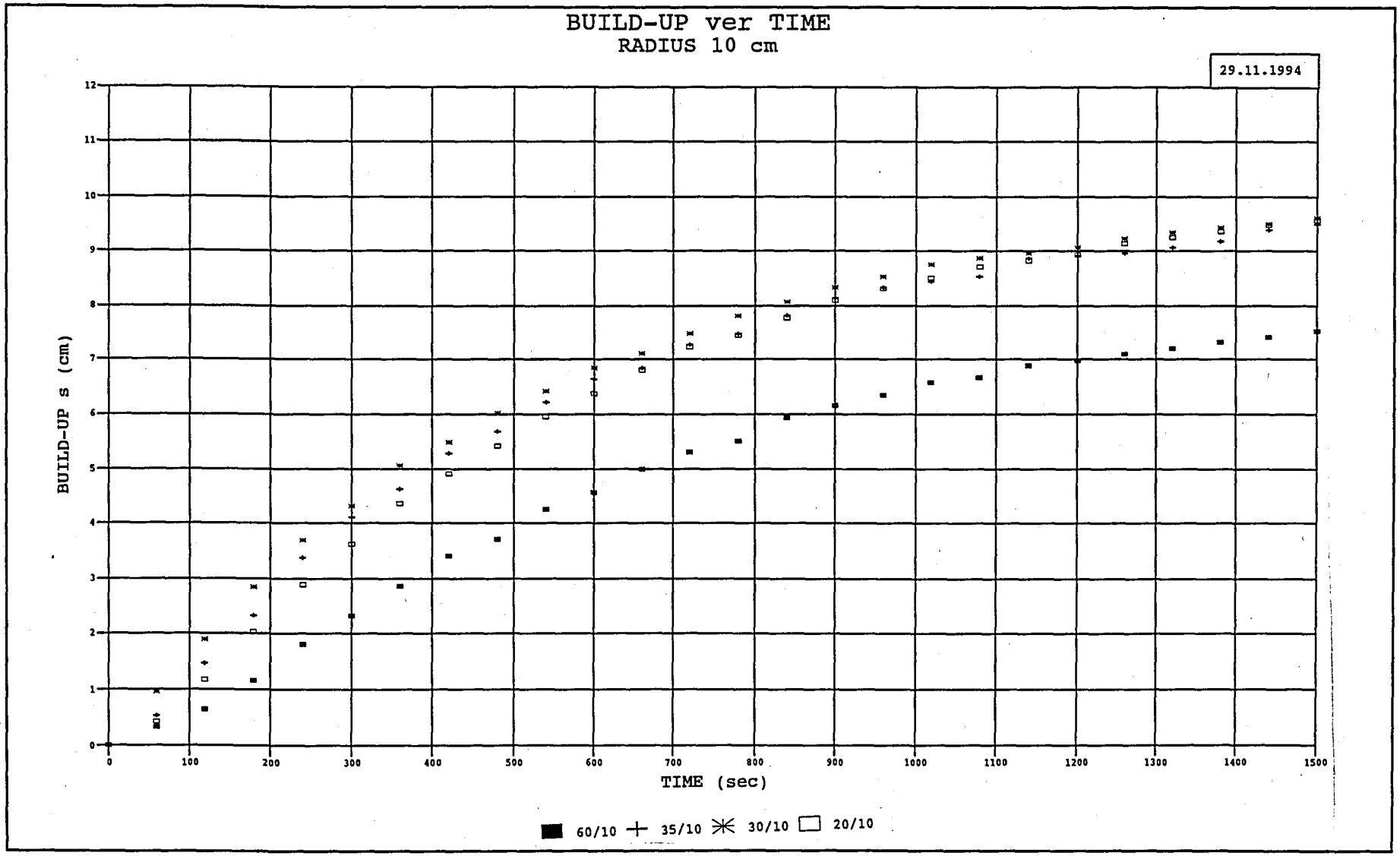

Figure 5.1 : Test results at piezometers at various radiuses

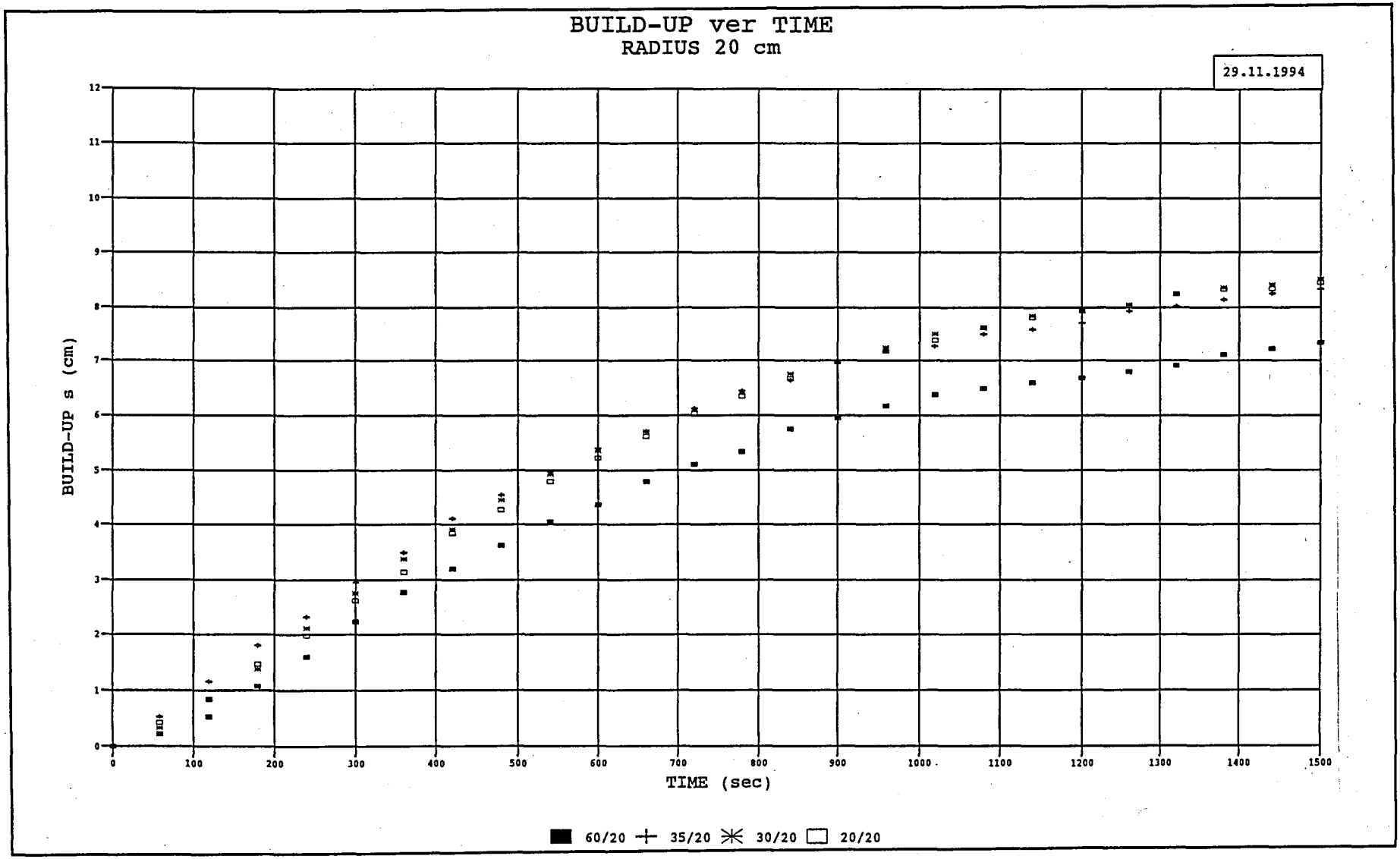

Figure 5.2 : Test results at piezometers at various radiuses

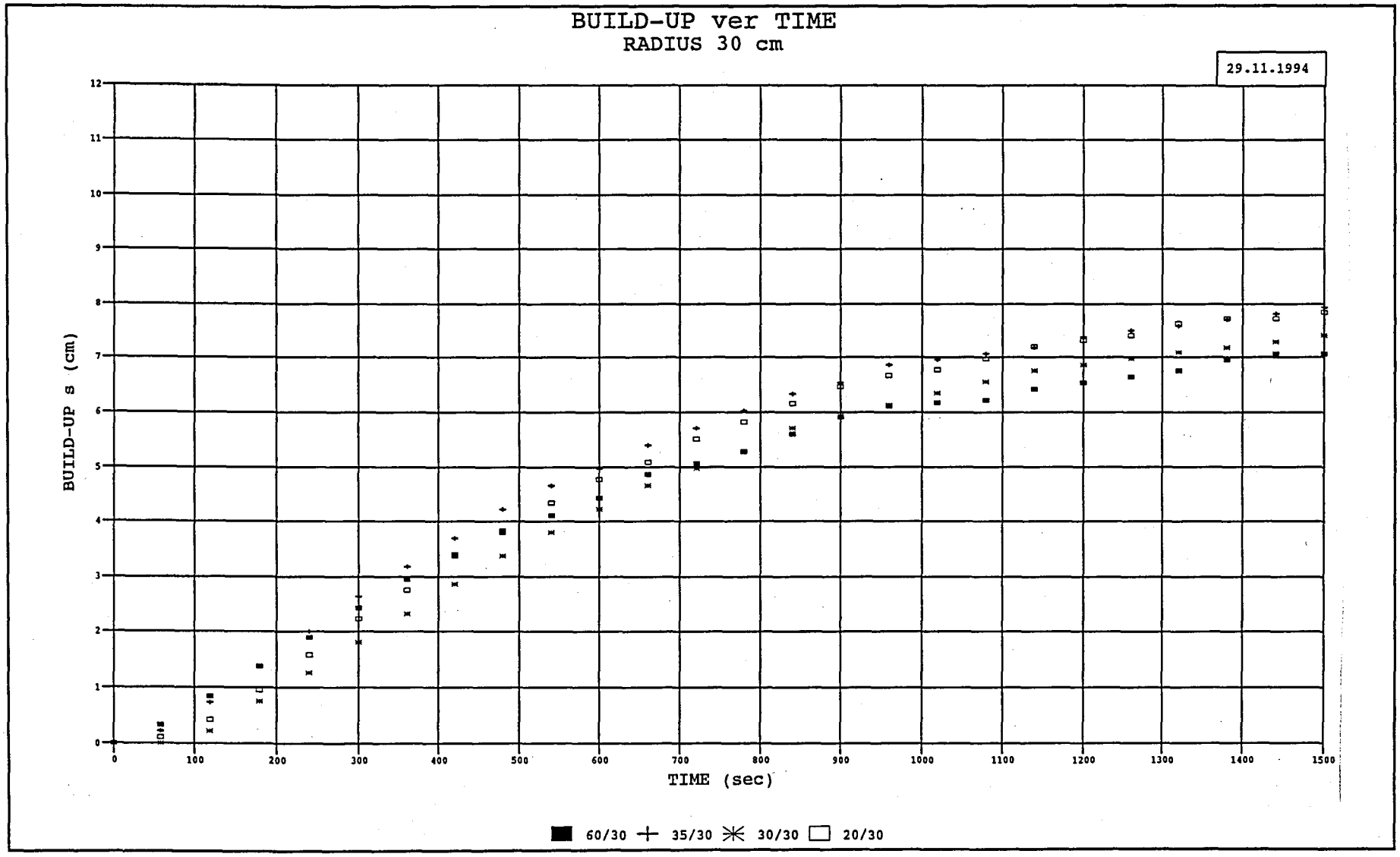

Figure 5.3 : Test results at piezometers at various radiuses

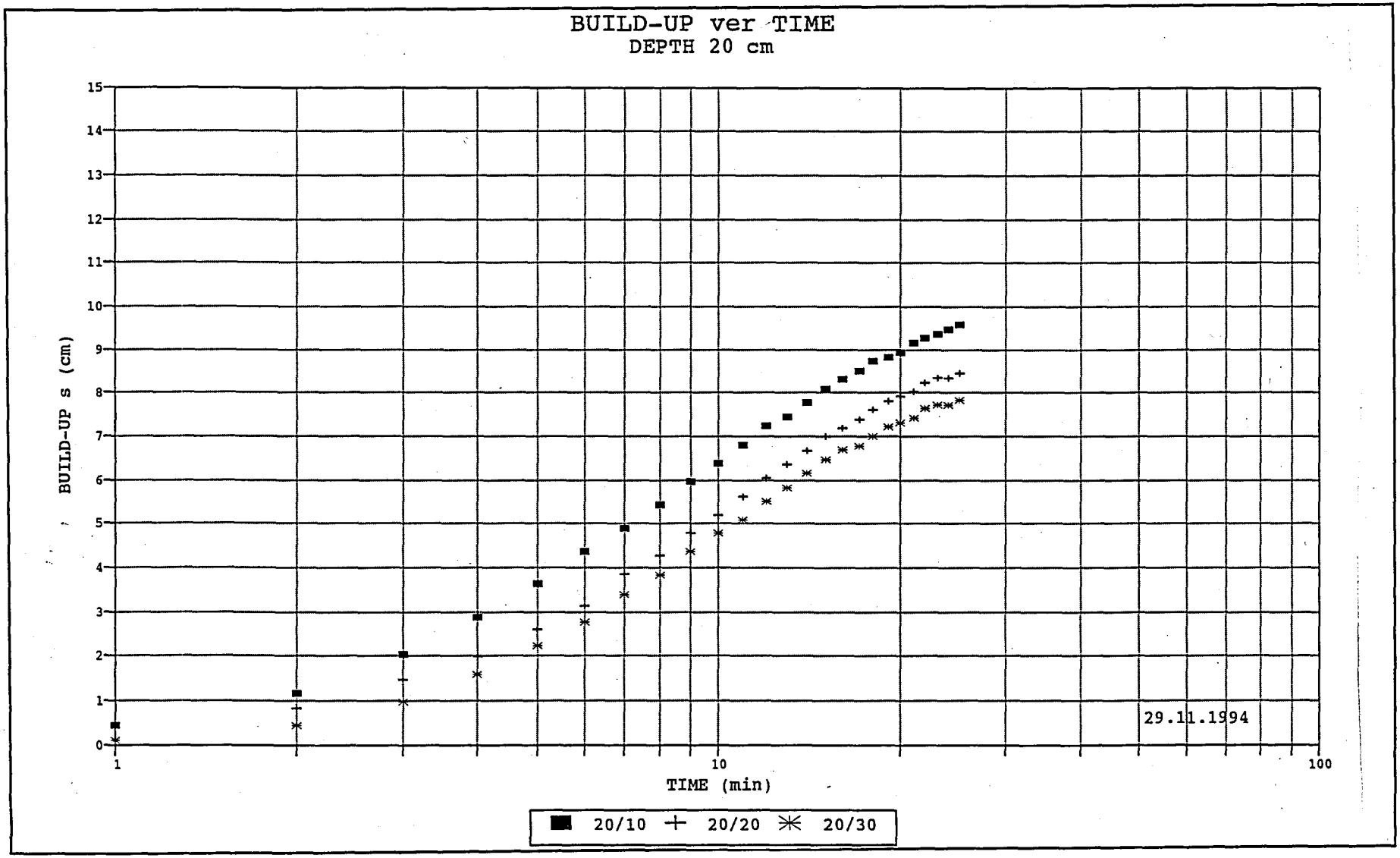

Figure 5.4 : Test results at the same radial plane (semi-logarithmic plot)

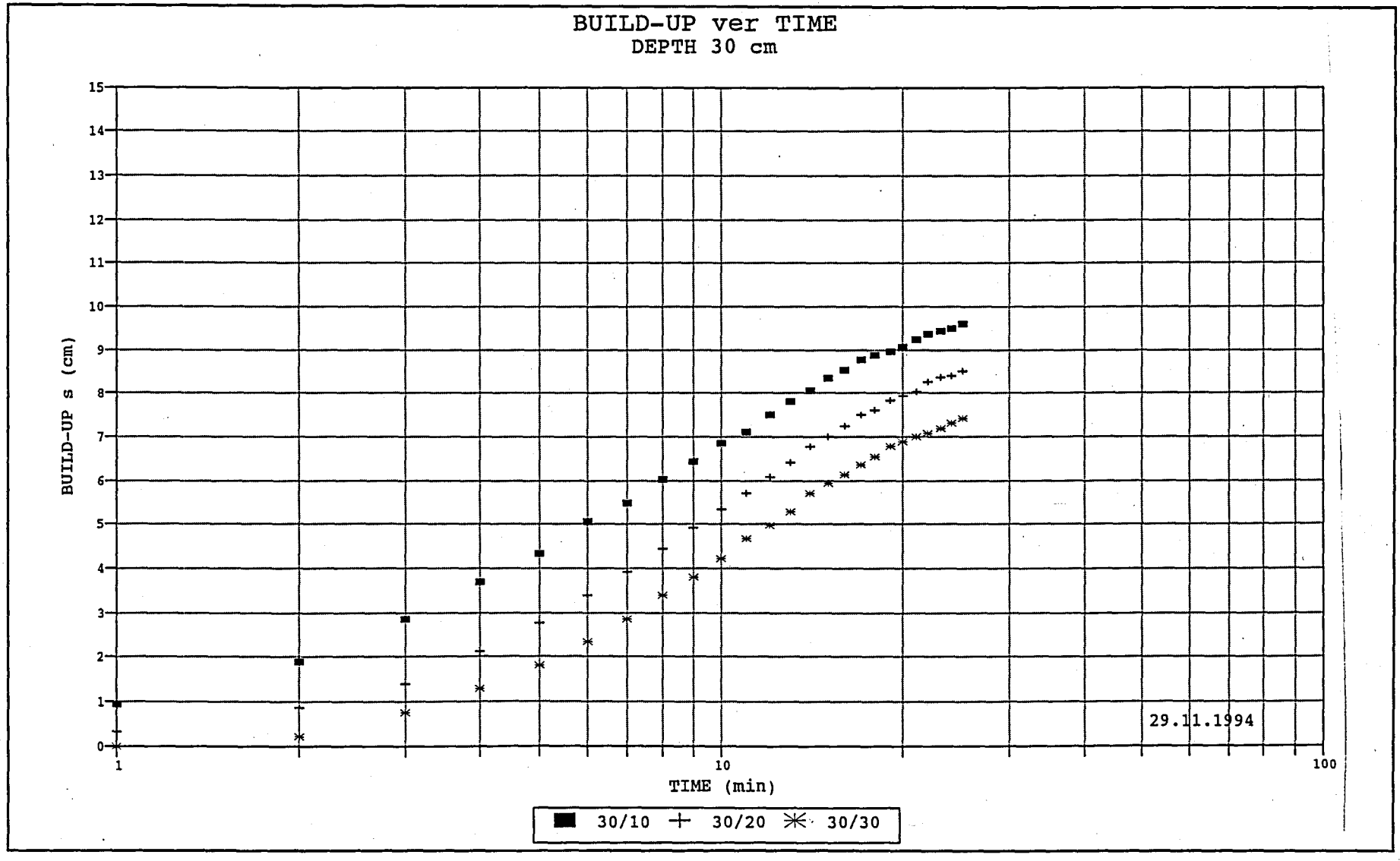

Figure 5.5 : Test results at the same radial plane (semi-logarithmic plot)

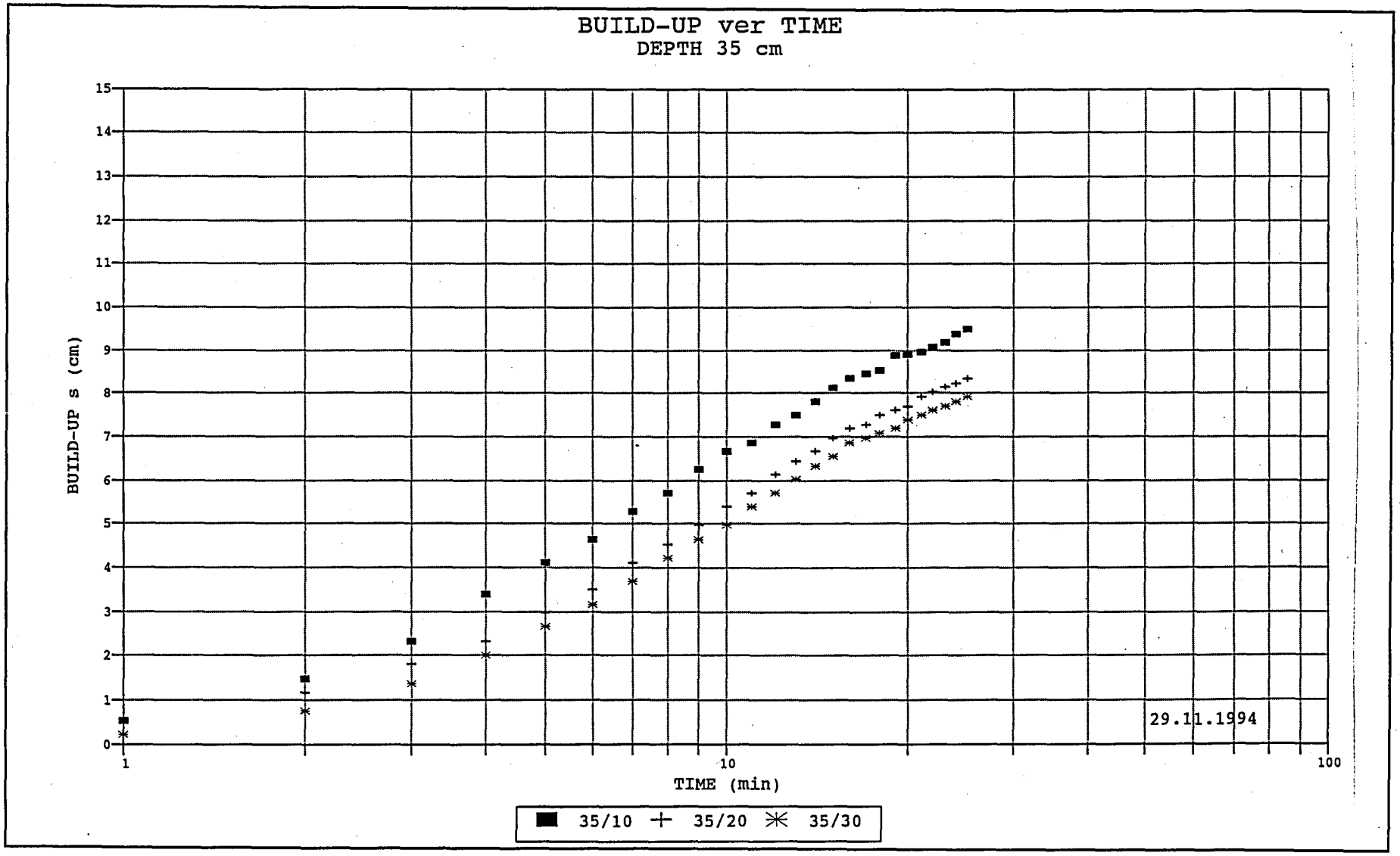

Figure 5.6 : Test results at the same radial plane (semi-logarithmic plot)

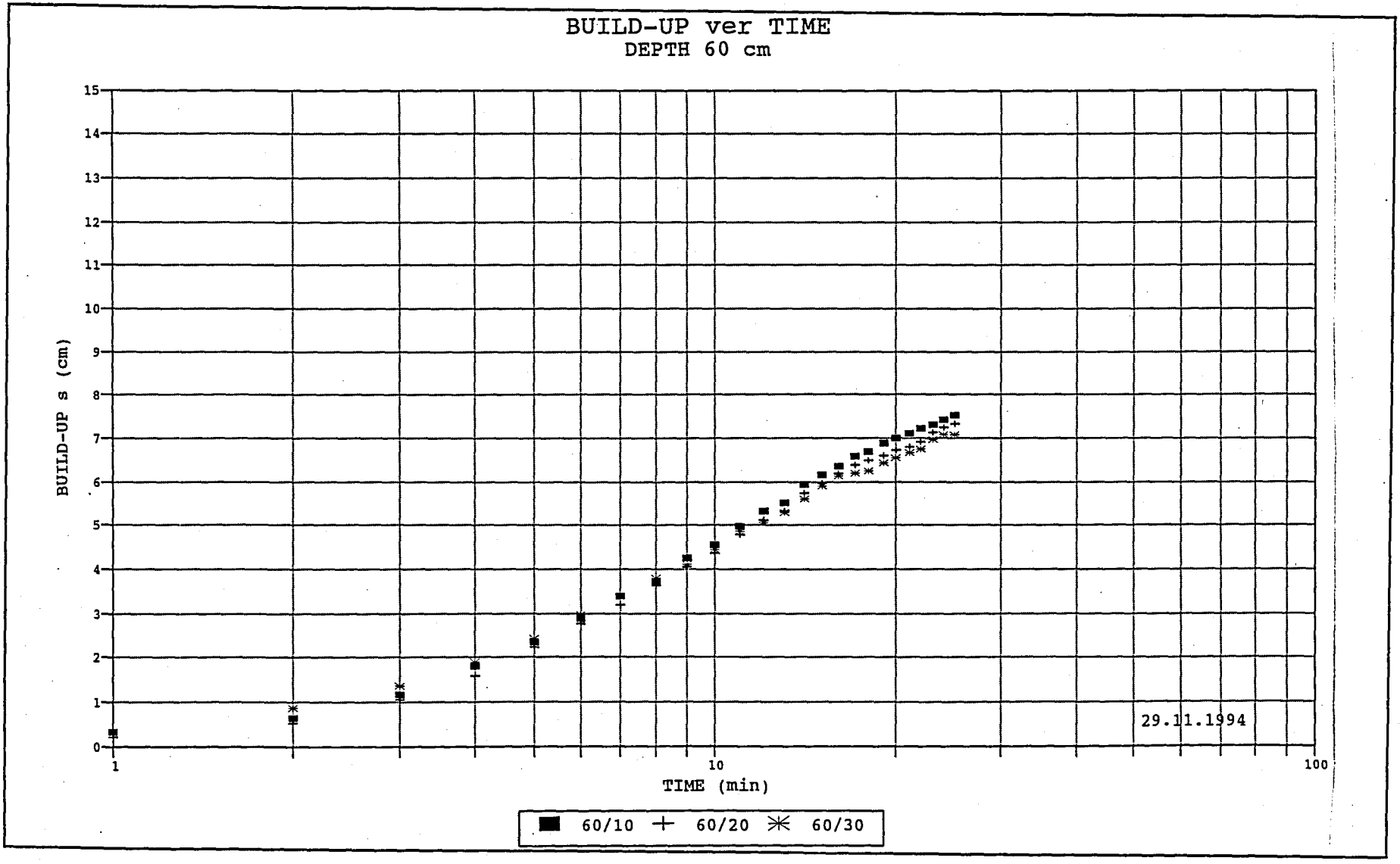

Figure 5.7 : Test results at the same radial plane (semi-logarithmic plot)

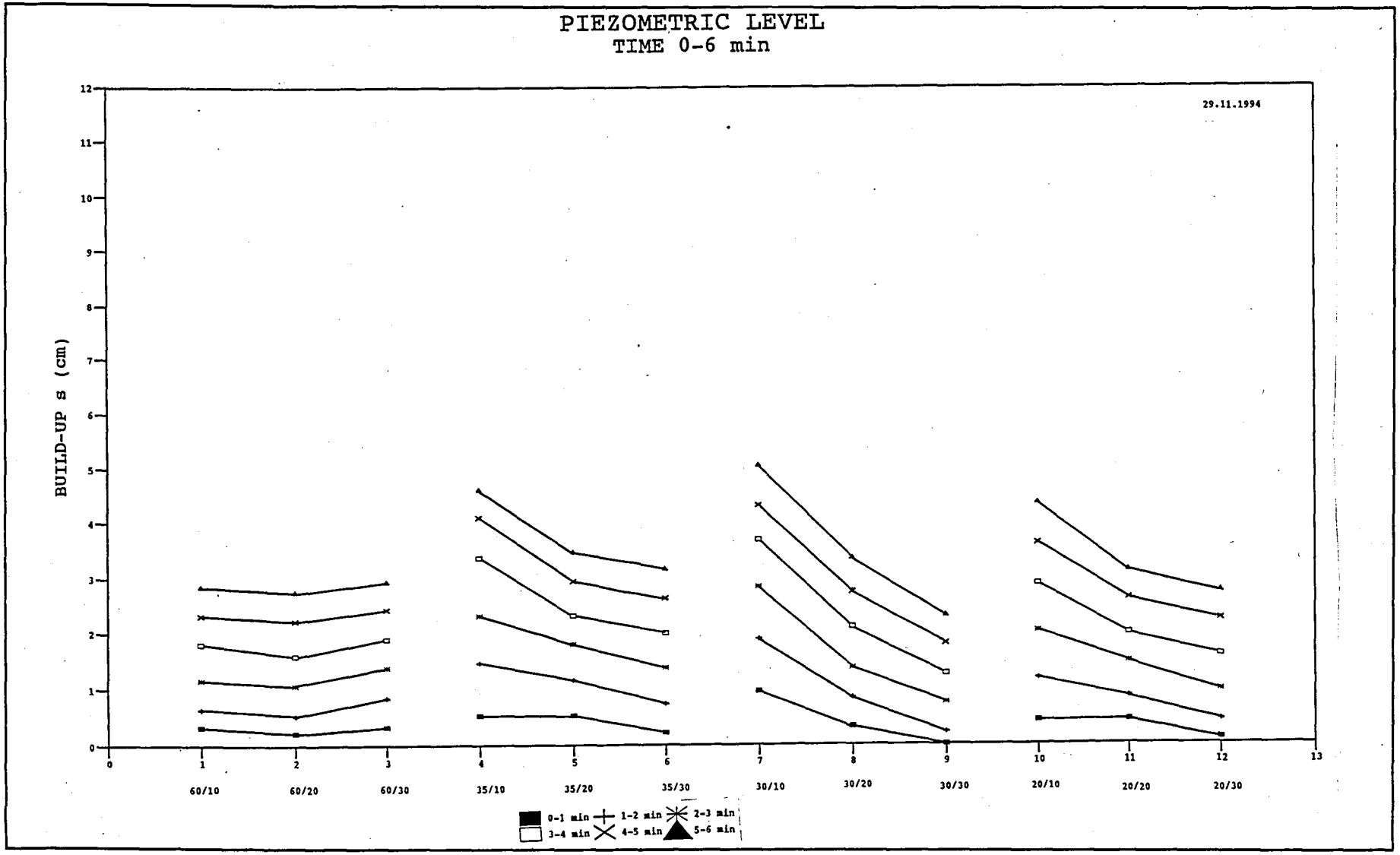

Figure 5.8 : Water levels of each piezometer in time

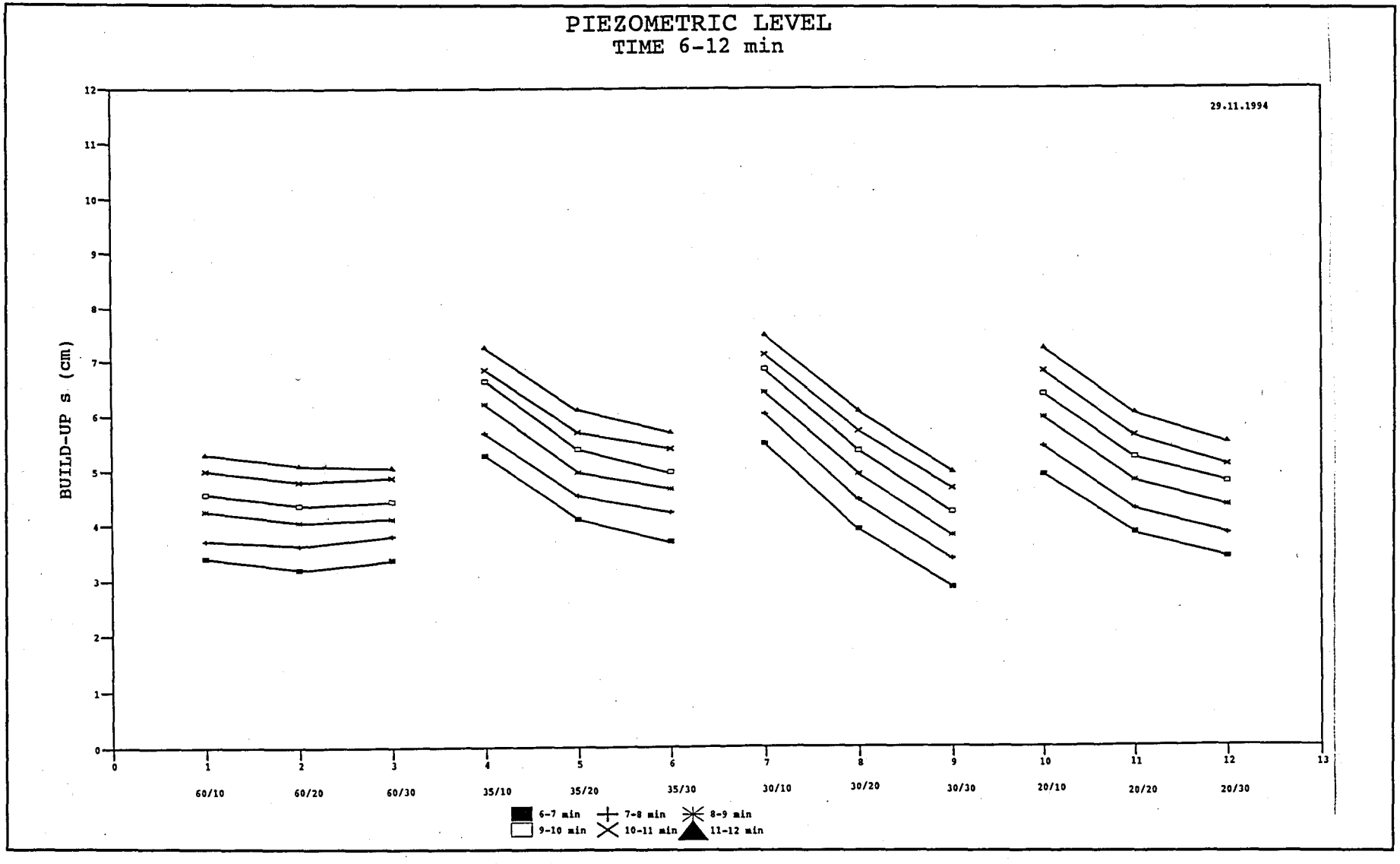

Figure 5.9 : Water levels of each piezometer in time

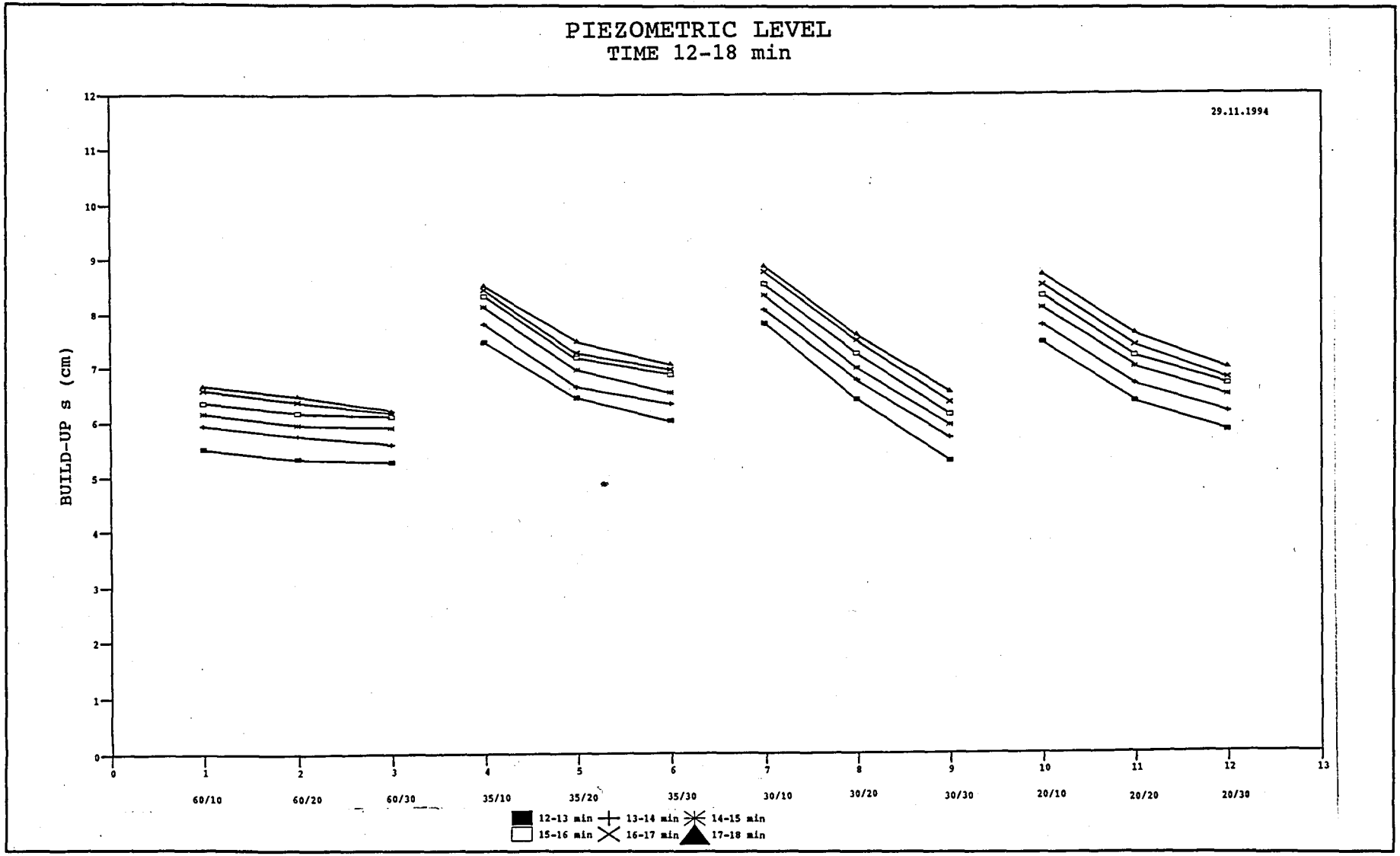

Figure 5.10 : Water levels of each piezometer in time

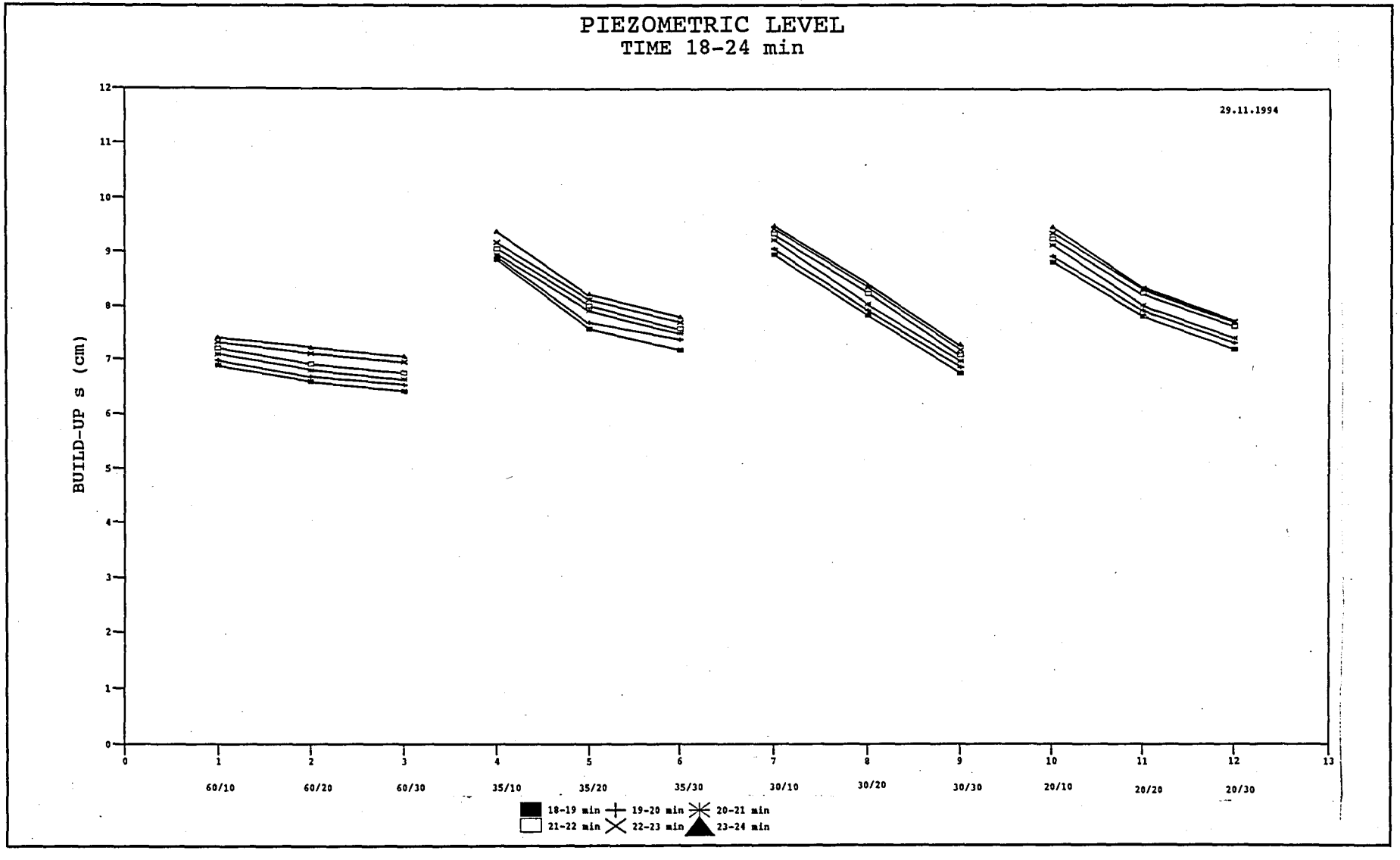

Figure 5.11 : Water levels of each piezometer in time

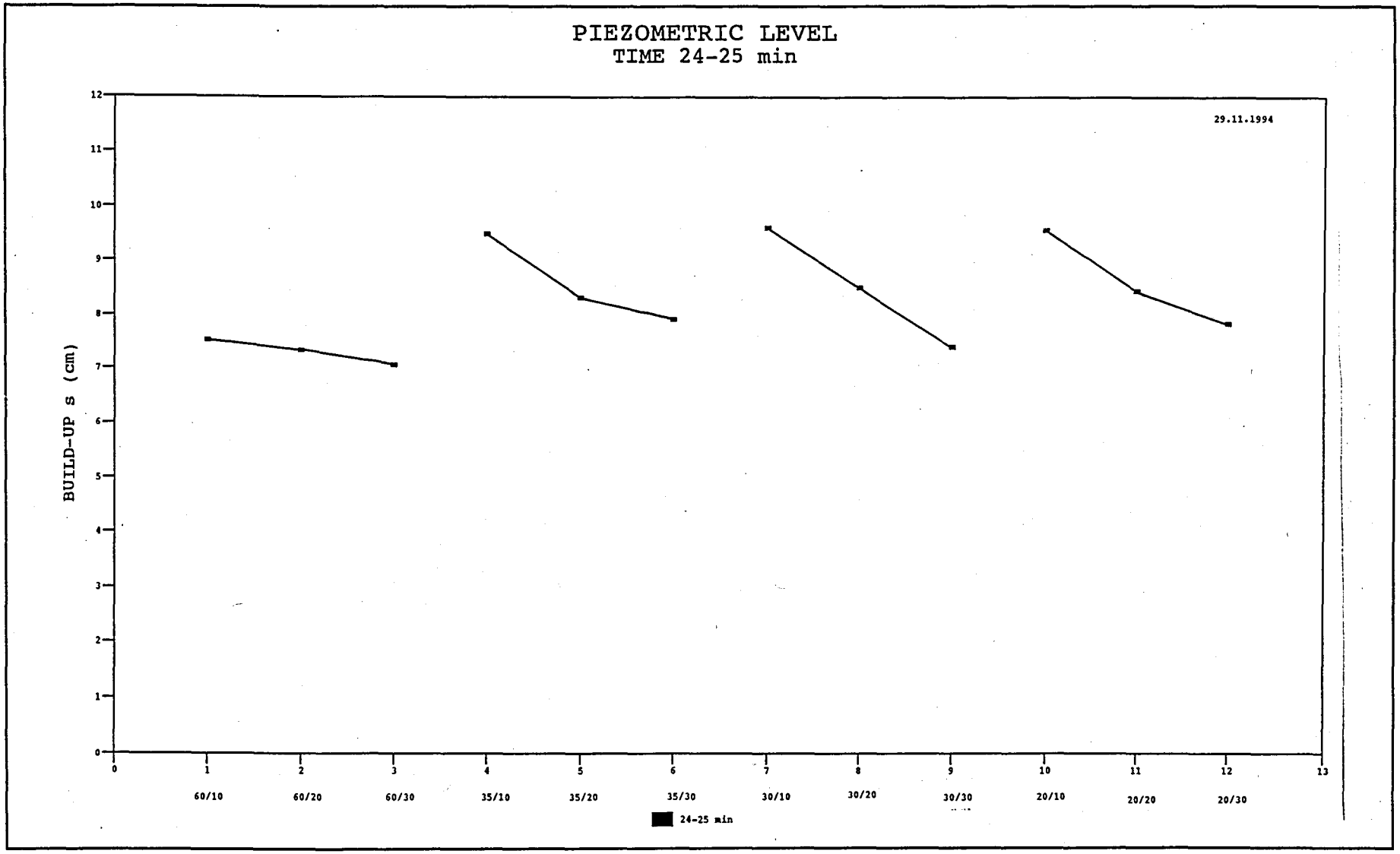

Figure 5.12 : Water levels of each piezometer in time

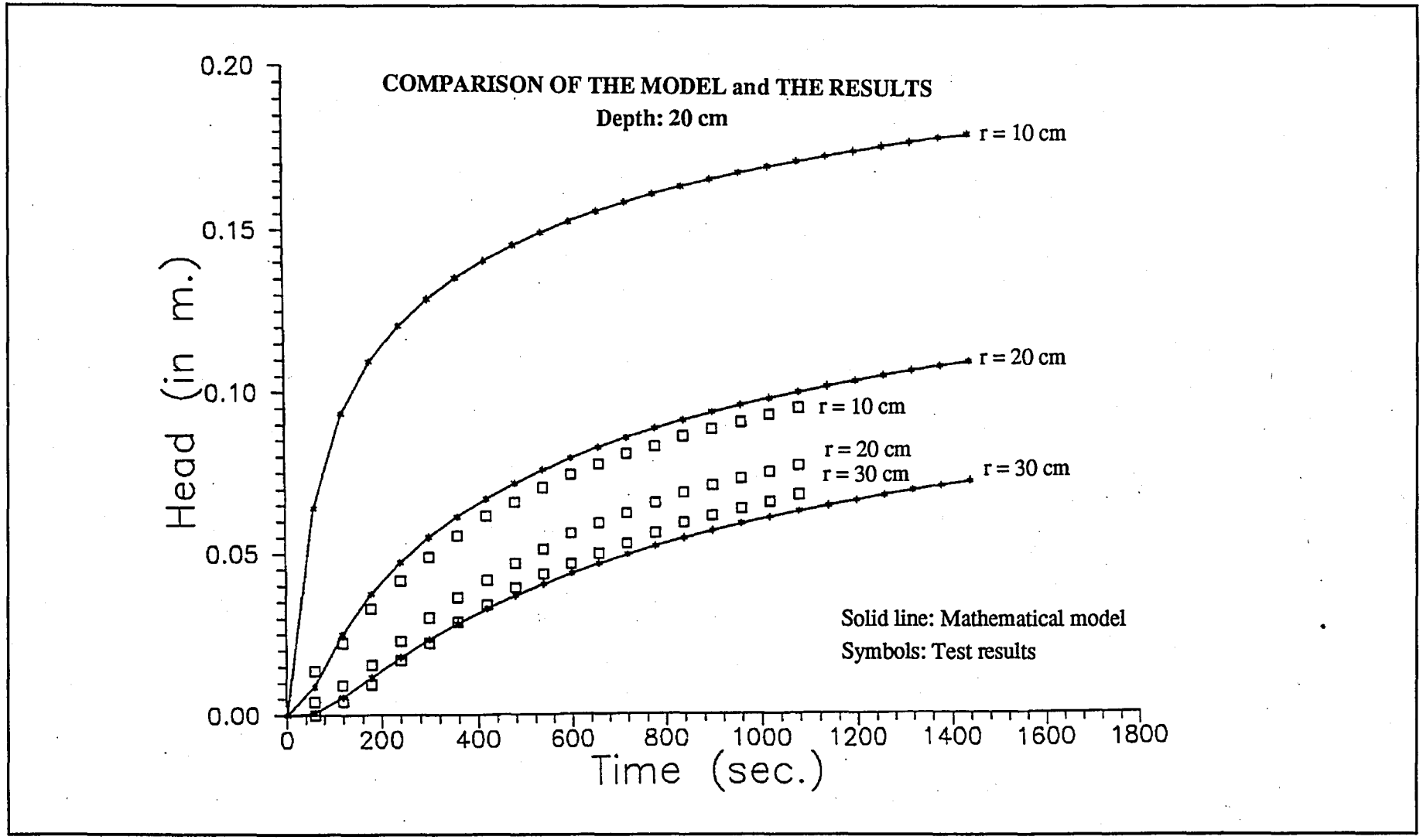

Figure 5.13 : The comparison of the mathematical model and the test results

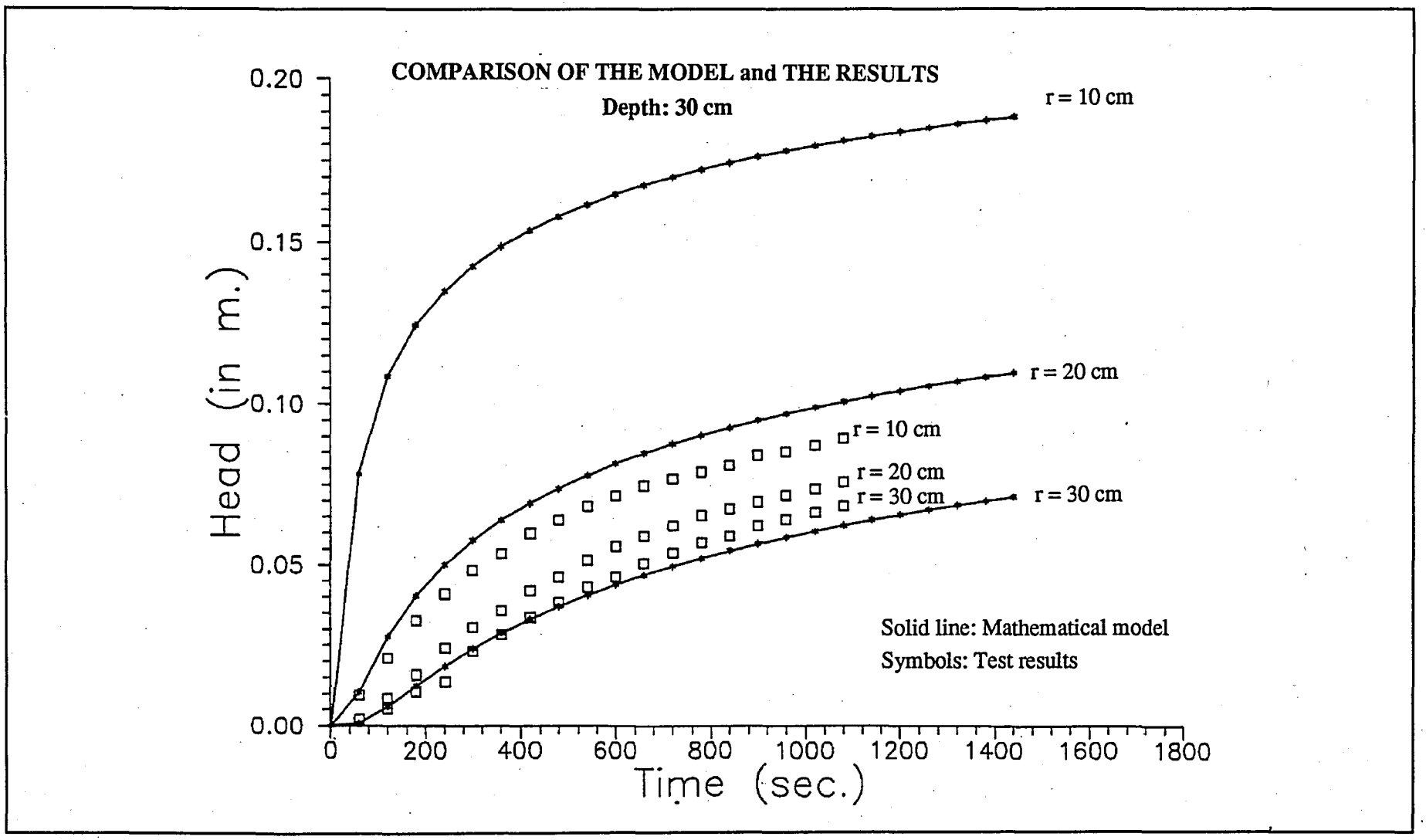

Figure 5.14 : The comparison of the mathematical model and the test results

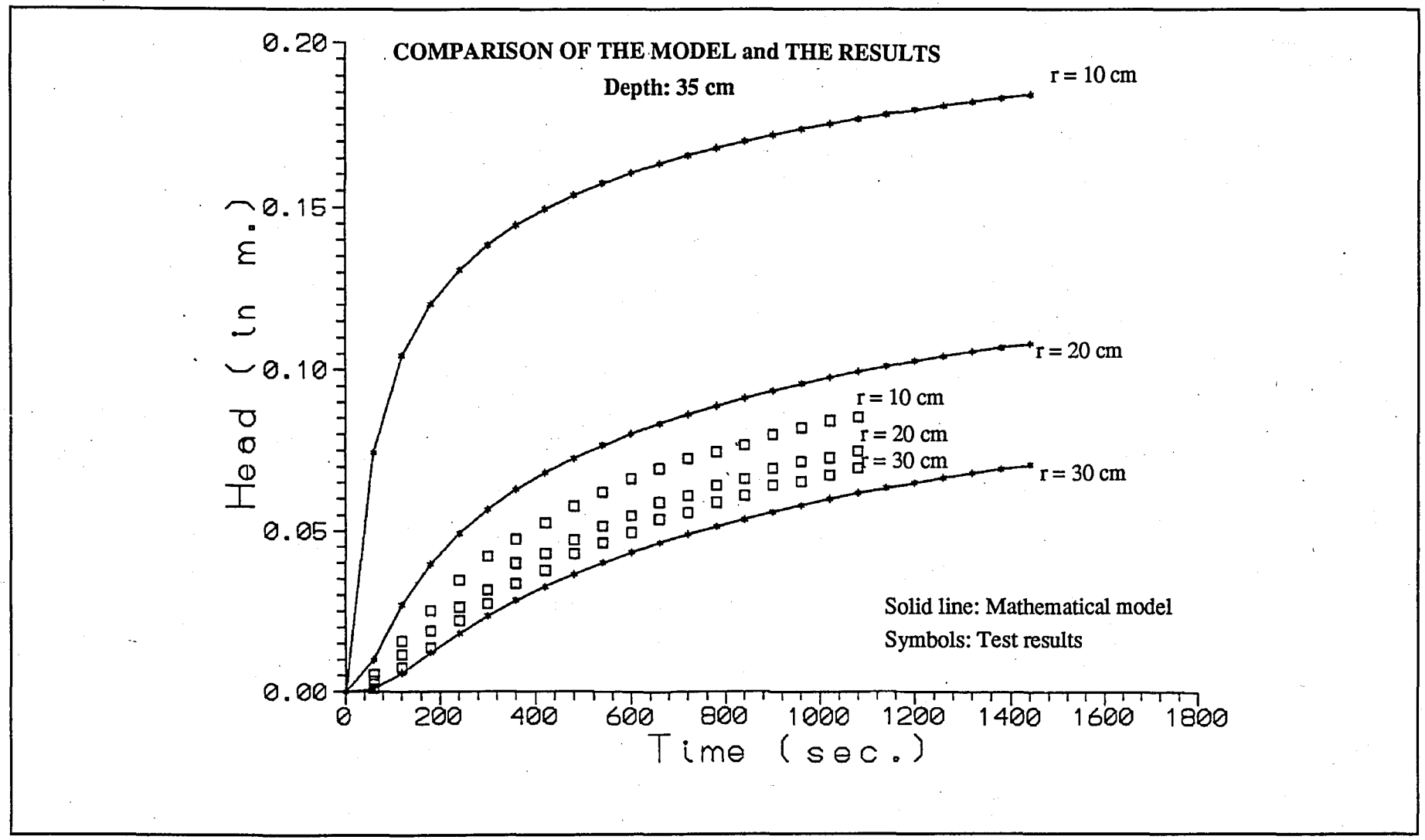

Figure 5.15 : The comparison of the mathematical model and the test results

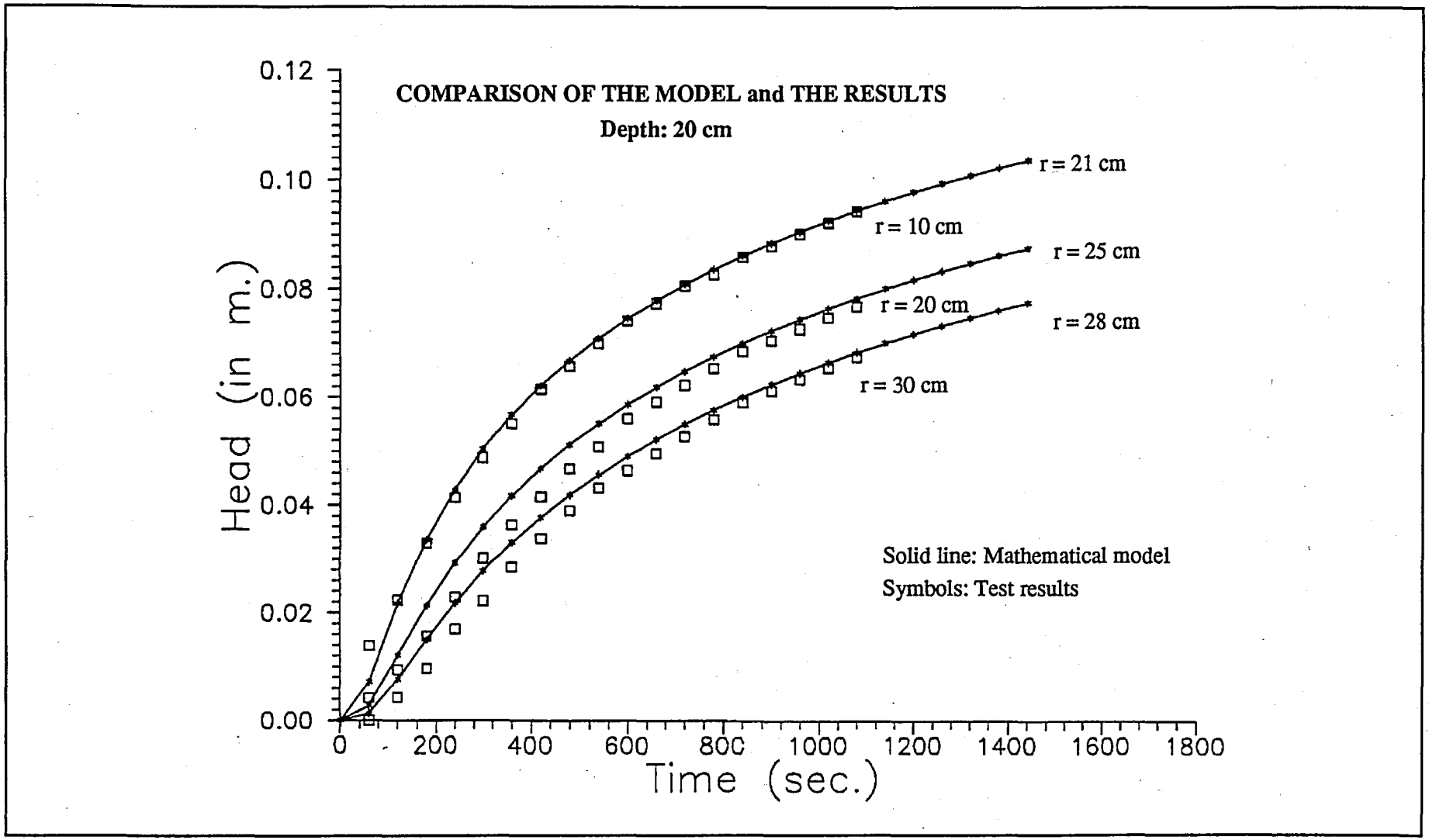

Figure 5.16 : The best match of the mathematical model and the test results

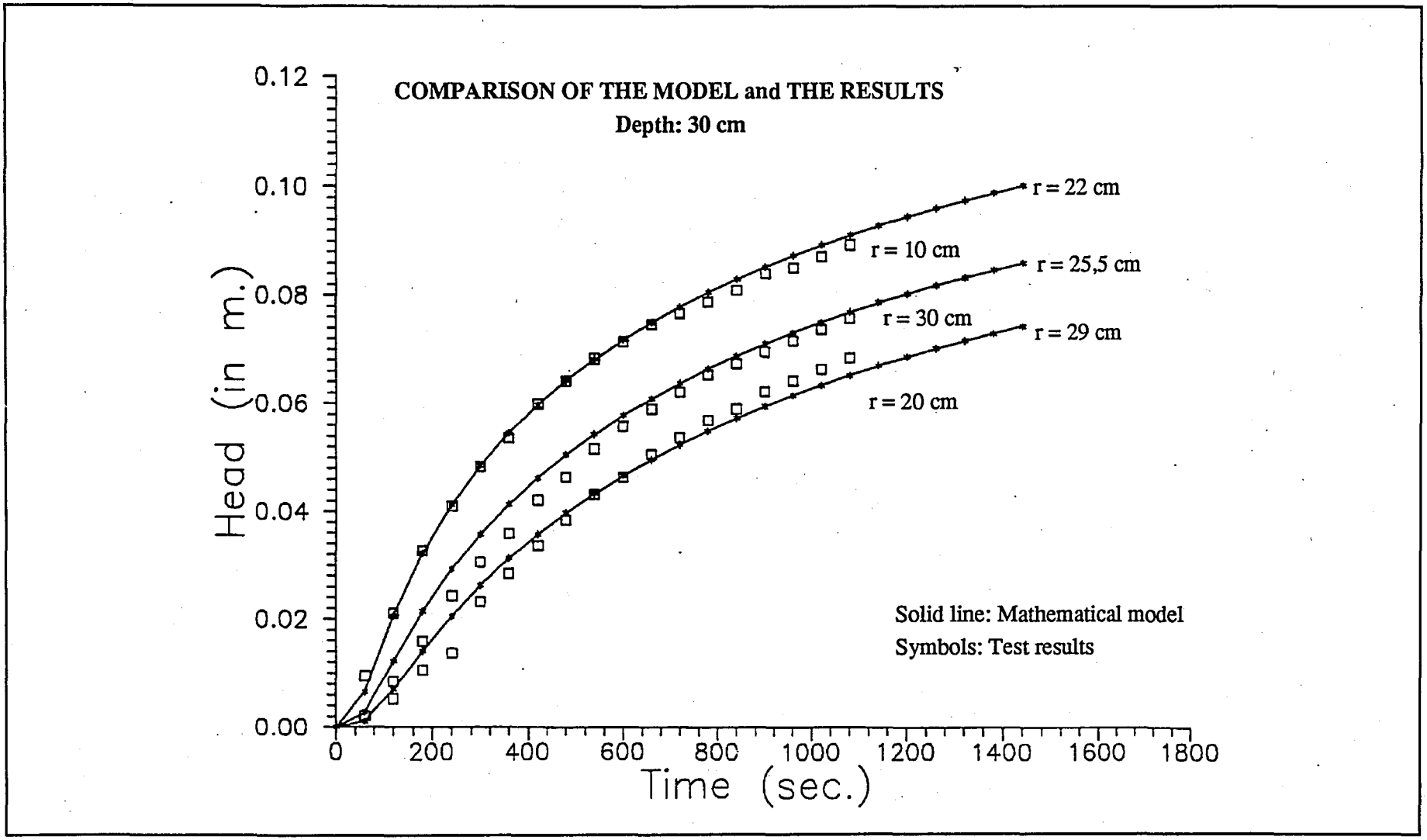

Figure 5.17 : The best match of the mathematical model and the test results

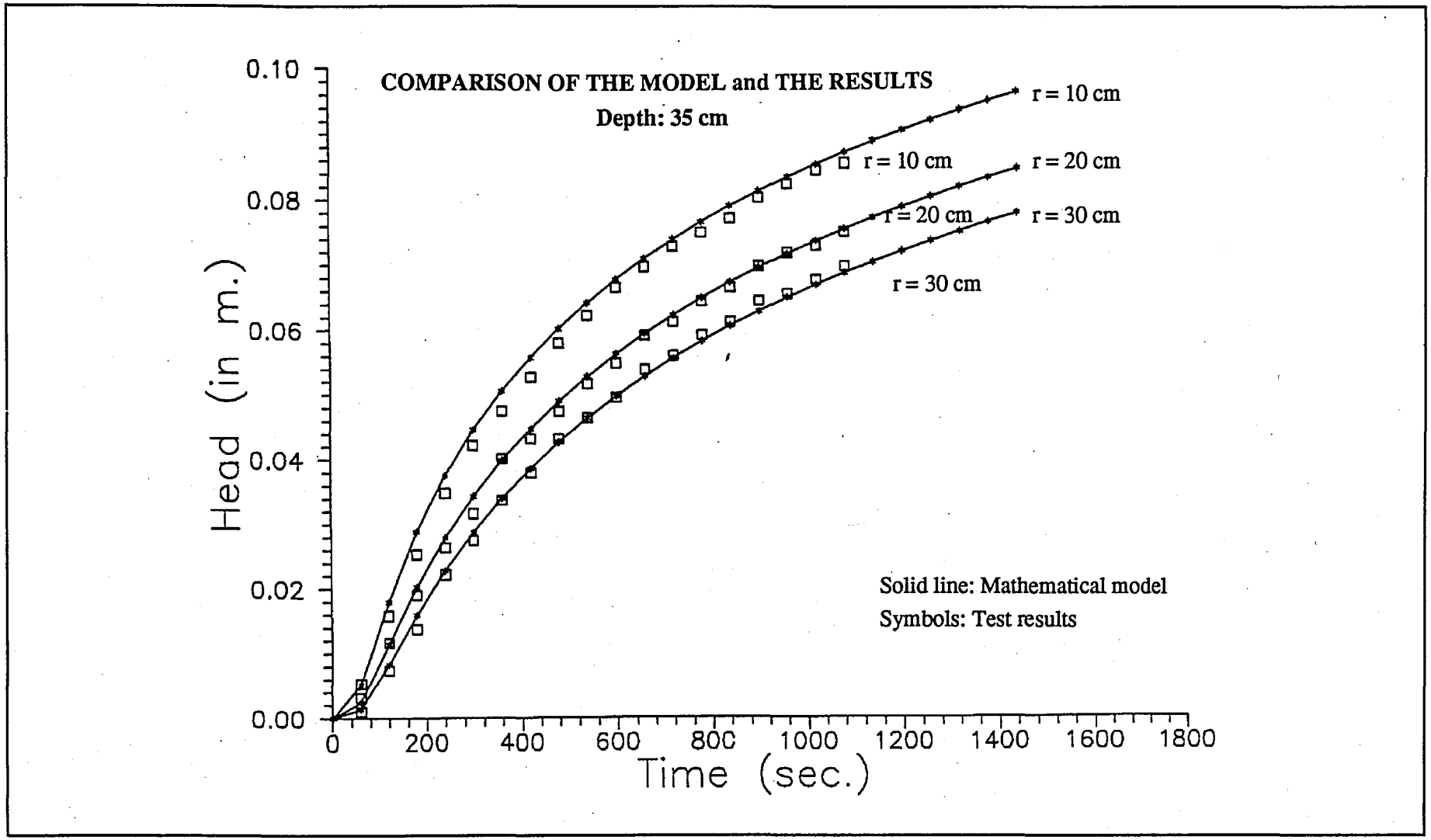

Figure 5.18 : The best match of the mathematical model and the test results

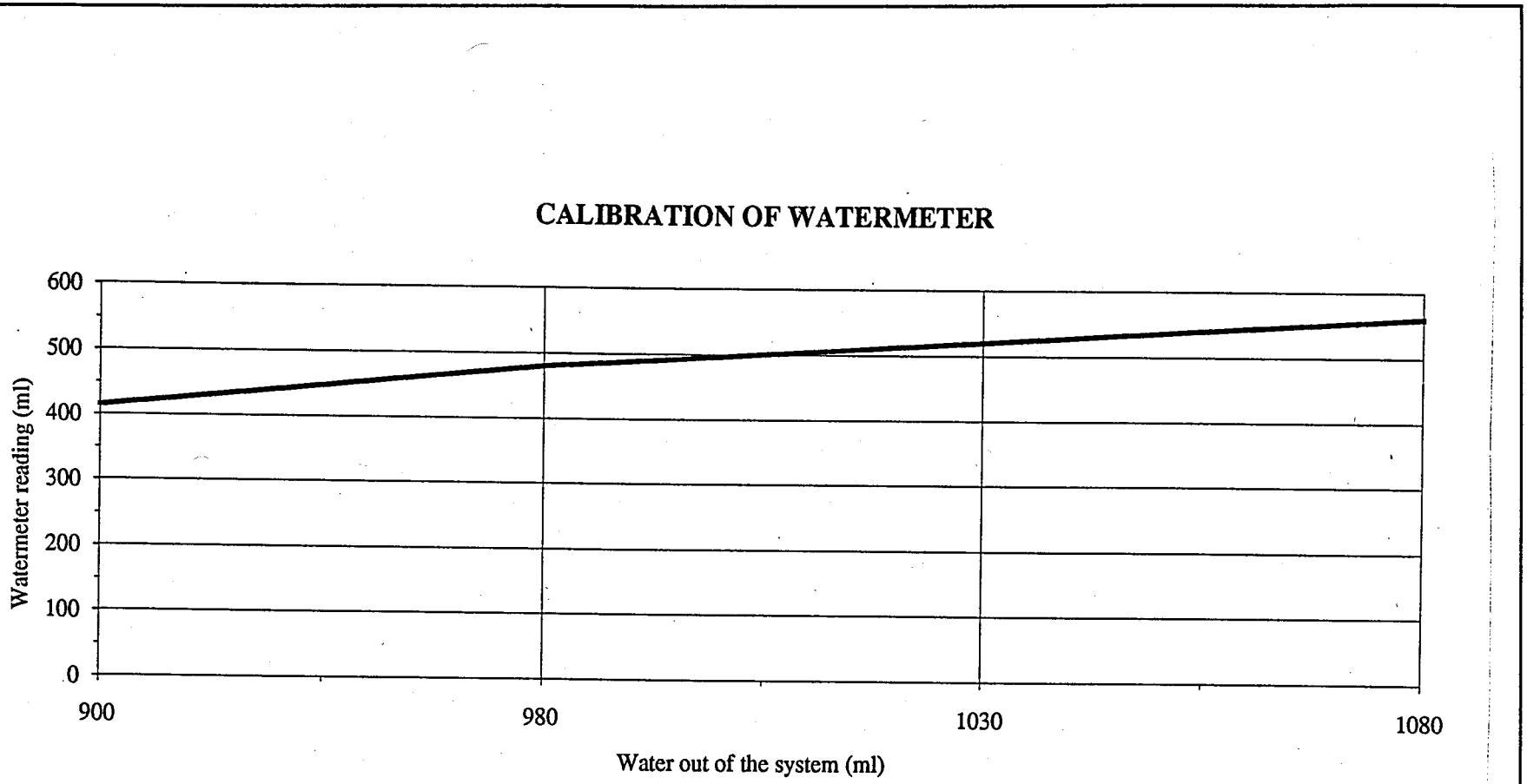
CALIBRATION OF WATERMETER
Watermeter reading (ml)
600
500
400
300
200
100
0
900
980
1030
1080
Water out of the system (ml)

Figure 5.19

6. CONCLUSIONS

A testing program was conducted for evaluating the derived mathematical model for flow from or towards a partially penetrating well in a finite thickness, anisotropic, homogeneous, confined or unconfined aquifer. A device designed for this task was constructed and utilized.

The boundary conditions of the derived model were simulated in the laboratory where the conditions were closely monitored and recorded. The derived model extrapolated the transient state values to steady-state hydraulic conductivity values through the use of shape factors that depend on various geometries.

The piezometric heads were measured to be higher closer to the well since an increased water head was kept constant within the well, the measured piezometer heads were as expected. The piezometric readings show the greatest hydraulic head pressure at 30 centimeter depth. The head values obtained at 30 centimeter depth are slightly higher than those head measurements at 20 centimeter and 35 centimeter depths. Considering that the center of the perforated portion of the well is at 30 centimeter depth from the surface, this is a very good match with what is expected. The fact that the piezometer at 60 centimeter depth get the least effect from the recharging hydraulic head in the well is also an indication that the system is functioning properly and that the measurement of the hydraulic heads were made correctly. The results that are obtained at 60 centimeter depth give very close values which shows that the recharging effect is not very significant at this depth.

The results were extrapolated on graphs obtained from the model and their match was controlled. The permeability and the storage coefficient effect the mathematical model considerably. The permeability determined by the mathematical model was $1 \cdot 10^{6}$ m/s whereas the permeability from the constant head test in the laboratory was $1 \cdot 10^{4}$ m/s. However, the fact that the steady-state is barely achieved at the end of 25 minutes indicates that the permeability measured in-situ reflects a more realistic value compared to the measurements made in the permeability apparatus. This can be due to the different size of the small permeability apparatus versus the large tank and due to the procedures followed in placement of the tested material .

It was concluded that the match for the piezometer located 10 centimeter radially from the centered well was not appropriate; however, for the other two on the same vertical plane, there was a satisfying similarity. Especially the most distant one gave a perfect relationship. The match between the measured and the calculated hydraulic heads fits each other for an observation well that is not close to the charged well This is satisfied from the very beginning of the test. So a waiting period is not required to reach the steady-state. This will save time and provide economy for field applications.

The rise of the piezometric level almost stabilized after a rapid initial increase. This is as expected due to the silty-sand that is used for the aquifer material.

The testing device was used to test the unconfined case, but can be used for the confined case as well by introducing a cover on top of the main tank. This cover will function as the confining layer. The problem can be that there is leakage from the boundaries of the model well and the rise of water head from the sides towards the inside. This was observed at several trial tests conducted.

The set-backs of the testing program were the number of utilizable tests and the measurement of the flow towards the aquifer. It is necessary to increase this number and to compare results with field data. It is important that the flow be determined accurately to better evaluate the proposed mathematical model. Therefore a more sensitive watermeter should be used. Also the floater for maintaining the water head constant during the testing period in the recharging reservoir and the centered model well should be sensing the changes more precisely. The surface of the recharging reservoir should be made smaller for this purpose.

The tests can be furthered by changing the depth of the penetration of the model well and monitoring its effects. Also the tested material can be inverted from silty-sand to more clayey soils with lower permeabilities to extend the flexibility of the mathematical model. A half circular plane of larger radius may be more efficient due to the axisymmetrical behavior. This provide that the boundary conditions are observed and are of less importance to the test results. If observation points are used, they should be chosen at a reasonable space from the charged well.

APPENDIX A

The graphs of the water head in the piezometer at various radii presented herein.

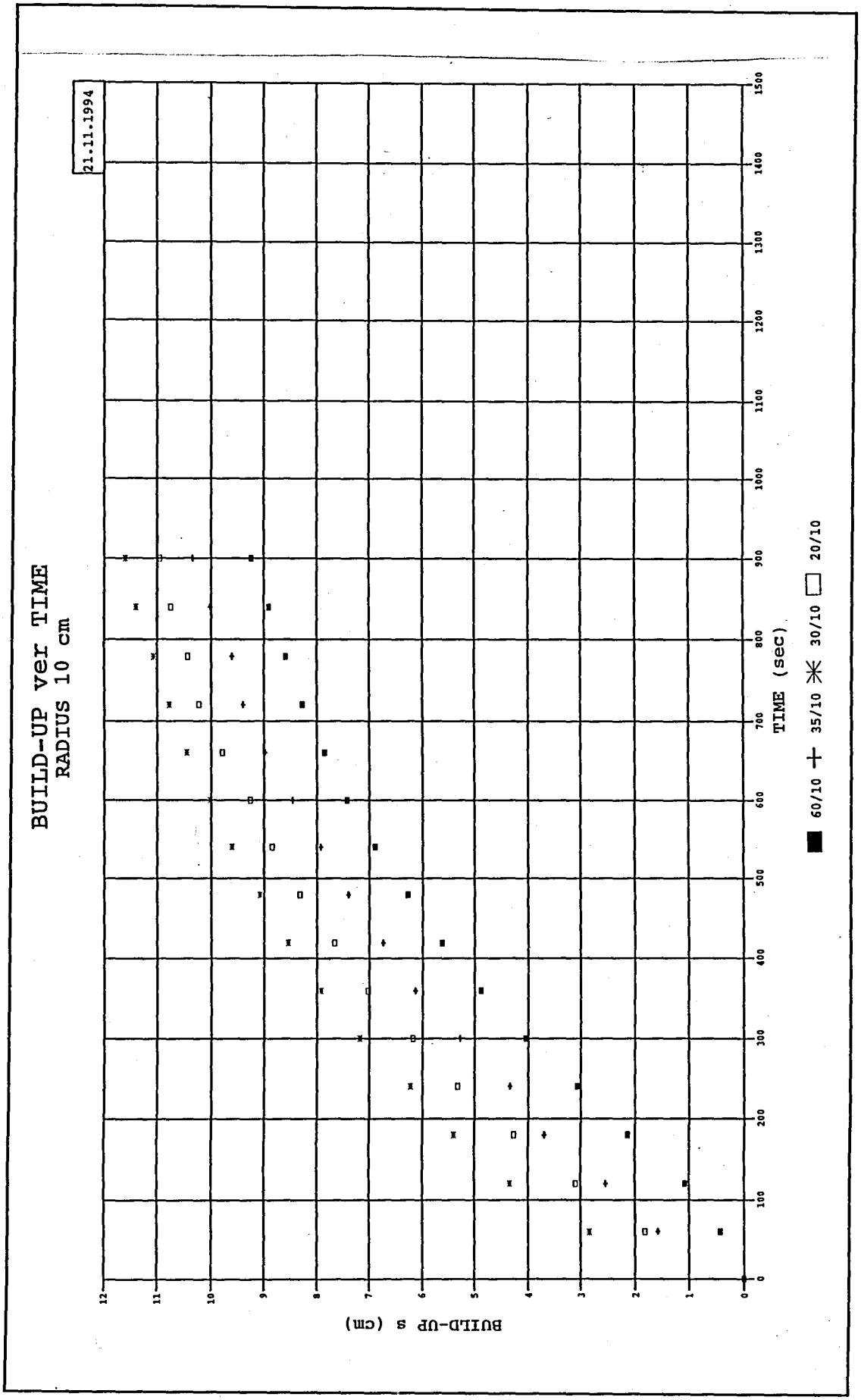
BUILD-UP ver TIME
RADIUS 10 cm
21.11.1994
BUILD-UP s (cm)
TIME (sec)
60/10
35/10
30/10
20/10

Fig. A.1

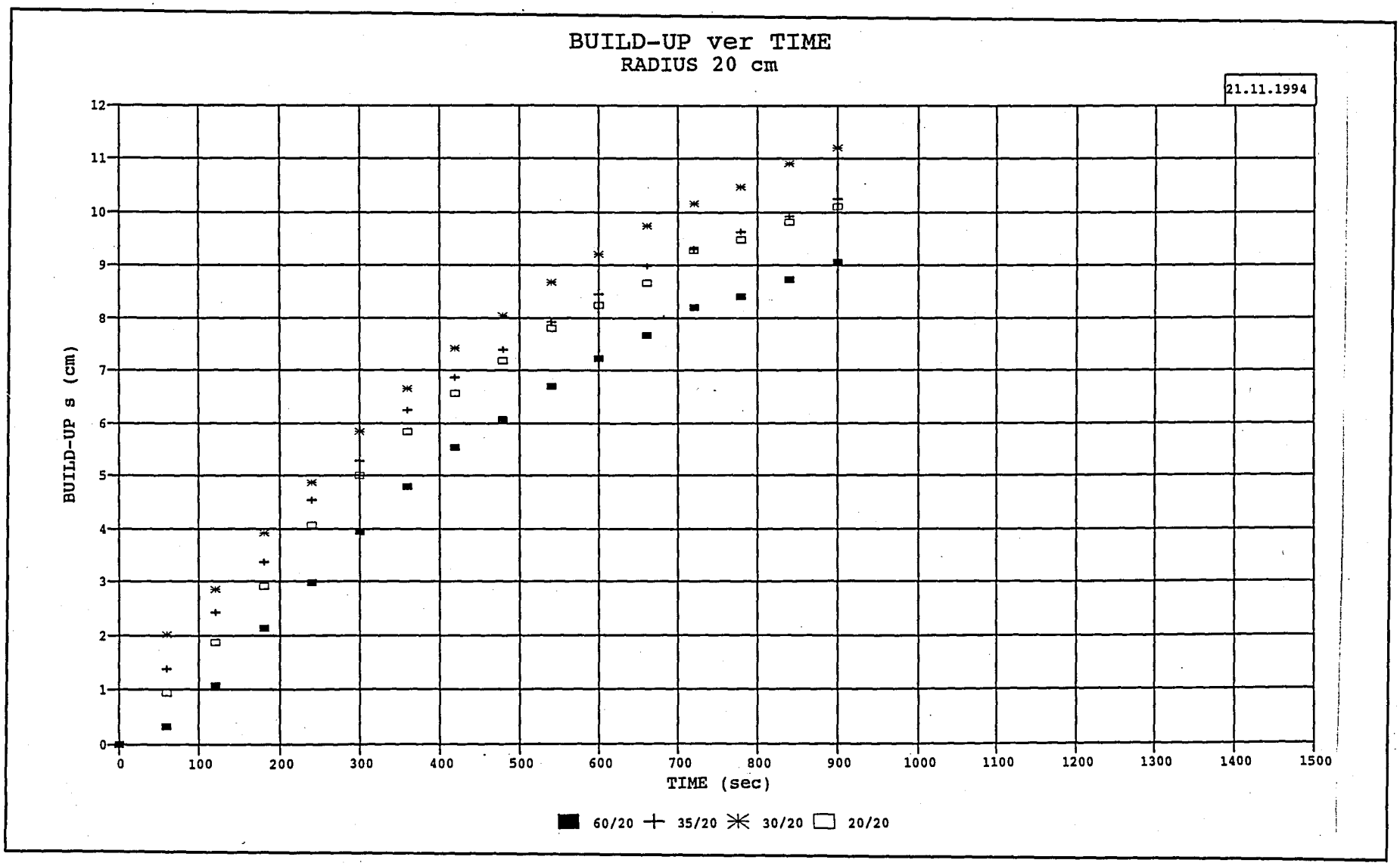
BUILD-UP ver TIME
RADIUS 20 cm
21.11.1994
BUILD-UP s (cm)
TIME (sec)
0
100
200
300
400
500
600
700
800
900
1000
1100
1200
1300
1400
1500
1
2
3
4
5
6
7
8
9
10
11
12
60/20
35/20
30/20
20/20

Fig. A.2

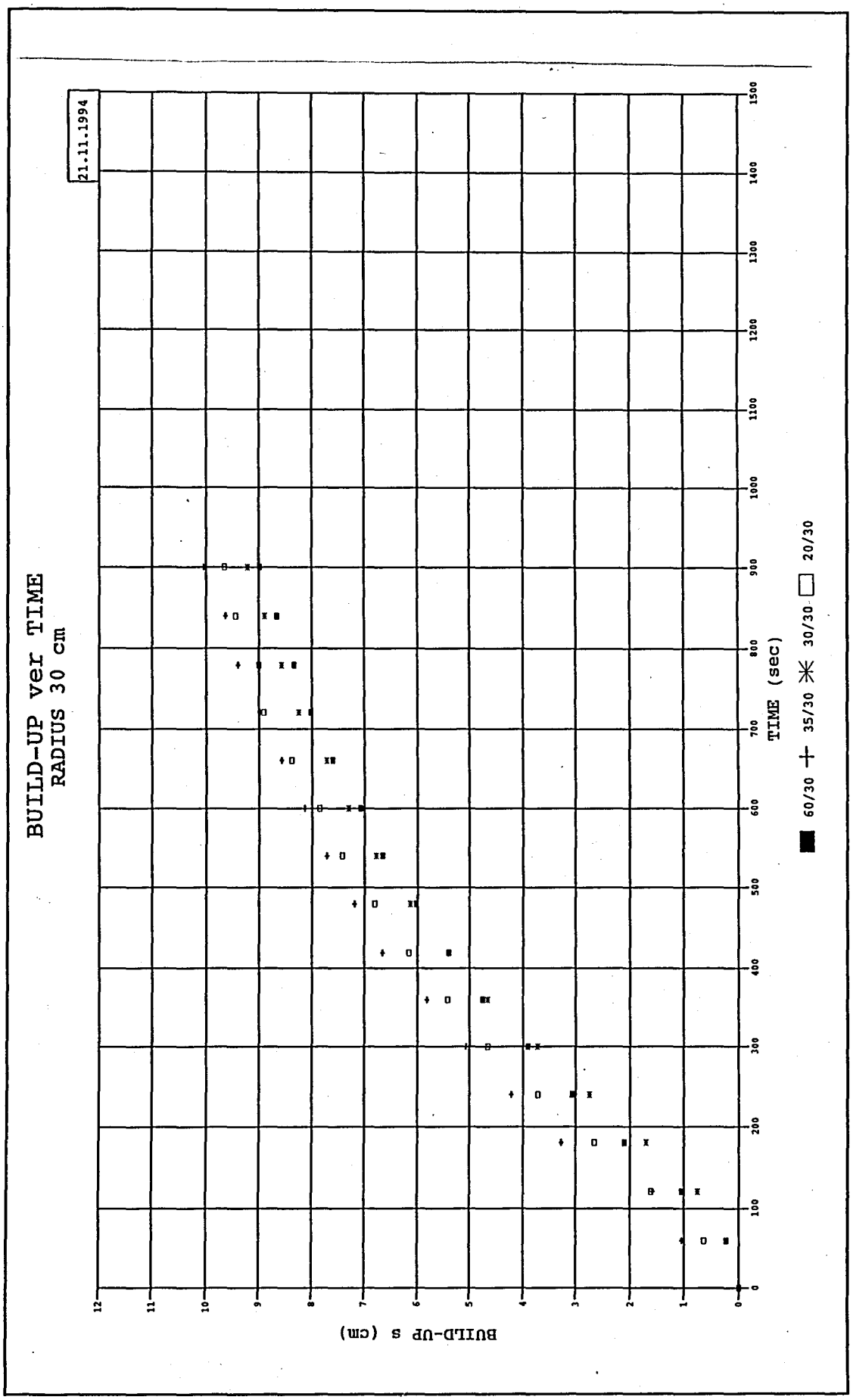
BUILD-UP ver TIME
RADIUS 30 cm
21.11.1994
BUILD-UP s (cm)
TIME (sec)
60/30
35/30
30/30
20/30

Fig. A.3

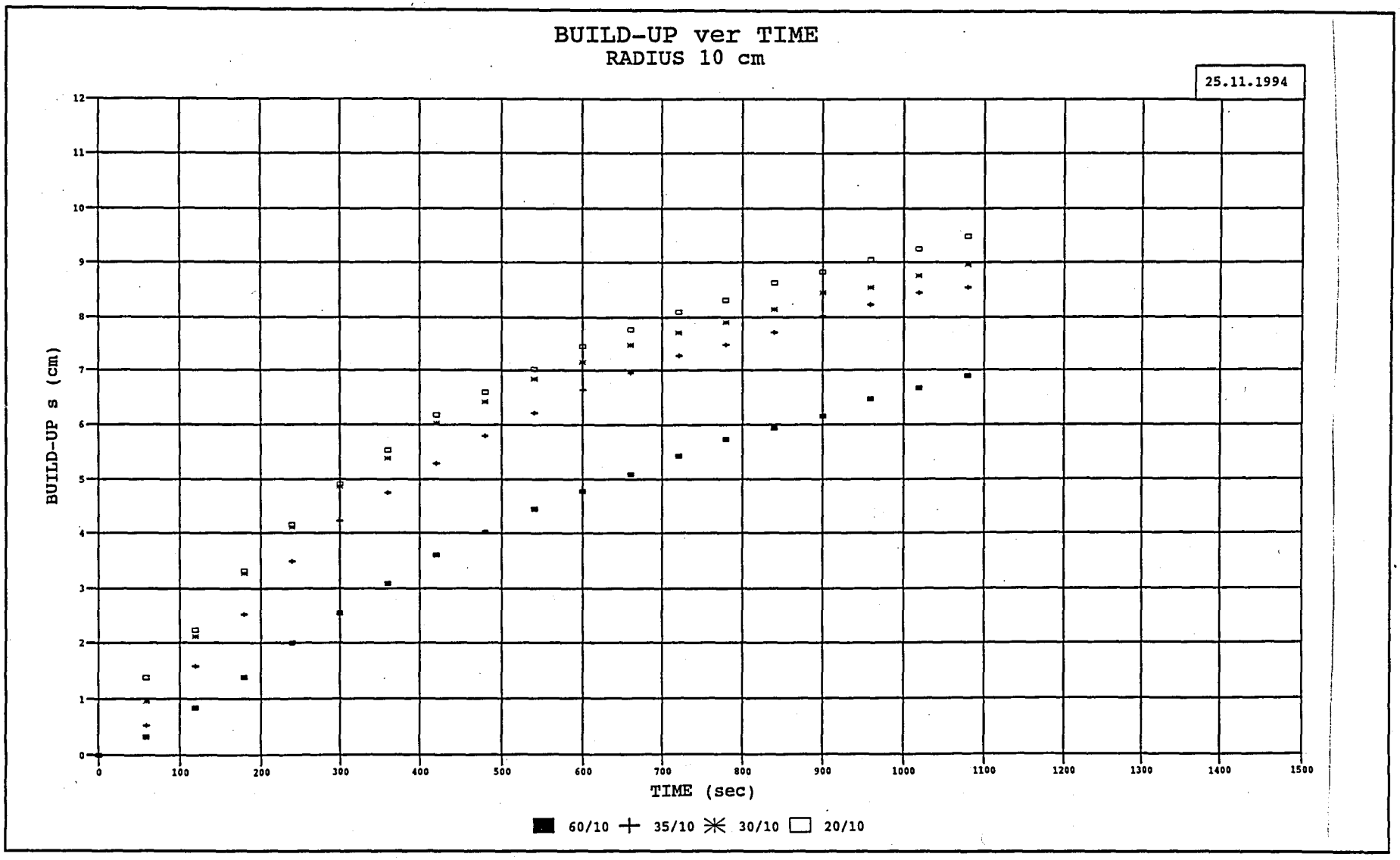
BUILD-UP ver TIME
RADIUS 10 cm
25.11.1994
BUILD-UP s (cm)
TIME (sec)
60/10
35/10
30/10
20/10

Fig. A.4

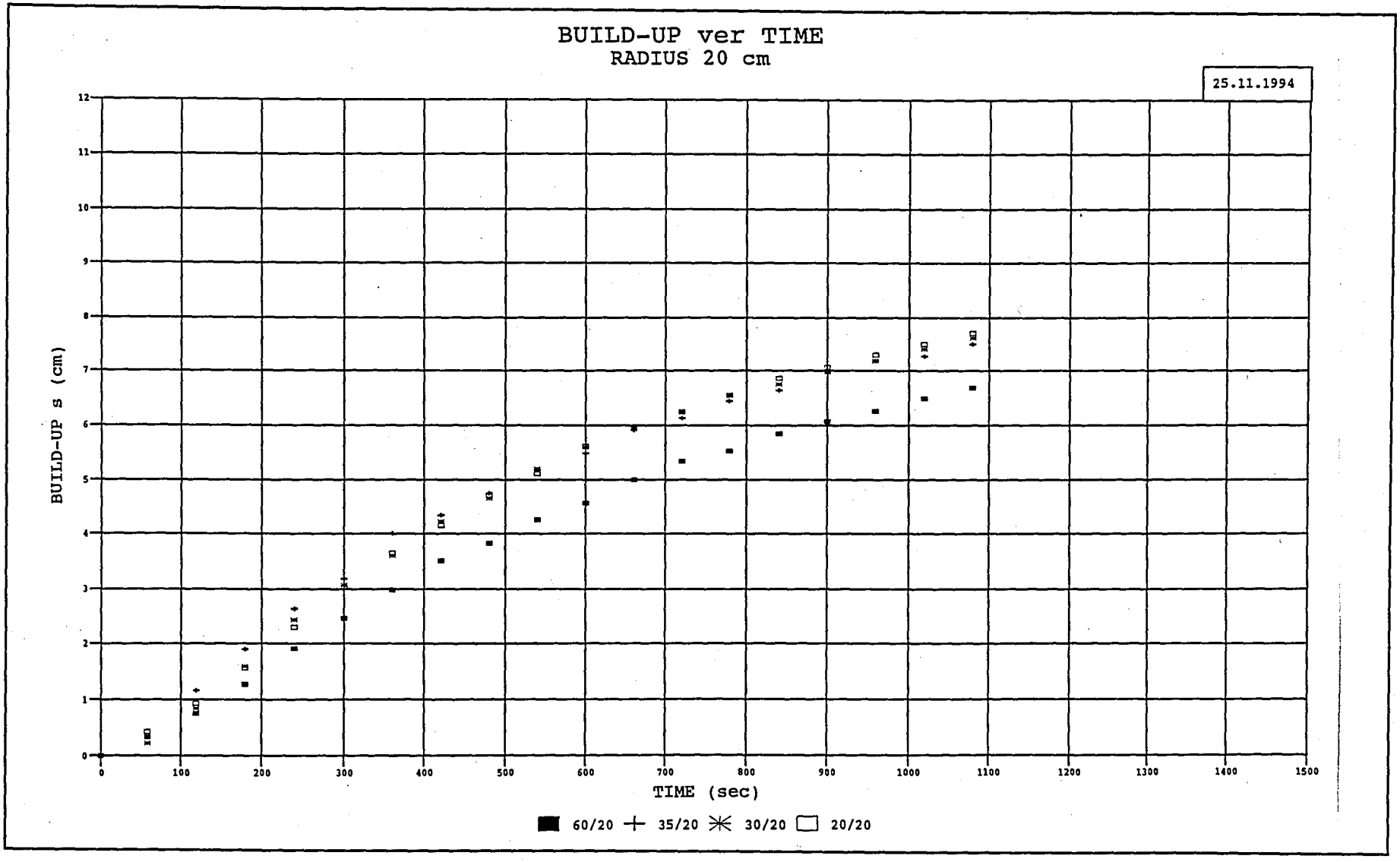
BUILD-UP ver TIME
RADIUS 20 cm
25.11.1994
BUILD-UP s (cm)
TIME (sec)
60/20
35/20
30/20
20/20

Fig. A.5

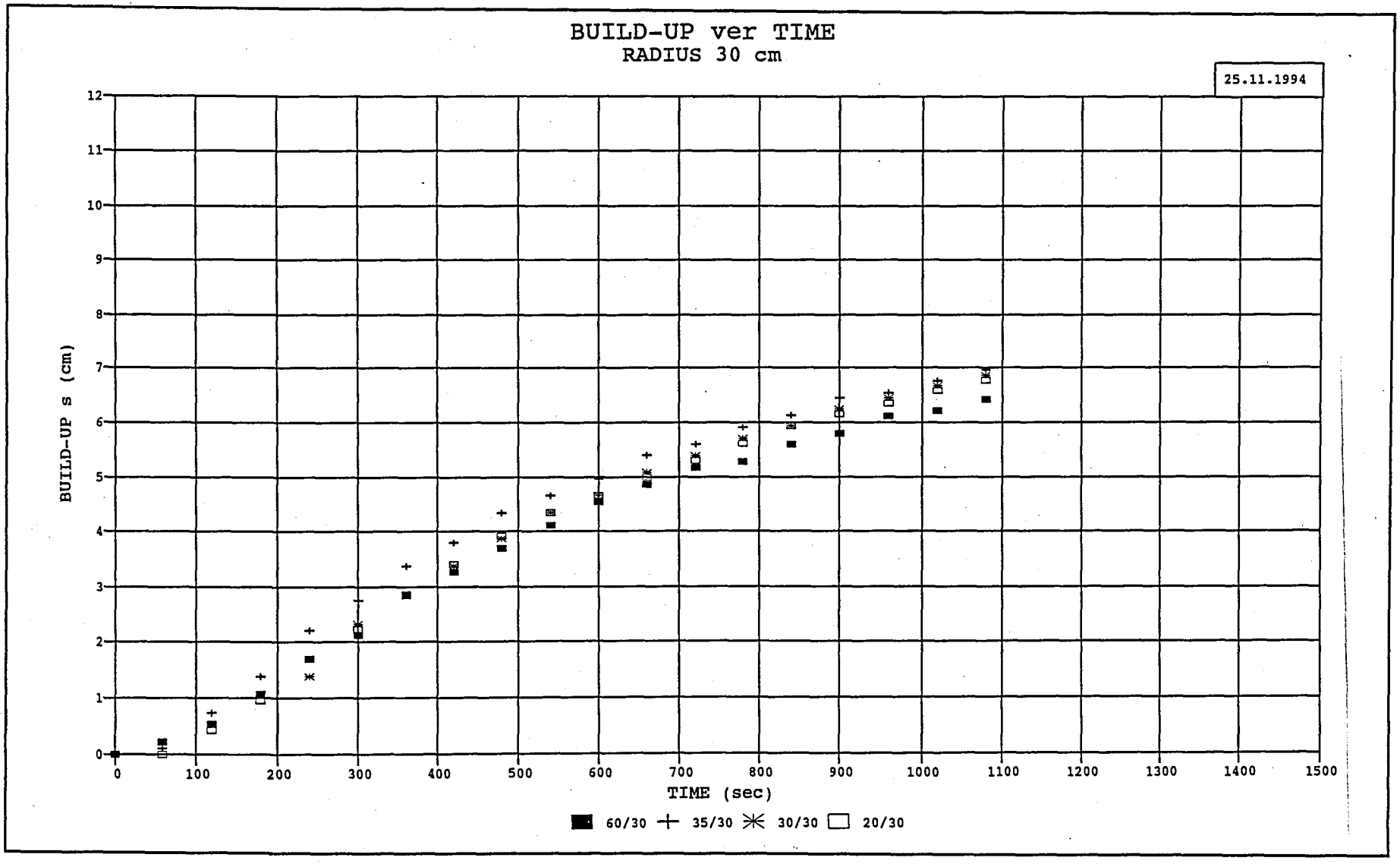
BUILD-UP ver TIME
RADIUS 30 cm
25.11.1994
BUILD-UP s (cm)
TIME (sec)
60/30
35/30
30/30
20/30

Fig. A.6

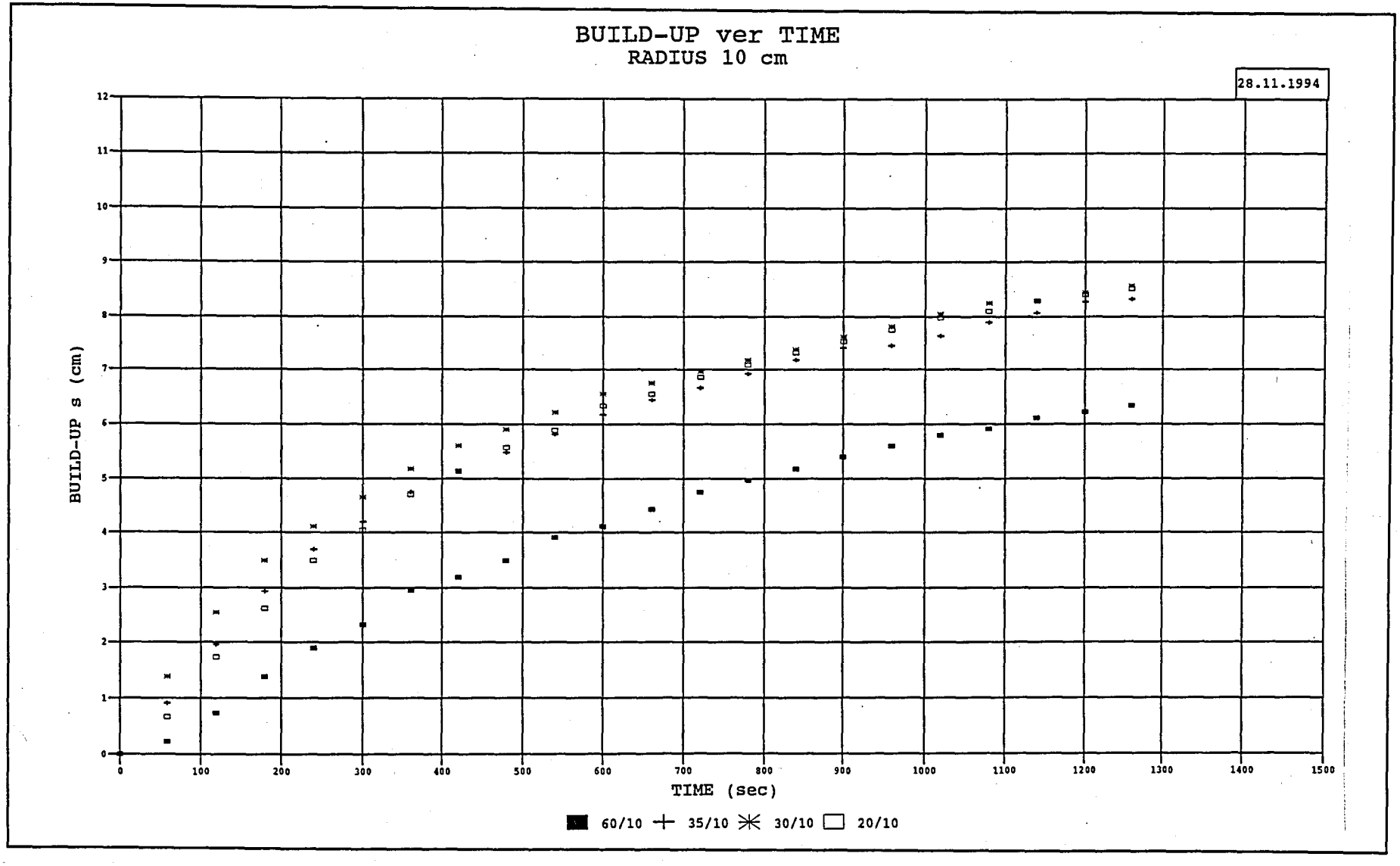
BUILD-UP ver TIME
RADIUS 10 cm
28.11.1994
BUILD-UP s (cm)
TIME (sec)
60/10
35/10
30/10
20/10

Fig. A.7

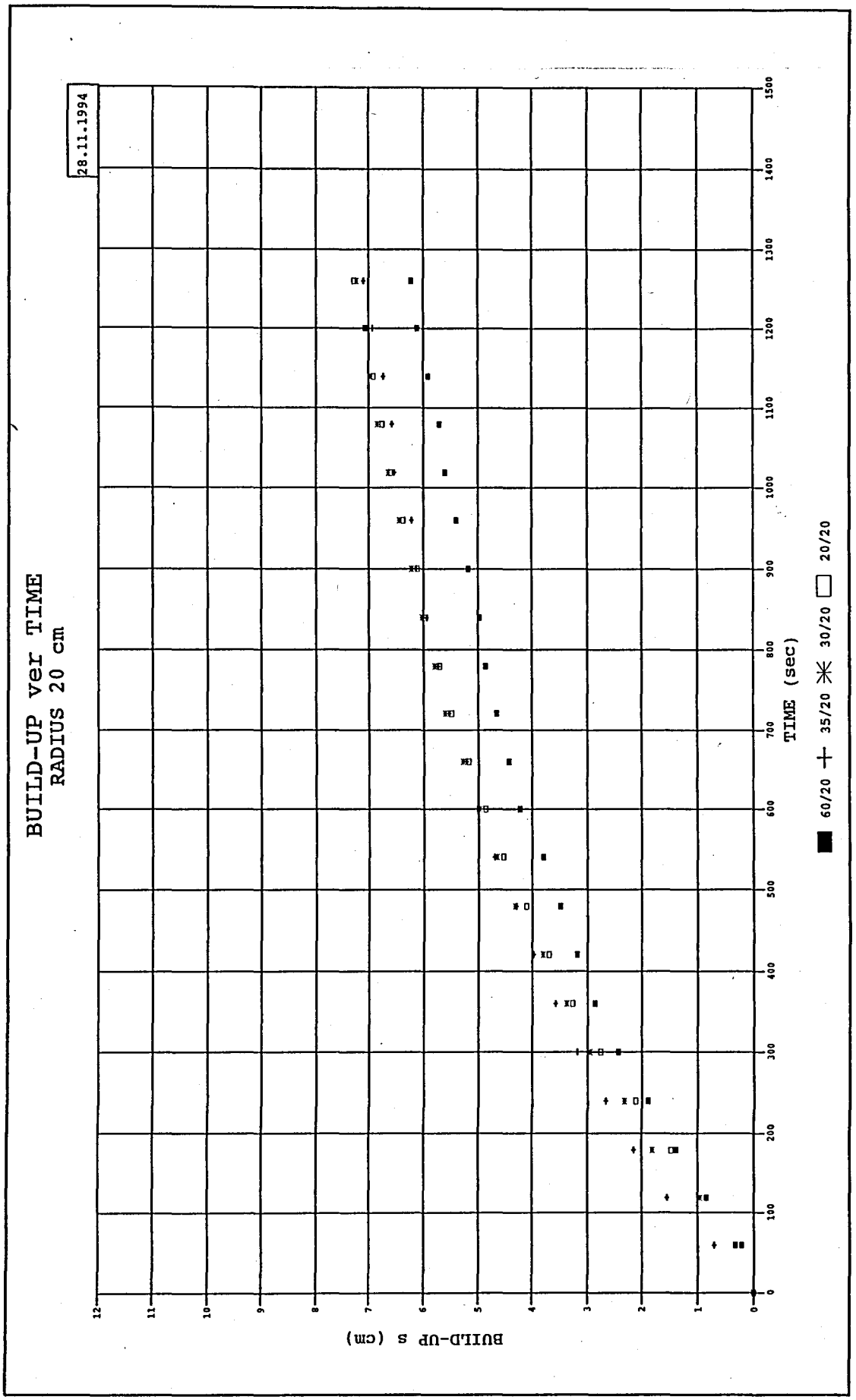
BUILD-UP ver TIME
RADIUS 20 cm
28.11.1994
BUILD-UP s (cm)
TIME (sec)
60/20
35/20
30/20
20/20

Fig. A.8

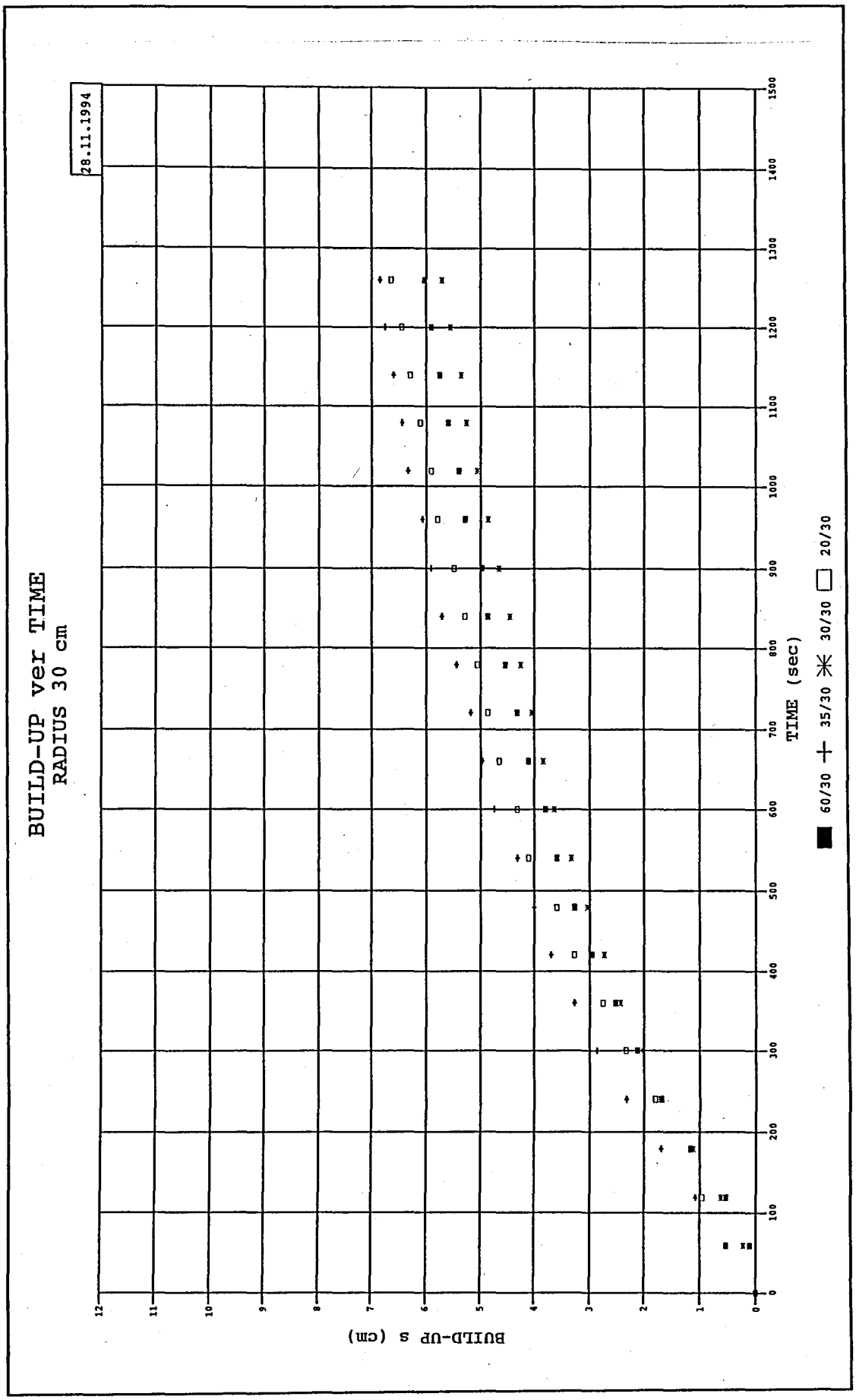
BUILD-UP ver TIME
RADIUS 30 cm
28.11.1994
BUILD-UP s (cm)
TIME (sec)
60/30
35/30
30/30
20/30

Fig. A.9

APPENDIX B

Semi-logaritmic plots of test results are given.

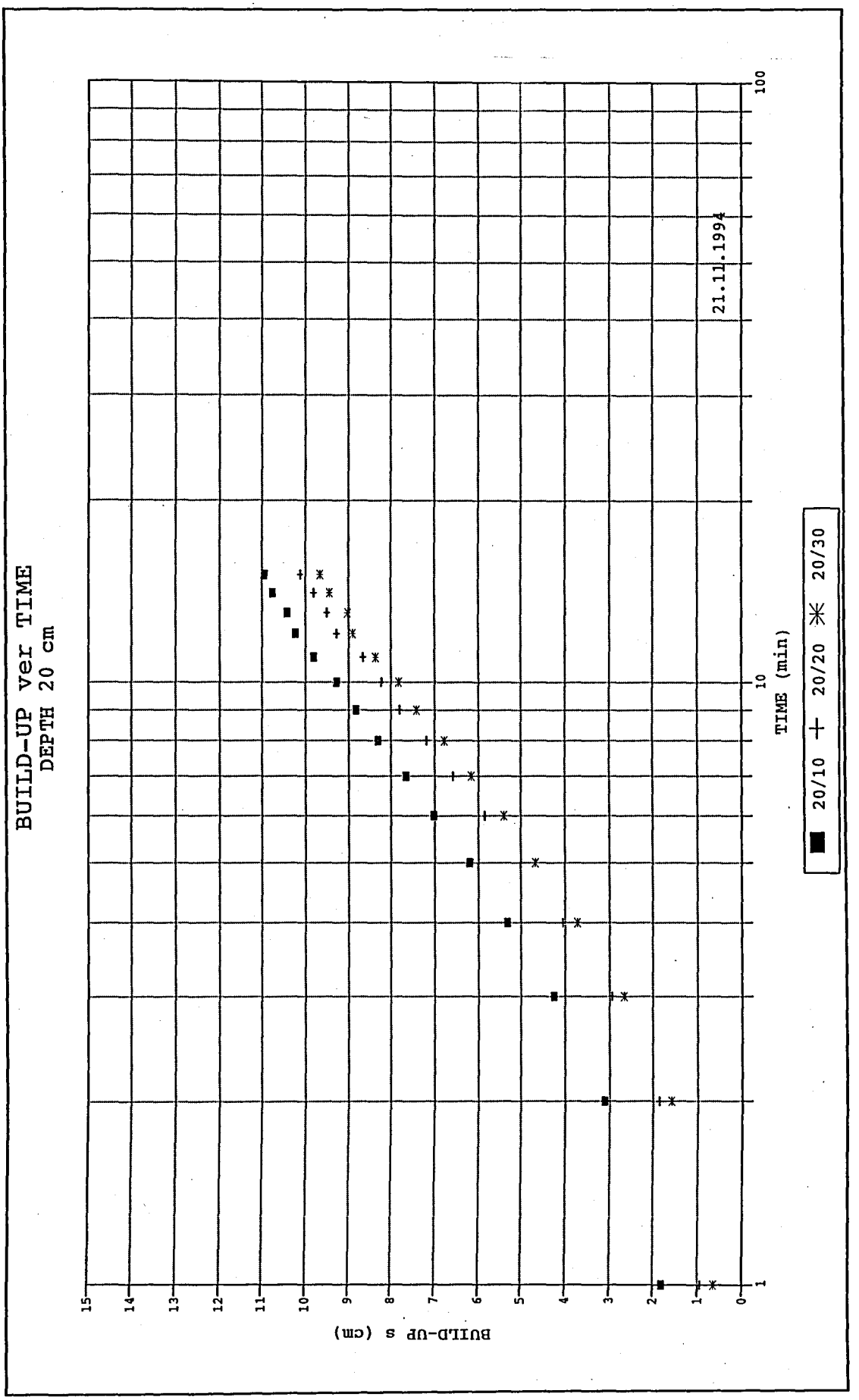
BUILD-UP ver TIME
DEPTH 20 cm
BUILD-UP s (cm)
TIME (min)
21.11.1994
20/10
20/20
20/30

Fig. B.1

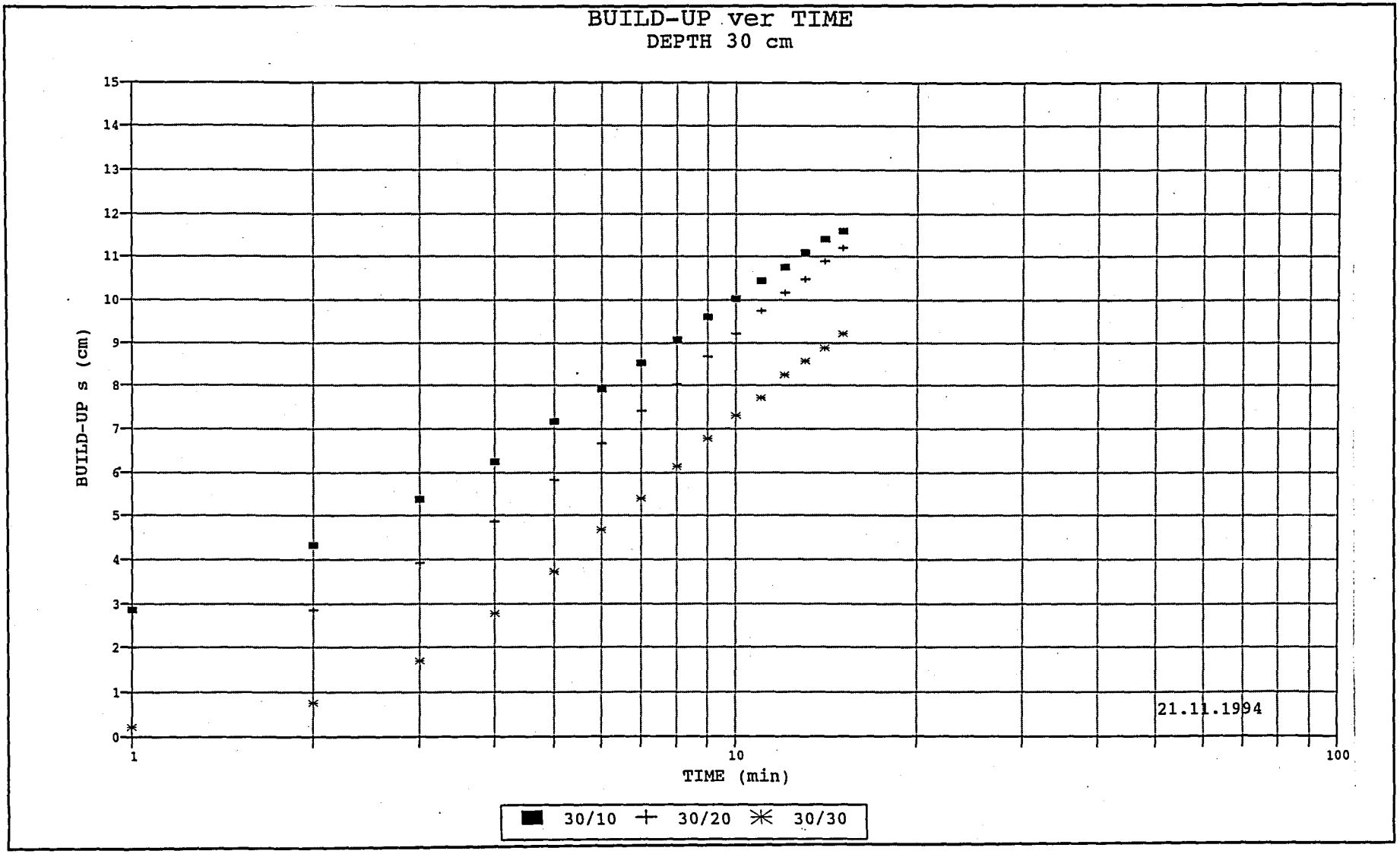
BUILD-UP ver TIME
DEPTH 30 cm
BUILD-UP s (cm)
TIME (min)
21.11.1994
30/10
30/20
30/30

Fig. B.2

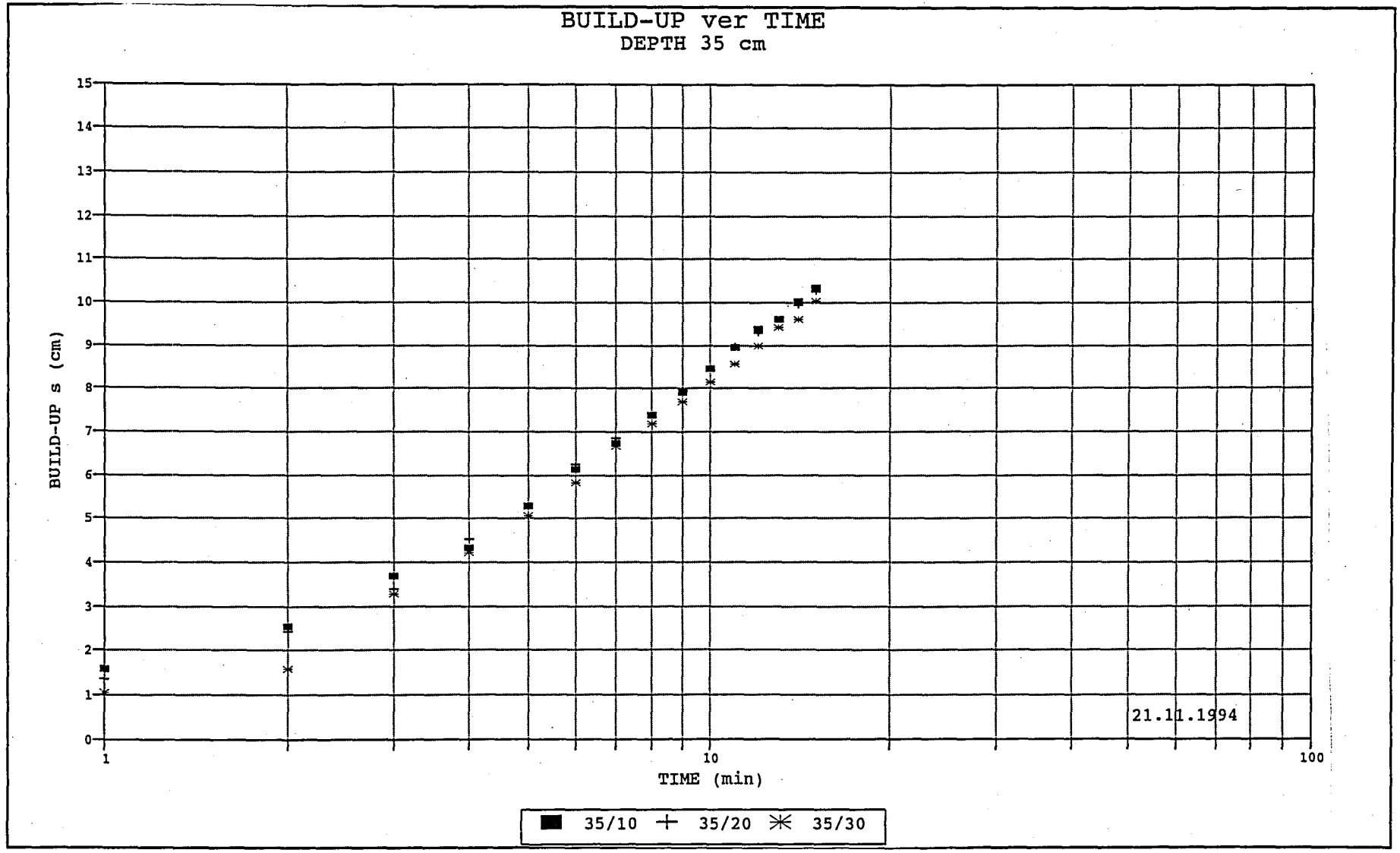
BUILD-UP ver TIME
DEPTH 35 cm
BUILD-UP s (cm)
TIME (min)
21.11.1994
35/10
35/20
35/30

Fig. B.3

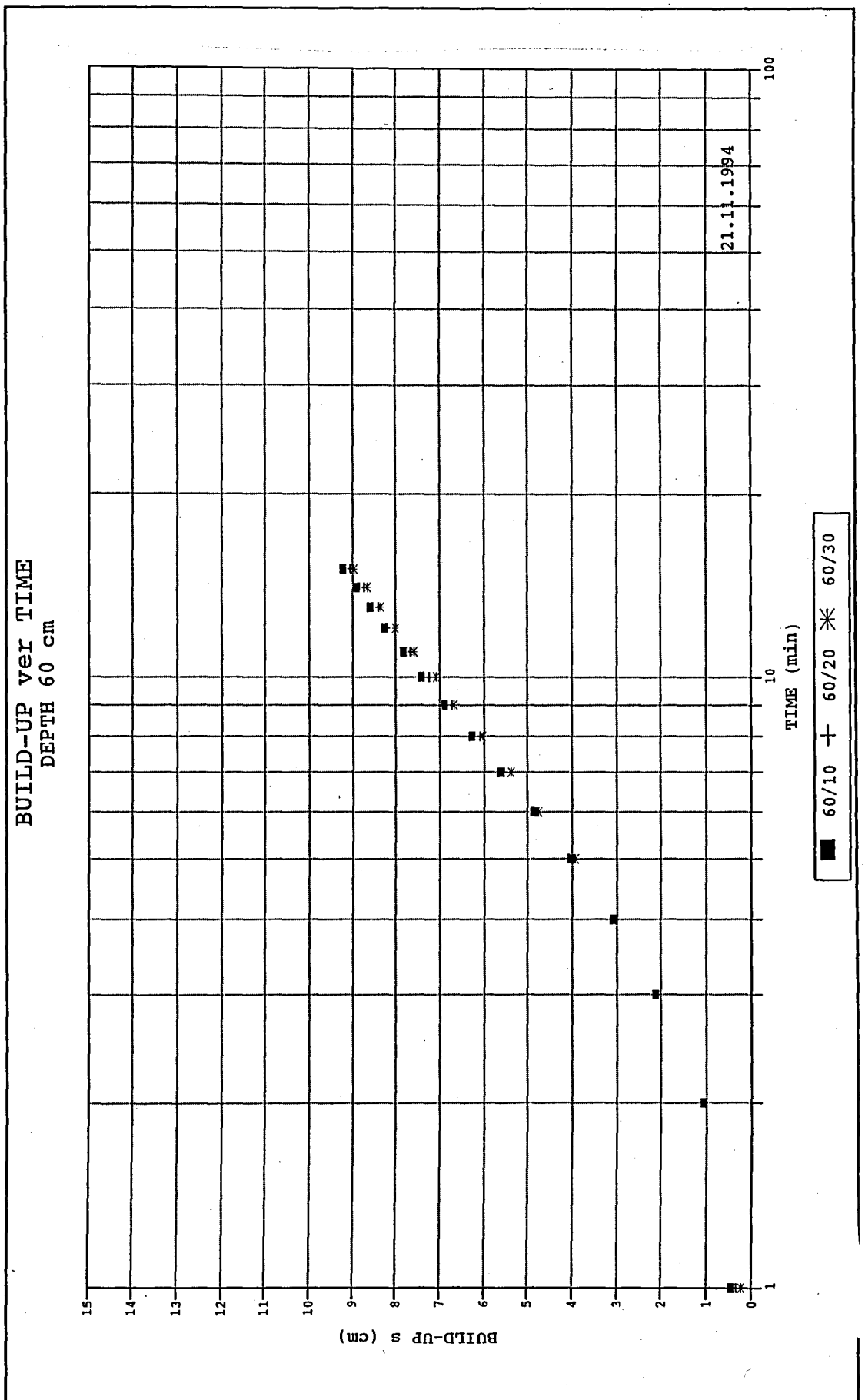
BUILD-UP ver TIME
DEPTH 60 cm
21.11.1994
BUILD-UP s (cm)
TIME (min)
60/10
60/20
60/30
0
1
2
3
4
5
6
7
8
9
10
11
12
13
14
15
1
10
100

Fig. B.4

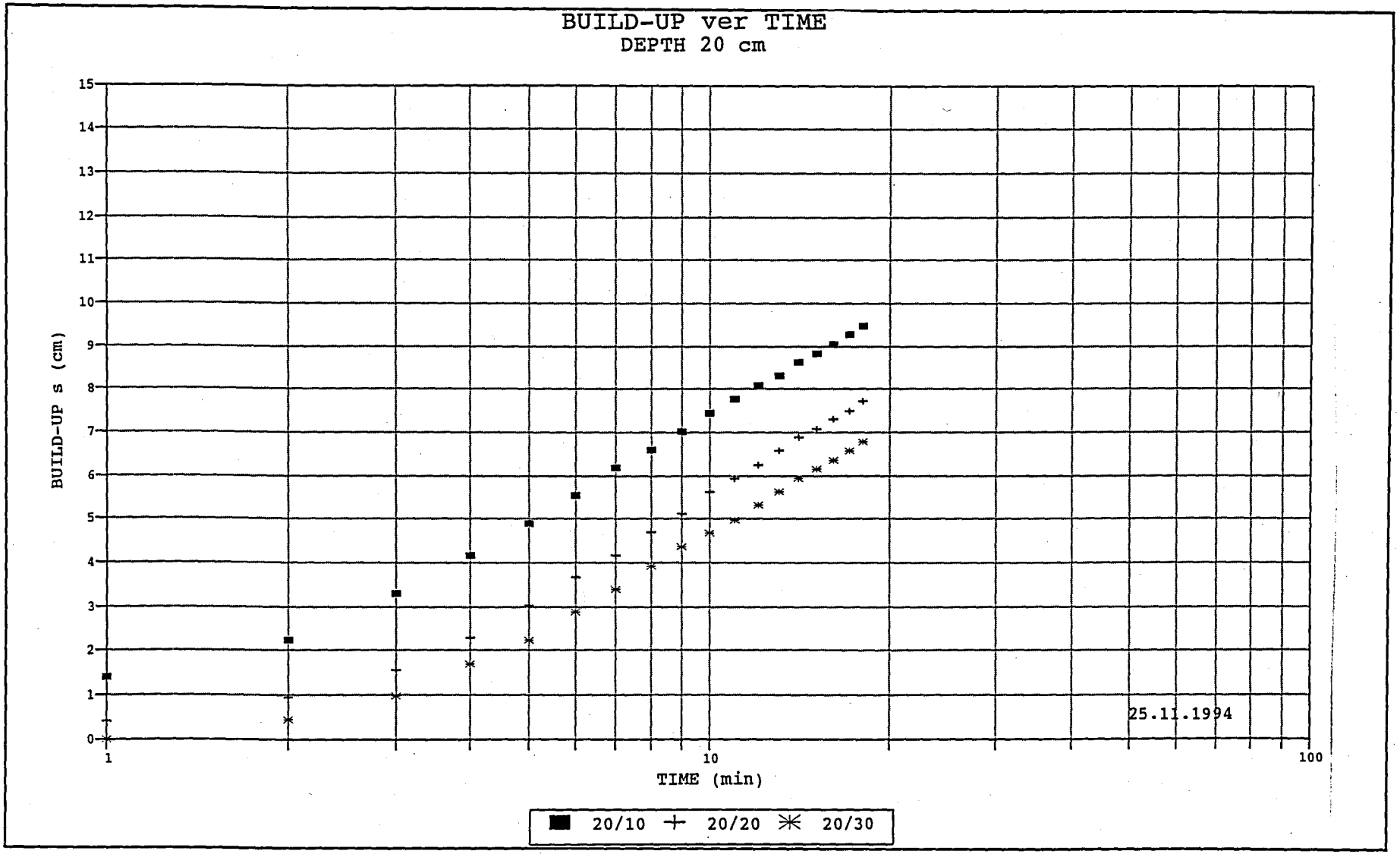
BUILD-UP ver TIME
DEPTH 20 cm
BUILD-UP s (cm)
TIME (min)
25.11.1994
20/10
20/20
20/30

Fig. B.5

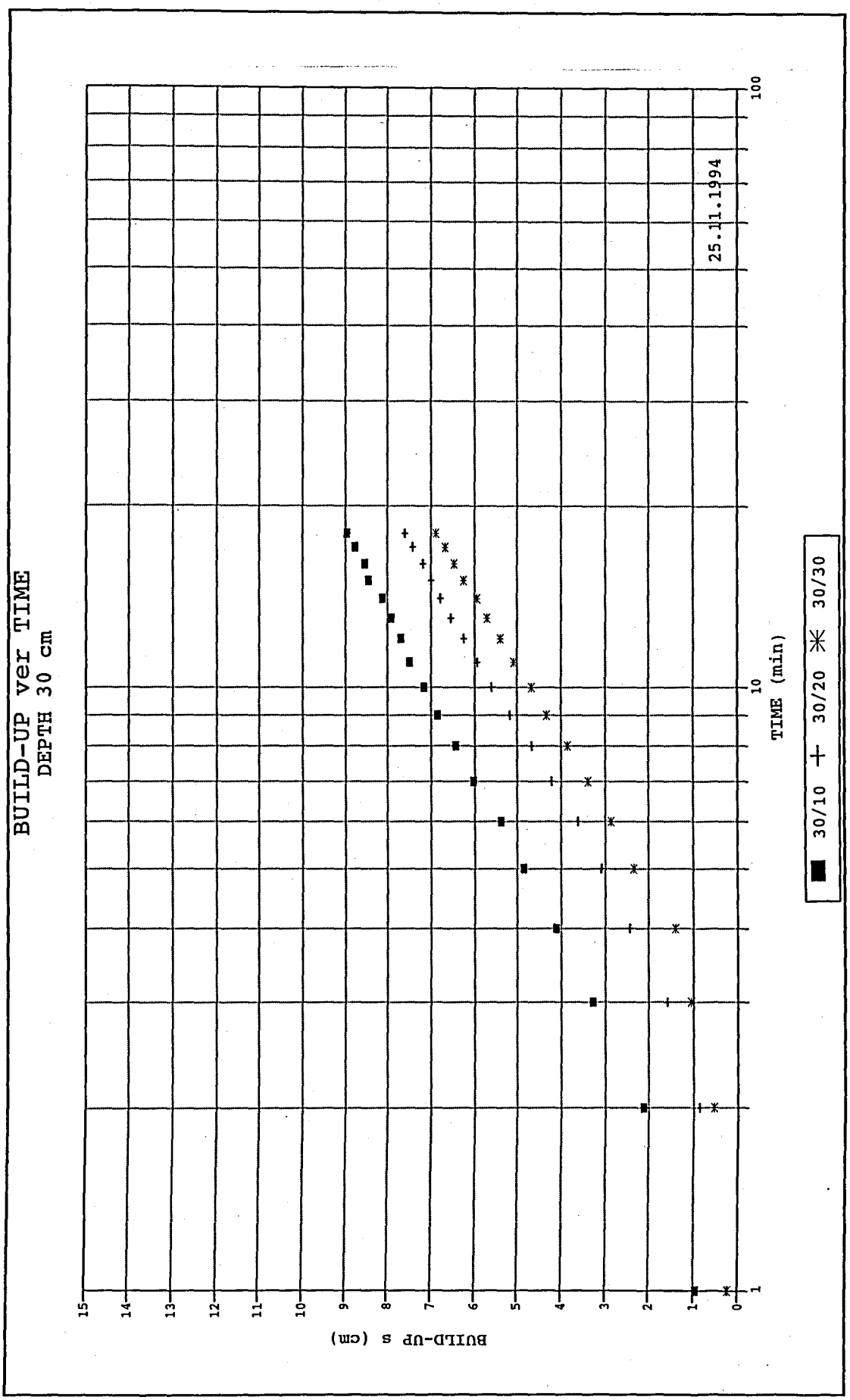
BUILD-UP ver TIME
DEPTH 30 cm
25.11.1994
BUILD-UP s (cm)
TIME (min)
30/10
30/20
30/30
0
1
2
3
4
5
6
7
8
9
10
11
12
13
14
15
1
10
100

Fig. B.6

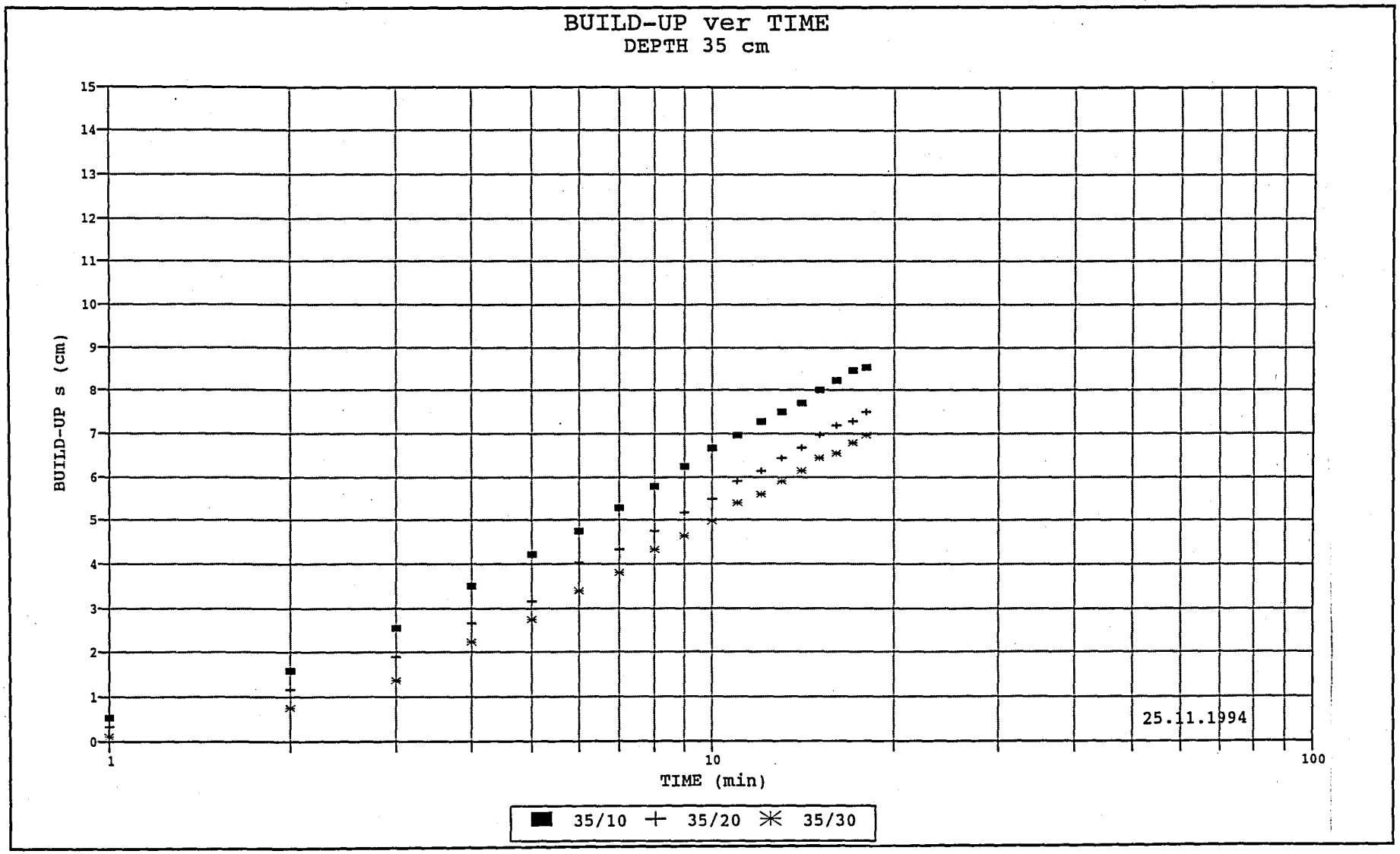
BUILD-UP ver TIME
DEPTH 35 cm
BUILD-UP s (cm)
0
1
2
3
4
5
6
7
8
9
10
11
12
13
14
15
1
10
100
TIME (min)
25.11.1994
35/10
35/20
35/30

Fig. B.7

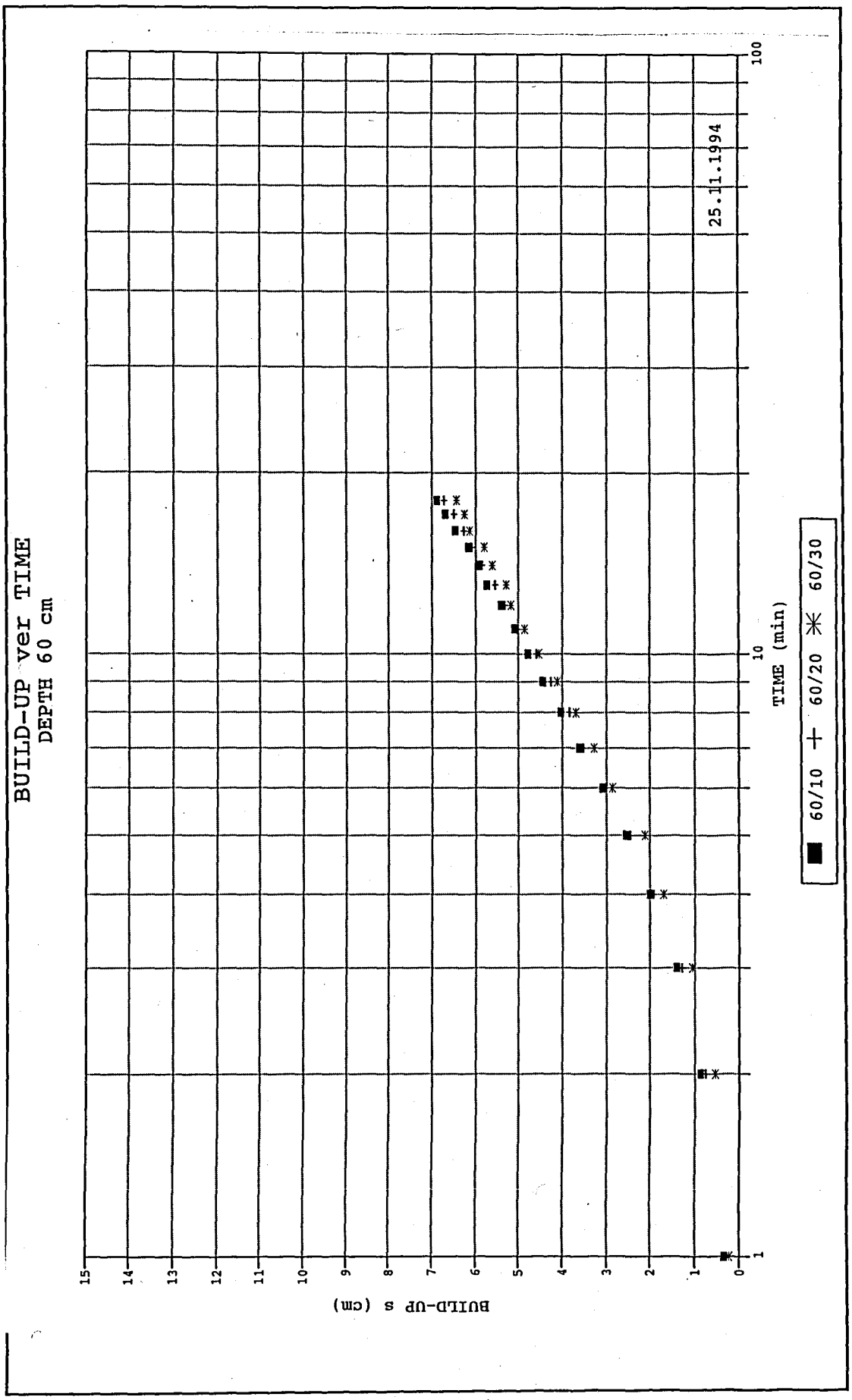
BUILD-UP ver TIME
DEPTH 60 cm
25.11.1994
BUILD-UP s (cm)
TIME (min)
60/10
60/20
60/30
0
1
2
3
4
5
6
7
8
9
10
11
12
13
14
15
1
10
100

Fig. B.8

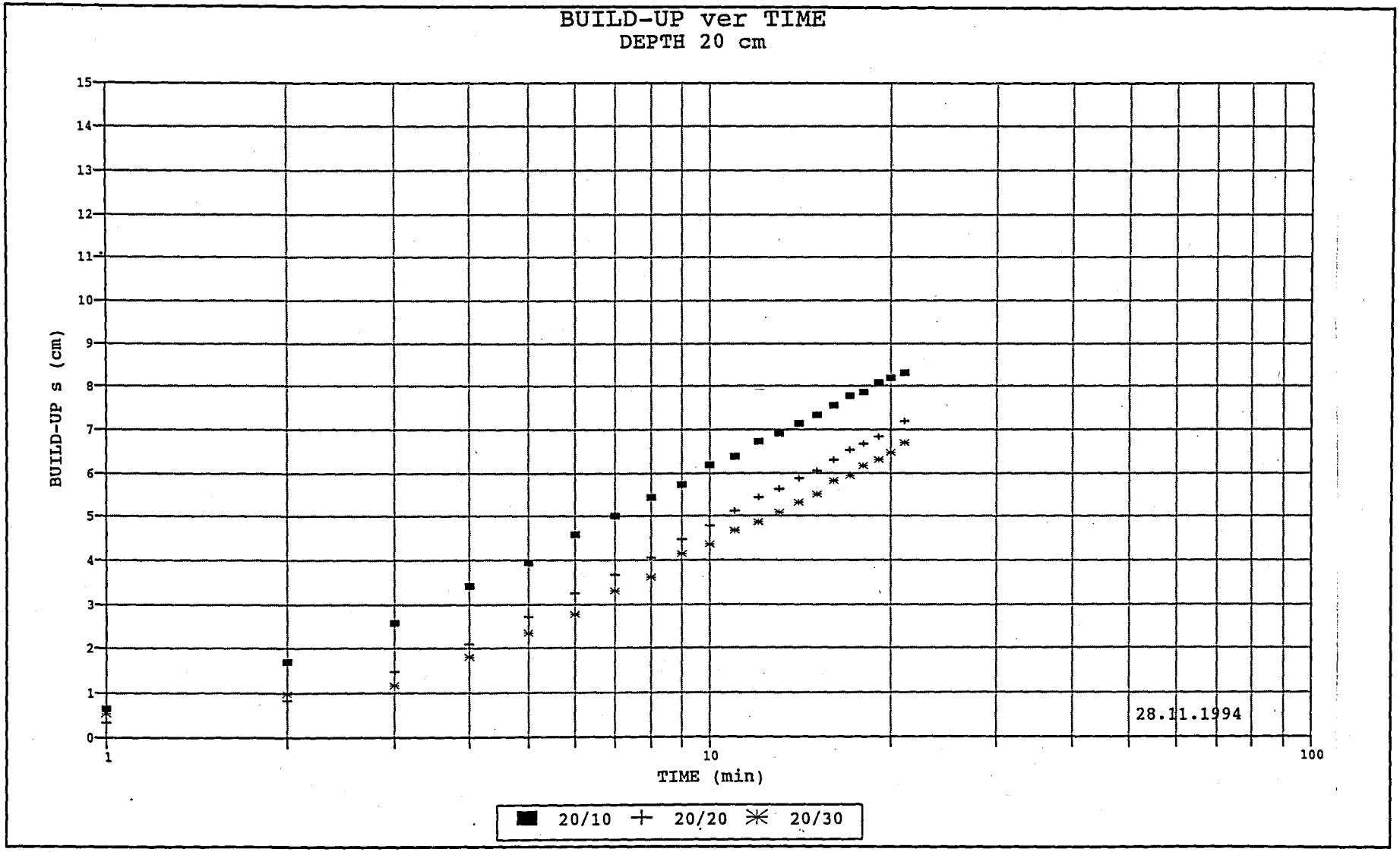
BUILD-UP ver TIME
DEPTH 20 cm
BUILD-UP s (cm)
TIME (min)
28.11.1994
20/10
20/20
20/30

Fig. B.9

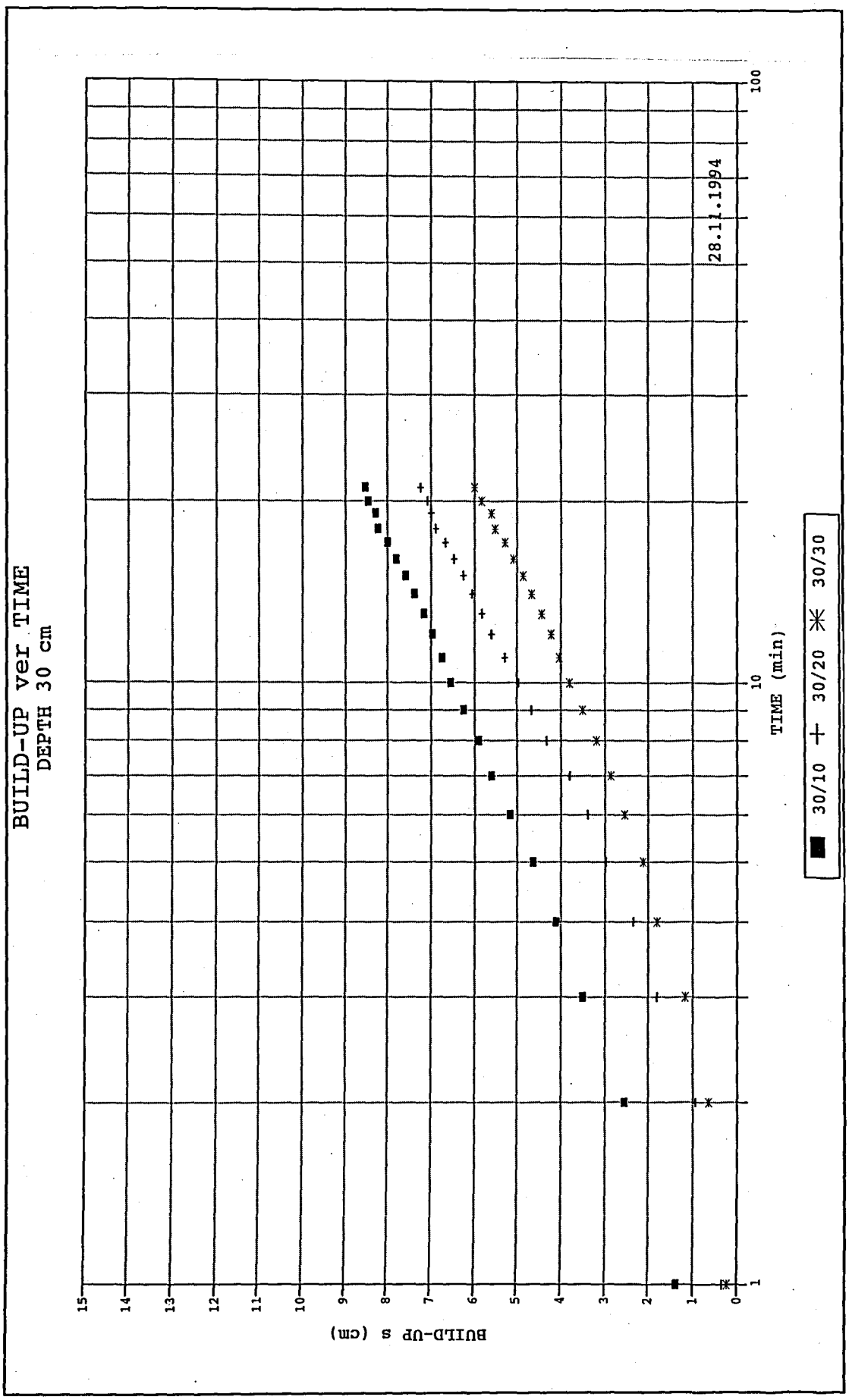
BUILD-UP ver TIME
DEPTH 30 cm
28.11.1994
BUILD-UP s (cm)
TIME (min)
30/10
30/20
30/30
0
1
2
3
4
5
6
7
8
9
10
11
12
13
14
15
1
10
100

Fig. B.10

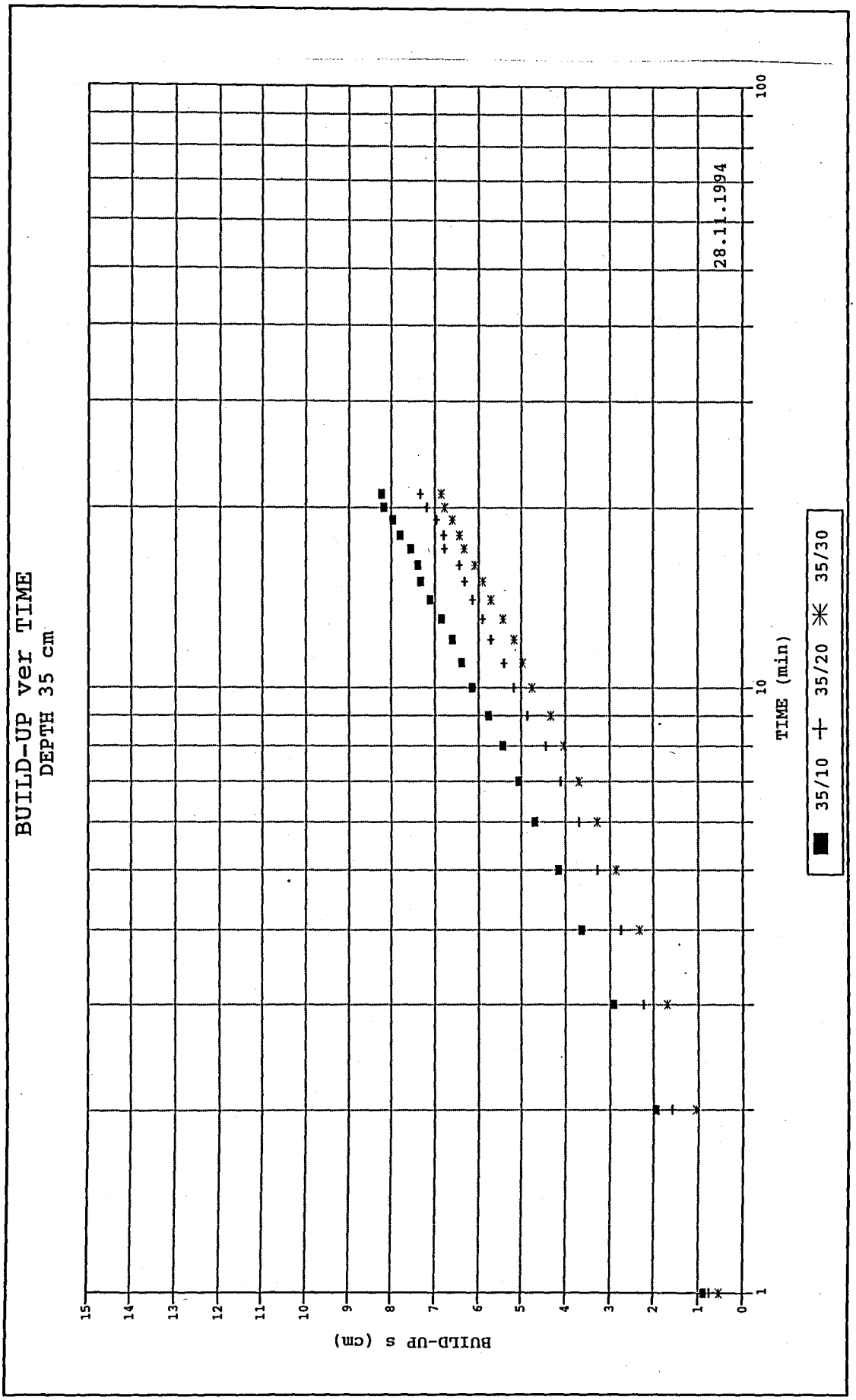
BUILD-UP ver TIME
DEPTH 35 cm
28.11.1994
BUILD-UP s (cm)
TIME (min)
35/10
35/20
35/30

Fig. B.11

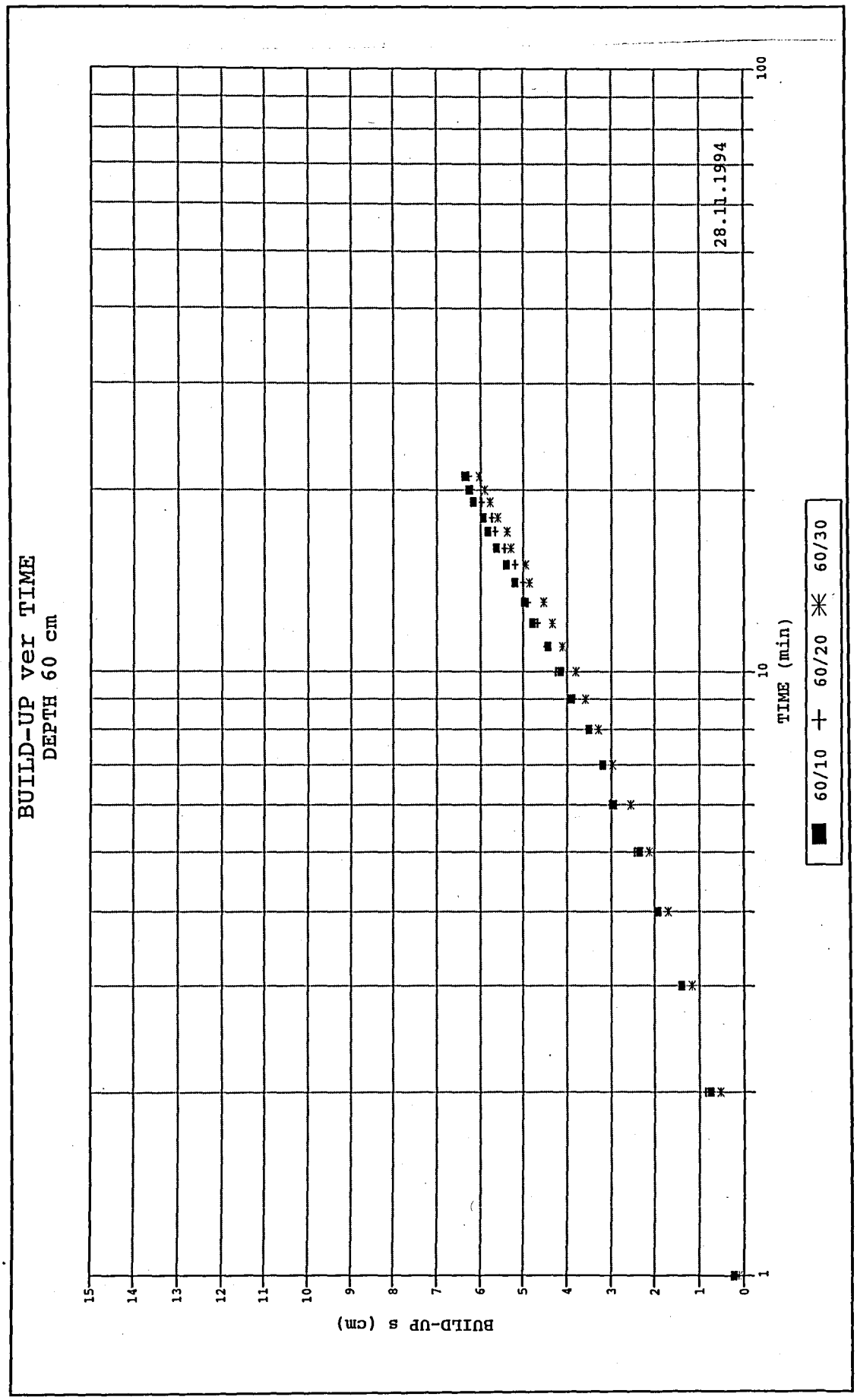
BUILD-UP ver TIME
DEPTH 60 cm
28.11.1994
BUILD-UP s (cm)
TIME (min)
60/10
60/20
60/30
0
1
2
3
4
5
6
7
8
9
10
11
12
13
14
15
1
10
100

Fig. B.12

APPENDIX C

The water levels at the piezometer in time are depicted.

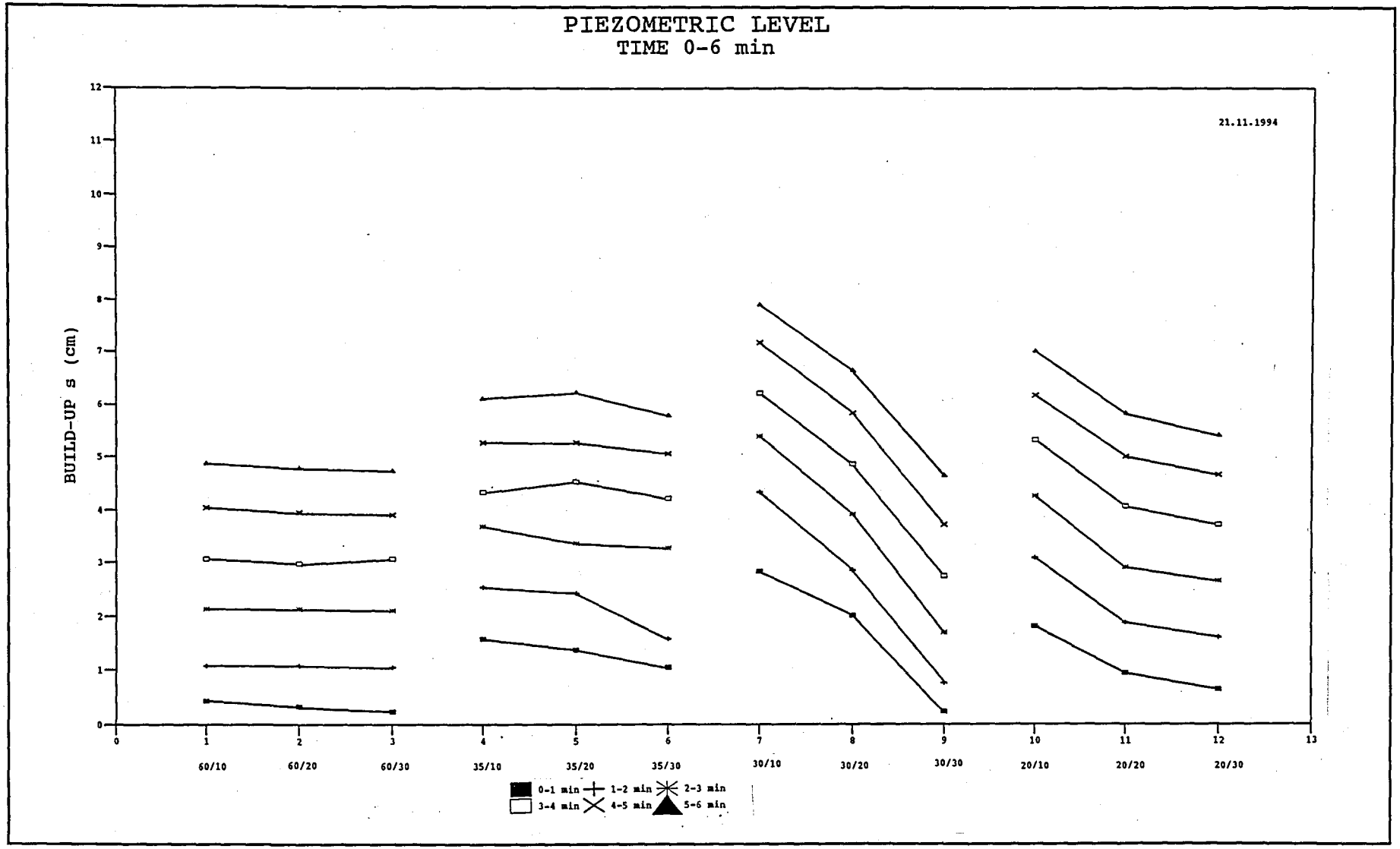
PIEZOMETRIC LEVEL
TIME 0-6 min
21.11.1994
BUILD-UP s (cm)
0
1
2
3
4
5
6
7
8
9
10
11
12
13
60/10
60/20
60/30
35/10
35/20
35/30
30/10
30/20
30/30
20/10
20/20
20/30
0-1 min
1-2 min
2-3 min
3-4 min
4-5 min
5-6 min

Fig. C.1

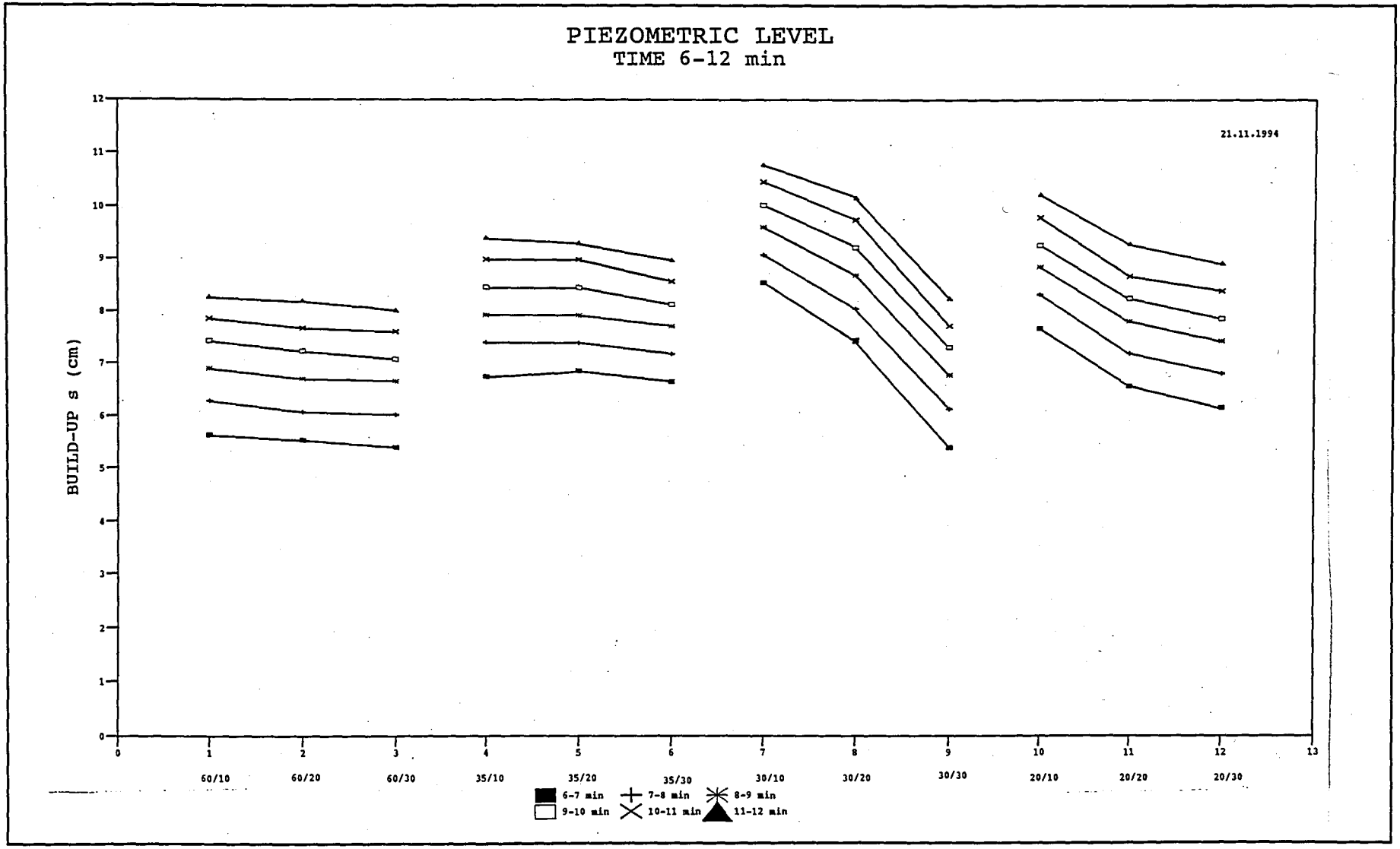
PIEZOMETRIC LEVEL
TIME 6-12 min
21.11.1994
BUILD-UP s (cm)
0
1
2
3
4
5
6
7
8
9
10
11
12
13
60/10
60/20
60/30
35/10
35/20
35/30
30/10
30/20
30/30
20/10
20/20
20/30
6-7 min
7-8 min
8-9 min
9-10 min
10-11 min
11-12 min

Fig. C.2

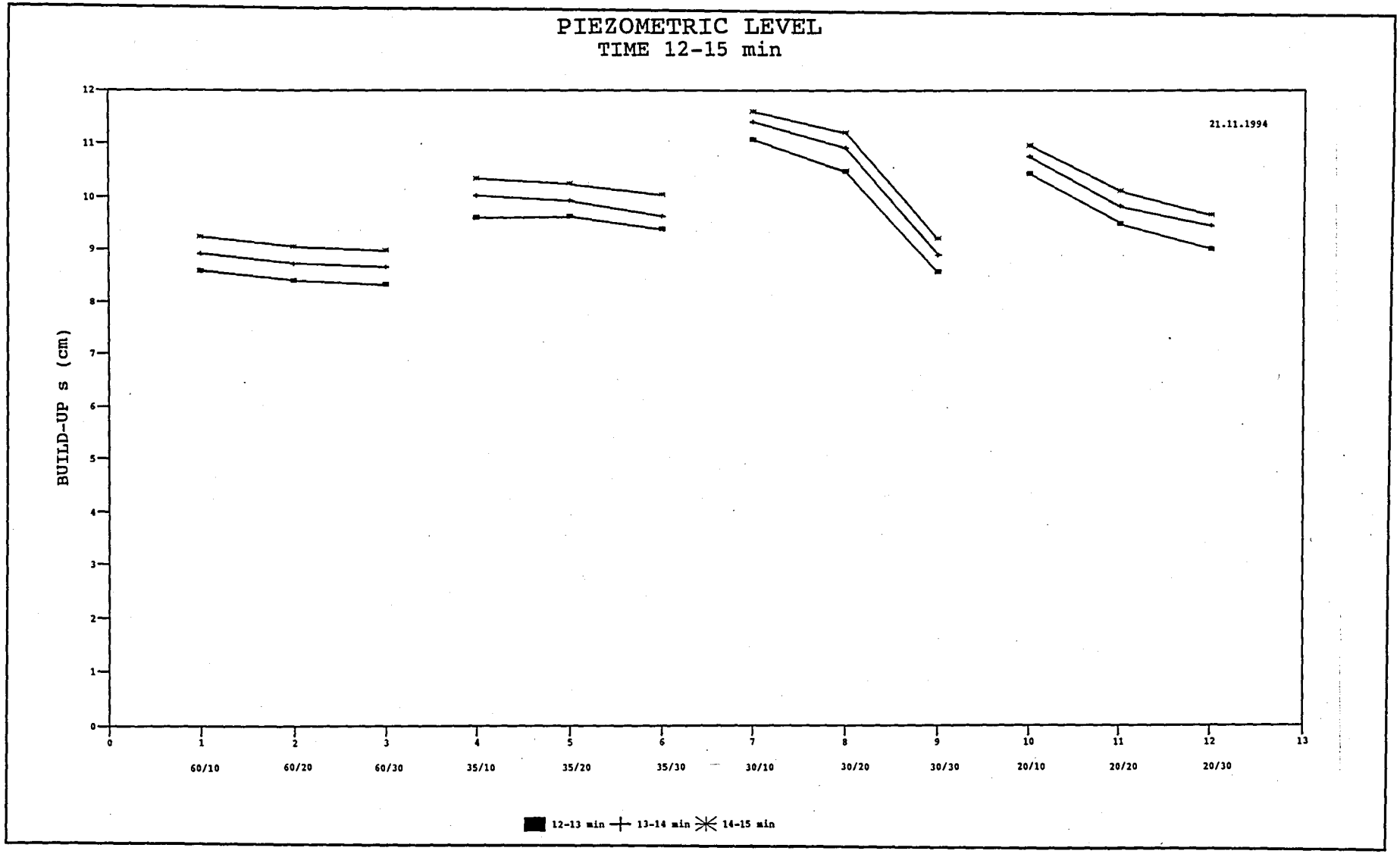
PIEZOMETRIC LEVEL
TIME 12-15 min
21.11.1994
BUILD-UP s (cm)
0
1
2
3
4
5
6
7
8
9
10
11
12
13
60/10
60/20
60/30
35/10
35/20
35/30
30/10
30/20
30/30
20/10
20/20
20/30
12-13 min
13-14 min
14-15 min

Fig. C.3

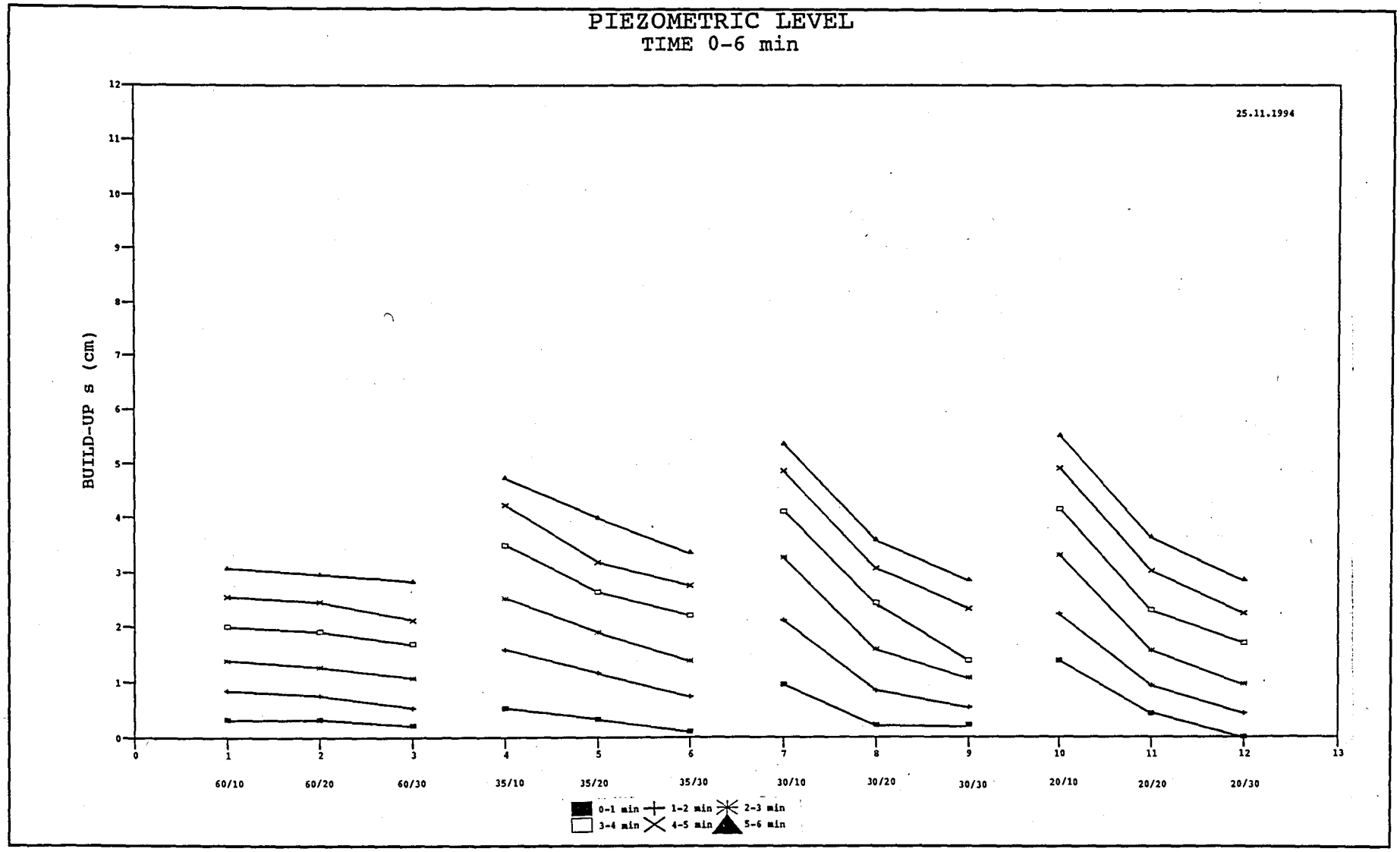
PIEZOMETRIC LEVEL
TIME 0-6 min
25.11.1994
BUILD-UP s (cm)
0
1
2
3
4
5
6
7
8
9
10
11
12
13
60/10
60/20
60/30
35/10
35/20
35/30
30/10
30/20
30/30
20/10
20/20
20/30
0-1 min
1-2 min
2-3 min
3-4 min
4-5 min
5-6 min

Fig. C.4

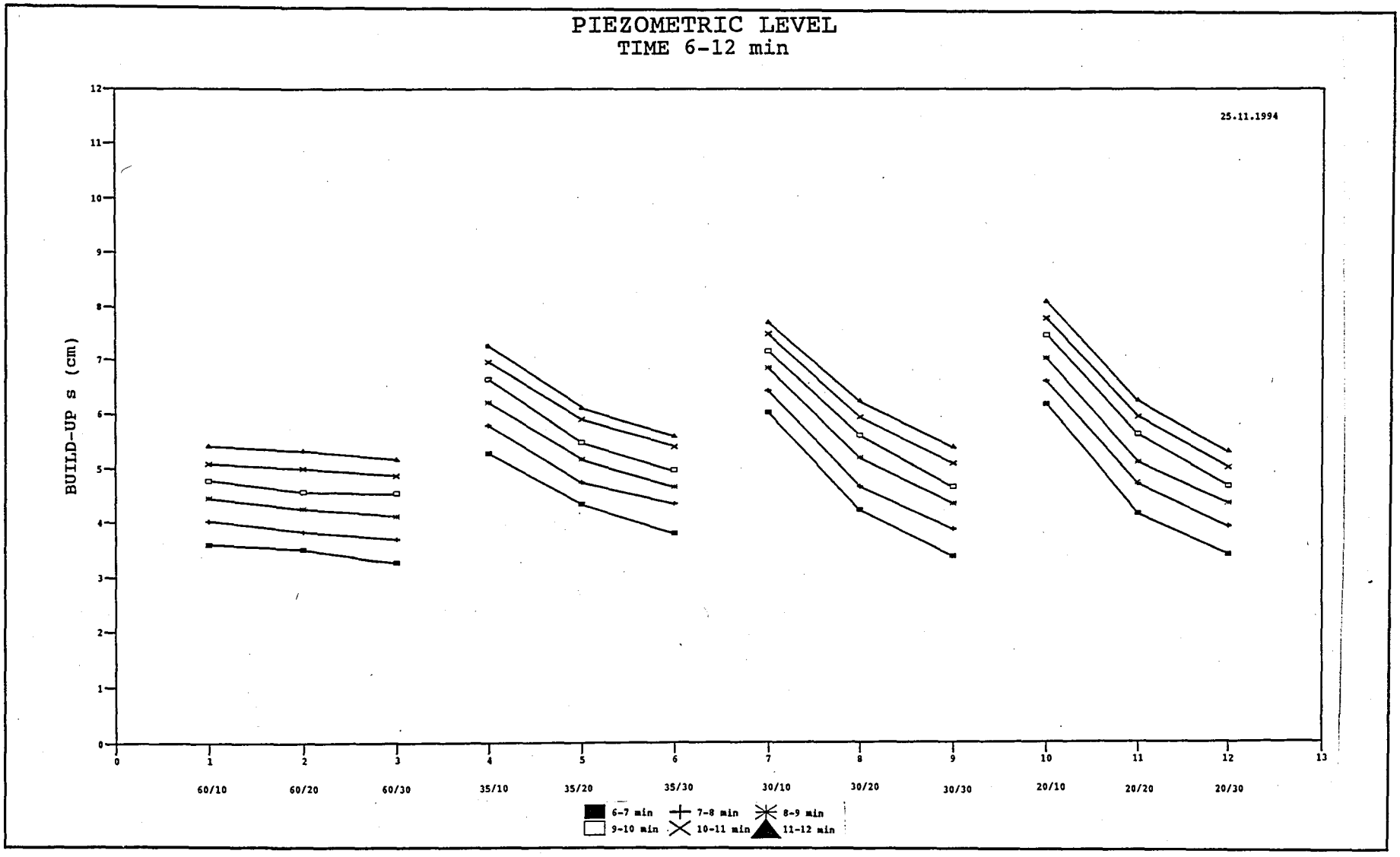
PIEZOMETRIC LEVEL
TIME 6-12 min
25.11.1994
BUILD-UP s (cm)
0
1
2
3
4
5
6
7
8
9
10
11
12
13
60/10
60/20
60/30
35/10
35/20
35/30
30/10
30/20
30/30
20/10
20/20
20/30
6-7 min
7-8 min
8-9 min
9-10 min
10-11 min
11-12 min

Fig. C.5

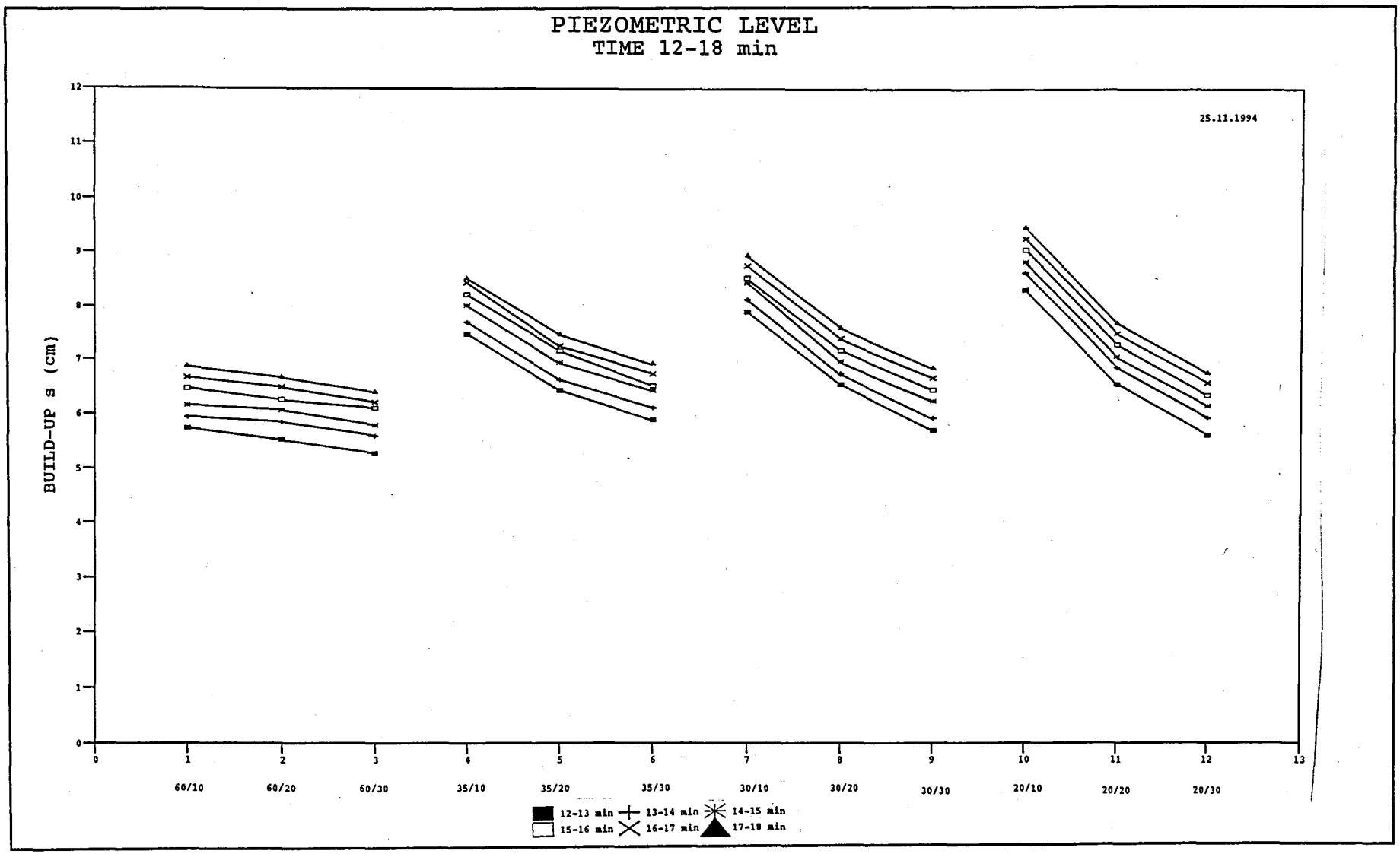
PIEZOMETRIC LEVEL
TIME 12-18 min
25.11.1994
BUILD-UP s (cm)
0
1
2
3
4
5
6
7
8
9
10
11
12
13
60/10
60/20
60/30
35/10
35/20
35/30
30/10
30/20
30/30
20/10
20/20
20/30
12-13 min
13-14 min
14-15 min
15-16 min
16-17 min
17-18 min

Fig. C.6

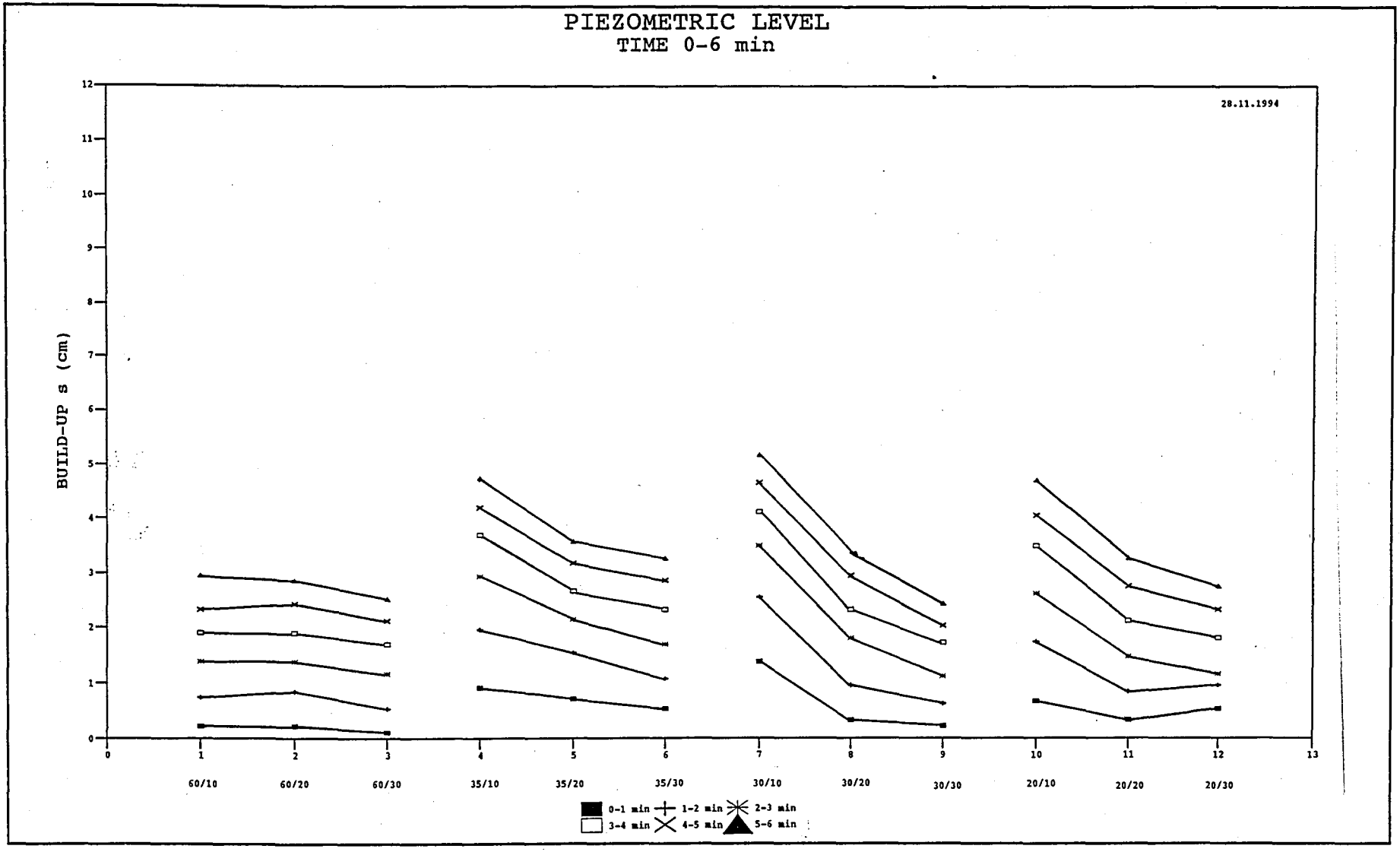
PIEZOMETRIC LEVEL
TIME 0-6 min
28.11.1994
BUILD-UP s (cm)
0
1
2
3
4
5
6
7
8
9
10
11
12
13
60/10
60/20
60/30
35/10
35/20
35/30
30/10
30/20
30/30
20/10
20/20
20/30
0-1 min
1-2 min
2-3 min
3-4 min
4-5 min
5-6 min

Fig. C.7

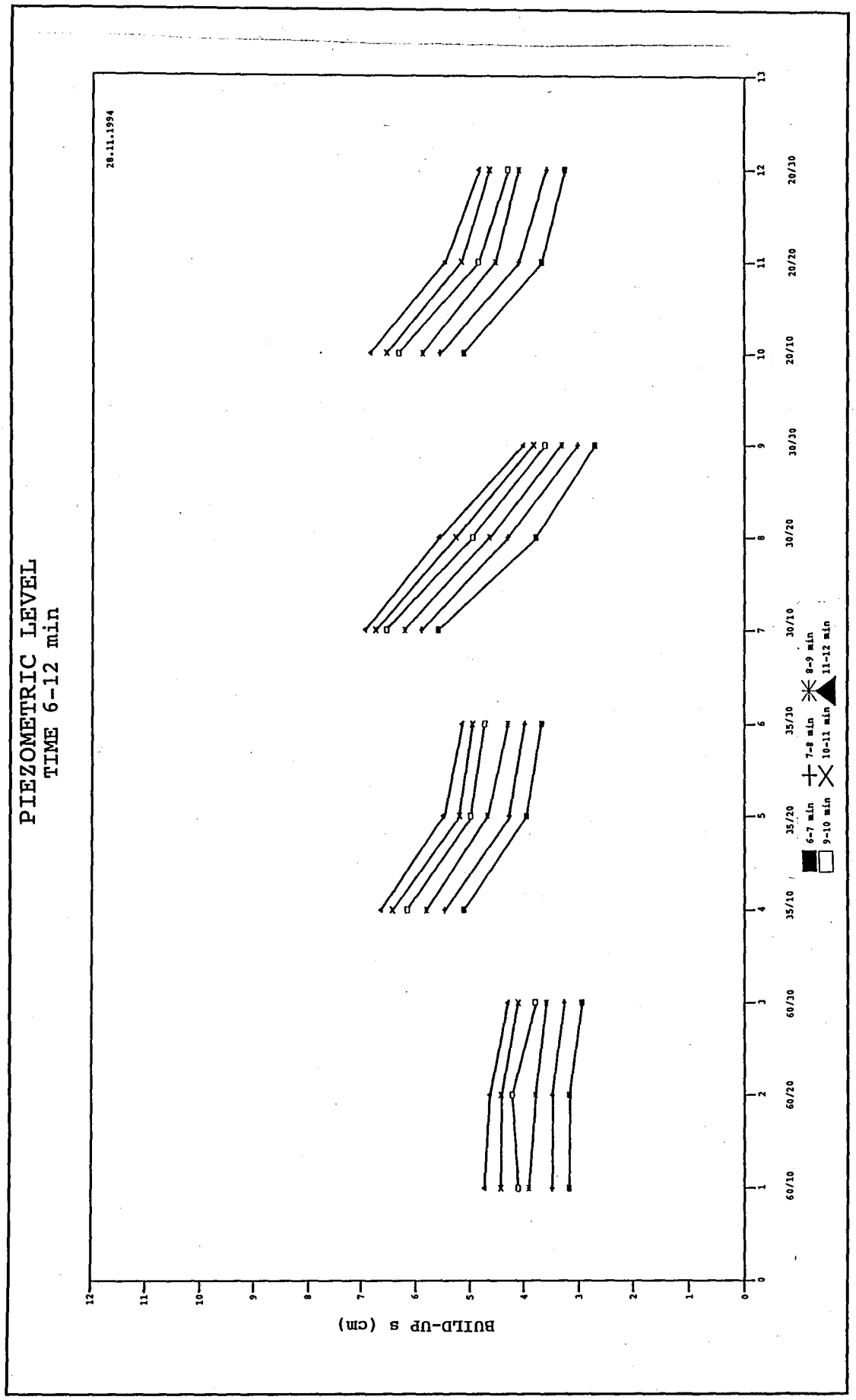
PIEZOMETRIC LEVEL
TIME 6-12 min
28.11.1994
BUILD-UP s (cm)
0
1
2
3
4
5
6
7
8
9
10
11
12
13
60/10
60/20
60/30
35/10
35/20
35/30
30/10
30/20
30/30
20/10
20/20
20/30
6-7 min
7-8 min
8-9 min
9-10 min
10-11 min
11-12 min

Fig. C.8

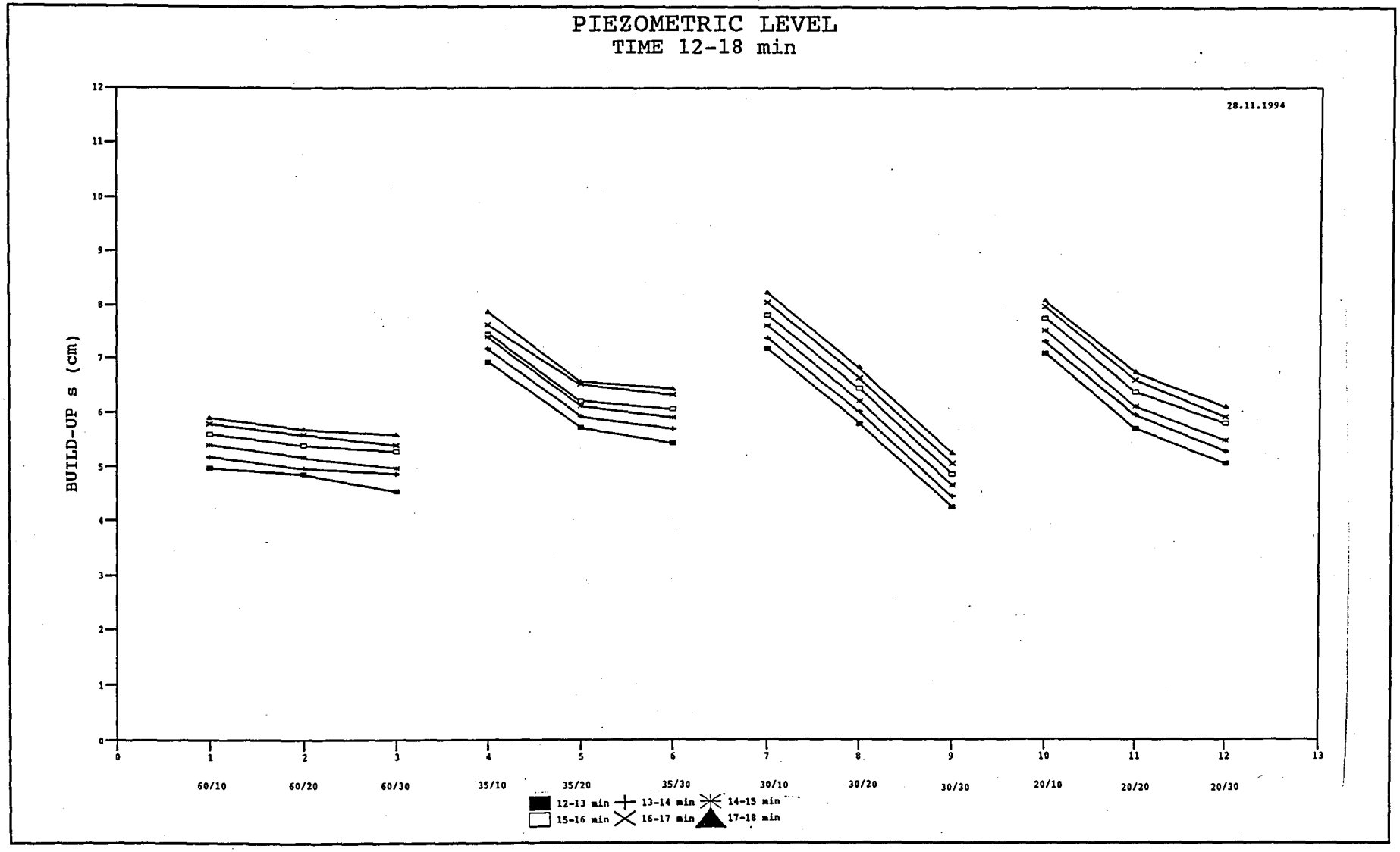
PIEZOMETRIC LEVEL
TIME 12-18 min
28.11.1994
BUILD-UP s (cm)
0
1
2
3
4
5
6
7
8
9
10
11
12
60/10
60/20
60/30
35/10
35/20
35/30
30/10
30/20
30/30
20/10
20/20
20/30
12-13 min
13-14 min
14-15 min
15-16 min
16-17 min
17-18 min

Fig. C.9

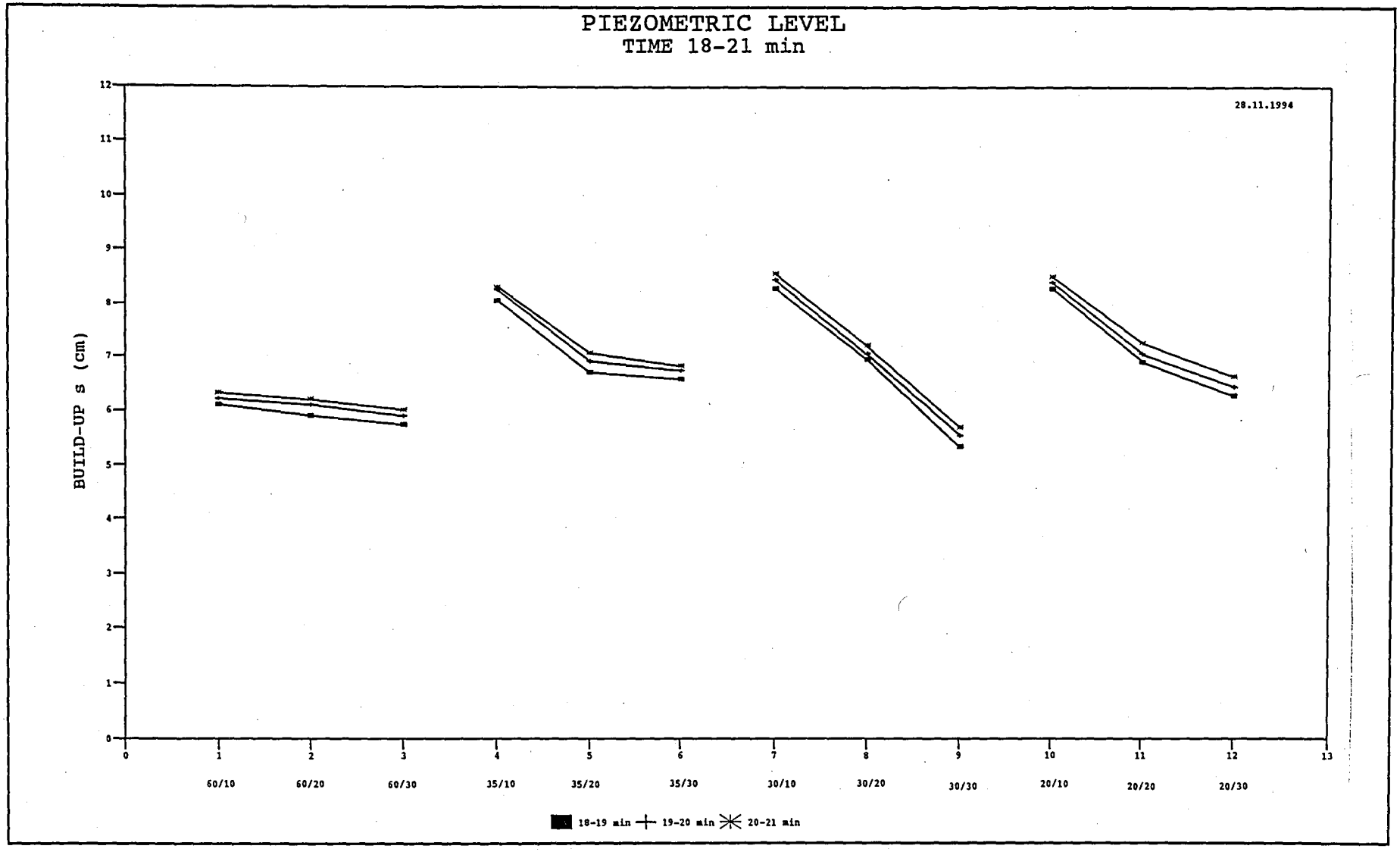
PIEZOMETRIC LEVEL
TIME 18-21 min
28.11.1994
BUILD-UP s (cm)
0
1
2
3
4
5
6
7
8
9
10
11
12
13
60/10
60/20
60/30
35/10
35/20
35/30
30/10
30/20
30/30
20/10
20/20
20/30
18-19 min
19-20 min
20-21 min

Fig. C.10

REFERENCES

1. Al-Dhahir, Z.A., and Morgenstern, N. R., "Intake Factors for Cylindrical Piezometer Tips ," *Soil Science*, Vol. 107, No. 1, pp. 17-21, 1969.

2. Anderson, D. C., Crawley, W., and Zabcik, J. D., "Effects of Various Liquids on Clay Soil: Bentonite Slurry Mixtures," in Hydraulic Barriers in Soil and Rock, ASTM STP 874, A.I. Johnson, R.K. Frobel, N.J. Cavalli, and C.B. Pettersson, (Eds.), ASTM, Philadelphia, pp. 93-103, 1985.

3. Anderson, D. C., Crawley, W., and Zabcik, J. D., "Effects of Various Liquids on Clay Soil: Bentonite Slurry Mixtures," in *Hydraulic Barriers in Soil and Rock, ASTM STP 874*, A.I. Johnson, R.K. Frobel, N.J. Cavalli, and C.B. Pettersson, (Eds.), ASTM, Philadelphia, pp. 93-103, 1985.

4. Avcı, C. B., "Analysis of In Situ Permeability Test in Nonpenetrating Well, *"Journal of Ground Water"* Vol. 32, No. 2, pp. 312-322, 1994.

5. Avcı, C. B., Güler, E., and Kılanç, B., "Variable Head Test Analysis in Partially Penetrating Wells, *"Journal of Geotechnical Engineering, ASCE,* (in print).

6. Avcı, C. B. and Kılanç, B., "Analysis of Constant Head Tests Performed in Cylindrical Piezometers, *"Journal of Geotechnical Engineering, ASCE* (in review).

7. Boonstra, J., "Aquifer Tests with Partially Penetrating Wells: Theory and Practice," *Journal of Hydrology,* Vol. 137, pp. 165-179, 1992.

8. Boynton, S. S., and Daniel, D.E., "Hydraulic Conductivity Tests on Compacted Clay," *Journal of Geotechnical Engineering, ASCE,* Vol. 111, No. 4, pp. 465-478, April 1985.

9. Brand, E. W., and Premchitt, J., "Shape Factors of Cylindrical Piezometers," *Geotechnique,* Vol. 30, No. 4, pp. 369-384, 1980.

10. Cedergren, H. R., *Seepage, Drainage, and Flow Nets,* John Wiley & Sons, Inc, 1968.

11. Chapius, R.P. "Shape Factors for Permeability Tests in Boreholes and Piezometers," *Ground Water,* Vol. 27, No. 5, pp. 647-654, September-October 1989.

12. Chapuis, R. P., Soulié, M., and Sayegh, G., "Laboratory Modeling of Field Permeability Tests in Cased Boreholes," *Canadian Geotechnical Journal,* Vol. 27, pp. 647-658, 1990.

13. Dagan, G., "A Note on Packer, Slug, and Recovery Tests in Unconfined Aquifers," *Water Resources Research,* Vol. 14, No. 5, pp. 929-934, October 1978.

14. Daniel, D. E. "Predicting Hydraulic Conductivity of Clay Liners," *Journal of Geotechnical Engineering,* ASCE, Vol. 110, No. 2, pp. 285-300, February 1984.

15. Daniel, D.E., "In-Situ Hydraulic Conductivity Tests for Compacted Clay," *Journal of Geotechnical Engineering,ASCE,* Vol. 115, No. 9, pp. 1205-1226, September 1989.

16. Daniel, D.E., Anderson, D. C., and Boynton,S.S., "Fixed Wall versus Flexible Wall Permeameters," in *Hydraulic Barriers in Soil and Rock, ASTM STP 874,* A.I. Johnson, R.K. Frobel, N.J. Cavalli, and C.B. Pettersson, (Eds.), ASTM, Philadelphia, pp. 107-126, 1985.

17. Day, S. R., and Daniel, D. E., "Hydraulic Conductivity of Two Prototype Clay Liners," *Journal of Geotechnical Engineering, ASCE,* Vol. 111, No. 8, pp. 957-970, August 1985.

18. Dougherty, D. E., and Babu, D. K., "Flow to a Partially Penetrating Well in a Double-Porosity Reservoir," *Water Resources Research,* Vol. 20, No. 8, pp. 1116-1122, August 1984.

19. Fernuik, N., and Haug, M., "Evaluation of In-Situ Permeability Testing Methods," *Journal of Geotechnical Engineering, ASCE,* Vol. 116, No. 2, pp. 297-311, February, 1990.

20. Gefell, M. J., Thomas, G. M., and Rossella, S. J., "Maximum Water-Table Drawdown at a Fully Penetrating Well," *Ground Water,* Vol. 32, No. 3, May-pp. 411-419, June 1994.

21. Gibson, R. E., "A Note on the Constant Head Test to Measure Soil Permeability In Situ," *Geotechnique,* Vol. 16, No. 3, pp. 256-259, 1966.

22. Gibson, R. E., "An Analysis of System Flexibility and its Effect on Time-Lag in Pore-Water Pressue Measurements," *Geotechnique,* Vol. 13, No. 1, pp. 1-11, 1963.

23. Gibson, R. E., "An Extension to the Theory of the Constant Head In-Situ Permeability Test," *Geotechnique,* Vol. 20, No. 2, pp. 193-197, 1970.

24. Hantush, M. S., "Drawdown Around a Partially Penetrating Well, *Journal of the Hydraulics Division,* ASCE, Vol. 87, No. HY 4, pp. 83-98, July 1961a.

25. Hantush, M. S., "Aquifer Tests on Partially Penetrating Wells," *Journal of the Hydraulics Division, ASCE,* Vol. 87, No. HY 5, pp. 171-195, September 1961b.

26. Harr, M. E., *Groundwater and Seepage,* Mc Graw-Hill Book Company, 1962.

27. Hausmann, M. R., *Engineering Principles of Ground Modification,* Mc Graw-Hill Co., 1990.

28. Hayashi, K., Ito, T., and Abé, H., "A New Method for the Determination of In-Situ Hydraulic Properties by Pressure Pulse Tests and Application to the Higashi Hachimantai Geothermal Field," *Journal of Geophysical Research,* Vol. 92, No. 139, pp. 9168-9174, August 1987.

29. Head, K. H., *Soil Technicians' Handbook,* John Wiley & Sons, 1989.

30. Holtz, R. D., and Kovacs, W. D., *An Introduction to Geotechnical Engineering,* Prentice-Hall, New Jersey, 1981.

31. Hvorslev, M. J., *Time Lag and Soil Permeability in Ground Water Levels and Pressures,* U.S. Army Corps of Engineers Waterways Experiment Station, Vicksburg, M. S., Bulletin No. 36, 1951.

32. Hyder, Z., Butler, Jr., J. J., Mc Elwee, C. D., and Liu, W., "Slug Tests in Partially Penetrating Wells," *Water Resources Research,* Vol. 30, No. 11, pp. 2945-2957, November 1994.

33. Kabala, Z J., "The Dipole Flow-Test: A New Single-Borehole Test for Aquifer Characterization," *Water Resources Research,* Vol. 29, No. 1, pp. 99-107, Janunary 1993.

34. Karasaki, K., Long, J. C. S., and Witherspoon, P. A., "Analytical Models of Slug tests, *"Water Resources Research,* Vol. 24, No. 1, pp. 115-126, 1988.

35. Kono, I., and Nishigaki, M., "A Method for Determination of Anisotropic Coefficients of Permeability and Specific Storage from Pumping Test Data," *Soils and Foundations,* Vol. 19, No. 1, pp. 55-62, March 1979.

36. Kruseman, G. P., and de Ridder, N. A., *Analysis and Evaluation of Pumping Test Data,* International Institute for Land Reclamation and Improvement ILRI Bulletin No. 11, 1983.

37. Lambe, T. W., and Whitman, R. V., *Soil Mechanics, I Version,* John Wiley & Sons, New York, 1979.

38. Mieussens, C., and Ducasse, P., "Measure en Place des Coefficients de Perméabilité et des Coefficients de Consolidation Horizontaux et Verticaux," *Canadian Geotechnical Engineering,* Vol. 14, pp. 76-90, 1977.

39. Moench, A. F., and Ogata, A., "Analysis of Constant Discharge Wells by Numerical Inversion of Laplace Transform Solutions," in *Ground Water Hydraulics,* J. S. Rosenshein and G. D. Bennett (Eds.), American Geophysical Union, Washington, D. C., Water Resources Monograph 9, 1984.

40. Novakowski, K. S., "Interpretation of the Transient Flow Rate Obtained from Constant-Head Tests Conducted In-Situ in Clays," *Canadian Geotechnical Journal,* Vol. 30, pp. 600-606, 1993.

41. Olson, R. E., and Daniel, D. E., "Measurement of the Hydraulic Conductivity of Fine-Grained Soils," *Permeability and Groundwater Transport, ASTM STP 746,* T. F. Zimmie and C. O. Riggs, (Eds.), ASTM, pp. 18-64, 1981.

42. Philip, J. R., "Approximate analysis of the Borehole Permeameter in Unsatwated Soil, *Water Resources Research,* Vol. 21, No. 7 pp. 1025-1033, 1985.

43. Randolph, M. F., and Booker, J. R., "Analysis of Seepage into Cylindirical Permeameter, *"Proceedings of the Fourth International Conference on Numerical Methods in Geomechaniscs,* Edmonton, Voy. 1, pp. 349-357, A. A. Balkema, 1982.

44. Raymond, G.P. and Azzouz, M.M., "Permeability Determination for Predicting Rates of Consolidation," *Institute of Civil Engineers*, London, pp. 285-293, 1969.

45. Reynolds, W. D., and Elrick, D. E., "A Method for Simultaneaus In-Situ Measurement in the Vadose Zone of Field-Saturated Hydraulic Conductivity, Sorptivity and the Conductivity-Pressure Head Relatianships," *Ground Water Monitoring Rev.*, Vol. 6, No. 1, pp. 84-95, 1986.

46. Reynolds, W. D., and Elrick, D. E., "In Situ Measurement of Field-Saturated Hydraulic Conductivity, Sorptivity, and the α - Parameter Using the Guelph Permeameter," *Soil Science,* Vol. 140, No. 4, pp. 292-302, October 1985.

47. Reynolds, W. D., Elrick, D. E., and Clothier, B. E., "The Constant Head Well Permeameter: Effect of Unsaturated Flow, *"Soil Science"*, Vol. 139, No. 2, pp. 172-180, 1987.

48. Sageev, A., "Slug Test Analysis, *"Water Resources Research,* Vol. 22, No. 8, pp. 1433-1436, 1986.

49. Samarasinghe, A. M., Huang, Y. H., and Drnevich, V. P., "Permeability and Consolidation of Normally Consolidated Soils," *Journal of Geotechnical Engineering,* ASCE, Vol. 108, No. GT6, pp. 835-850, June 1982.

50. Sivaram, B., and Swamee, "A Computational Method for Consolidation Coefficient," *Soils and Foundations,* Vol. 17, No. 2, pp. 48-52, 1977.

51. Smiles, D. E., and Youngs, E. G., "Hydraulic Conductivity Determinations by Several Field Methods in a Sand Tank," *Soil Science,* Vol. 99, No. 2, pp. 83-87, 1965.

52. Stephens, D. B., and Neuman, S. P., "Vadose Zone Permeability Test: Summary, *"Journal of Hydrolics Division, ASCE,* Vol. 108, No. 5, pp. 623-639, 1982a.

53. Stephens, D. B., and Neuman, S. P., "Vadose Zone Permeability Test: Steady-state results, *"Journal of Hydrolics Division, ASCE,* Vol. 108, No. 5, pp. 40-659, 1982a.

54. Stephens, D. B., and Neuman, S. P., "Vadose Zone Permeability Test: Steady-State Results, *"Journal of Hydrolics Division, ASCE,* Vol. 108, No. 5, pp. 660-677, 1982b.

55. Stephens, D. B., and Neuman, S. P., "Vadose Zone Permeability Test: Unsteady Flow, *"Journal of Hydrolics Division, ASCE,* Vol. 108, No. 5, pp. 660-677, 1982c.

56. Stephens, D. B., Lambert, K, and Watson, D., "Regression Models for Hydraulic Conductivity and Field Test of the Borehole Permeameter," Vol. 23, No. 12, pp. 2207-2214, 1987.

57. Tavenas, F., Diene, M., and Leroueil, S., "Analysis of the In-Situ Constant-Head Permeability Test in Clays," *Canadian Geotechnical Journal*, Vol. 27, pp. 305-314, 1990.

58. Tavenas, F., Jean, P., Leblond, P., and Leroueil, S., "The Permeability of Natural Soft Clays. Part II: Permeability Characteristics, "*Canadian Geotechnical Journal,* Vol. 20, pp. 6454-660, 1983.

59. Wilkinson, W. B., "Constant Head In Situ Permeability Tests in Clay Strata," *Geotechnique,* Vol. 18, No. 2, pp. 172-194, 1968.

REFERENCES NOT CITED

1. Balasutramaniam, A. S., Chandra, S., Bergada, D. T., and Nutalaya, P. (Eds.), *Environmental Geotechnics, and Problematic Soils and Rocks,* Proceedings of the Symposium on Environmental Geotechnics and Problematic Soils and Rocks, A. A. Balkema, Broakfield, 1988.

2. Craig, R. F., *Soil Mechanics,* Chapman & Hall, 1993.

3. Eroskay, S.O., and Uz, N.Ö., Yeraltısuyu Kuyu Verilerinin Değerlendirilmesi, İstanbul University Publication No.2816, 1981.

4. Ervin, M. C. (Ed.), *Proceedings of an Extension Course on In-Situ Testing for Geotechnical Investigations,* A. A. Balkema, Rotterdam, 1983.

5. *Permeability and Capillarity of Soils,* ASTM Special Technical Publication No. 417, 1967.

6. Das, B. M., *Advanced Soil Mechanics,* Mc Graw - Hill, Singapore, 1983.

7. Das, B. M., *Principles of Geotechnical Engineering,* PWS Publishing Company, Boston, 1994.